RESERVE

D3.9

WP3 Drafting of Ancillary Services and Network codes definitions V2

The research leading to these results has received funding from the European Union's Horizon 2020 Research and Innovation Programme, under Grant Agreement no 727481.

Project Name	RESERVE
Contractual Delivery Date:	30.09.2019
Actual Delivery Date:	30.09.2019
Contributors:	Alireza Soroudi (UCD), Alireza Nouri (UCD), Andrew Keane (UCD), Sriram Karthik Gurumurthy (RWTH), Antonello Monti (RWTH), David Ryan (WIT), Miguel Ponce De Leon (WIT), Niall Grant (WIT), Darren Leniston (WIT), Zain Mehdi (EDD), Robert Farac (EDD), Ronan Murphy (ESB), Tom Clancy (ESB), Artur Löwen (GH)
Workpackage:	WP3 – Voltage Stability by Design
Security:	PU
Nature:	R
Version:	1.0
Total number of pages:	120

Abstract:

This deliverable presents the updated Ancillary Services and Network codes definitions developed in WP3 of RESERVE project. The proposed network codes and validations are related to the dynamic and static active voltage management (SV_A and SV_B), requirements. The trialled network codes related to the technical aspects and ancillary services, ICT testing as well as the related simulation activities are reported.

Keyword list:

Distribution Network Code, Ancillary Service, Reactive support, Voltage stability, Volt-Var curve, impedance measurement

Executive Summary

The deliverable **D3.9** drafts the network code definitions (version 2) related to Task 3.7 within the wider context of WP3. The reactive power support and voltage control are essential ancillary services for ensuring the grid reliability and facilitating hosting RES technologies.
This is a final second version of **D3.8** which is deprecated. The main role of this deliverable is identifying a structure and key attributes through which all energy actors will integrate and communicate with a voltage and network control system in a secure resilient fashion and draft ancillary service and network code definitions based on these insights. This deliverable is dedicated to the network code requirements as well as the ICT validation of the SV_A and SV_B strategies.

The network code recommendation for DER control considering static voltage control strategies are listed. The power factor requirements of different DER technologies are discussed and mathematically formulated. Additionally, the standard operating voltage conditions in different network codes are analysed. Finally, the concept of decentralised voltage control strategy using Volt-var curves is explained and discussed. The active voltage management using Volt-var optimization can be utilised as a powerful tool in futuristic distribution networks. The simulation results provided in chapter **2** show the effectiveness of the proposed methodologies (related to SV_B) in this chapter.

In Chapter **3**, network codes and ancillary services definition arising from the Dynamic Voltage Stability Monitoring (DVSM) technique is defined and elaborated. The proposed technique addresses solution for power grids undergoing transition towards 100% RES and for power grids which are already operating at 100% RES. Unlike the conventional grids where power has a market, we propose a huge potential market for impedances since impedances reveals the dynamics of the grid and specifying the impedances to every converter allows the power grid to dynamically behave in a controlled manner. A programmable impedance measurement device is proposed and developed in RESERVE. The proposed device has high bandwidth and hence fast control, has the capability of noise injection through its control loops and enables extraction of grid impedance. The proposed device is mobile, low weight and low cost and can be used by DSOs for making real-time impedance measurements and evaluate the stability of the grid. The proposed device offers high plug-play capability owing to its mobile nature. Existing PV inverters can incorporate this concept and can offer ancillary service to the grid operator by providing the impedance information. In RESERVE, the new paradigm is that every grid connected household PV inverter acts as an impedance sensor allowing the grid operator to monitor and counteract instability.

Chapter **4,** Centres on the description of how the ICT architectures defined in D3.6 were used to implement the AVM in the field and the challenges faced. It also describes Servo Live from a technological level and how its components are used to assess the impact of the AVM in the field from a power system level. The role of 5G in fulfilling the key requirements of the voltage techniques is explained. The cost-effective and easy connection of the high number of new devices that will be introduced, ultra-low latency, high reliability and availability, security, and privacy. Connection of massive number of devices in secured and reliable way with ultra-low latency is part of the 5G design. This deliverable describes how 5G fulfils the new voltage techniques requirements provided with the 5G solutions like network slicing, edge cloud computing and private mobile networks.

Chapter **5** refers to the validation and assessment of Voltage Control in the trial sites. In selecting specific technologies for the AVM Field Trials, it was decided to mix more established technologies such as Solar PV with more cutting edge technologies such as Vehicle-2-Grid chargers. These selections allowed us to compare and contrast the impact of technologies on the effectiveness of the control technique across a range of network configurations located in both rural and urban environments. All AVM trial sites are located in Ireland and connected to low voltage distribution networks which are operated by a single Distribution System Operator, ESB Networks. This has allowed for standardised connection design and monitoring and facilitated consistent analysis of network impact

The outcome of the findings in this deliverable on inclusion of ICT features in NC recommends including only generic aspects on ICT features rather than hard requirements, as they would be too stringent regarding the different configurations and algorithms. Therefore, the presented

general recommendations on ICT aspects in NC should be seen as guidelines for setting a basis for DER ancillary services in future distribution grids.

Authors

Partner	Name	e-mail
UCD		
	Álireza Soroudi	Alireza.soroudi@ucd.ie
	Alireza Nouri	Alireza.nouri@ucd.ie
	Andrew Keane	Andrew.Keane@ucd.ie
RWTH		
	Sriram Karthik Gurumurthy	Sgurumurthy@eonerc.rwth-aachen.de
	Antonello Monti	Amonti@eonerc.rwth-aachen.de
WIT		
	David Ryan	dryan@tssg.org
	Miguel Ponce De Leon	miguelpdl@tssg.org
	Niall Grant	ngrant@tssg.org
	Darren Leniston	dleniston@tssg.org
EDD		
	Robert Farac	robert.farac@ericsson.com
	Mehdi Zain	zain.mehdi@ericsson.com
ESB		
	Ronan Murphy	ronan.murphy@esb.ie
	Tom Clancy	tom.clancy2@esb.ie
GH		
	Artur Lowen	aloewen@gridhound.de

Table of Contents

1. Introduction

This deliverable summarises the activities of **Task 3.7** of WP3 and further discusses the new findings obtained in work package 3 of RESERVE project.

1.1 Task 3.7

Deliverable D3.9, *Drafting of Ancillary Services and Network codes definitions, V2* , summarizes the new findings and the lessons learned in the research activities and practical implementations of the RESERVE project related to dynamic and static voltage control and stability analysis. WP3 explores new concepts and theories surrounding steady state voltage regulation and dynamic voltage stability for distribution energy networks with 100% RES penetration. In the context of Task 3.7, the integration of any control mechanism will be totally contingent on interaction with all actors in the energy value chain. This task will identify a structure and key attributes through which all energy actors will integrate and communicate with a voltage and network control system in a secure resilient fashion and draft ancillary service and network code definitions based on these insights. This deliverable summarises the activities of Task 3.7 within the wider context of WP3.

1.2 Objectives of the Work Report in this Deliverable

- **O1.** To provide a list of recommendations on distribution network codes related to static voltage control and stability techniques (SV_B introduced in **D1.5**)
- **O2.** To provide a list of recommendations on distribution network codes related to dynamic voltage control and stability techniques (SV_A introduced in **D1.5**)
- **O3.** To investigate the ICT requirements that should be reflected in network codes for implementing the voltage control and stability techniques proposed in WP3
- **O4.** To provide a valid simulation test-bed for developing and investigating the techniques,

The deliverable details the network code recommendations stemmed from the research efforts completed in WP3 of the RESERVE project in developing the voltage control and stability concepts. The network code recommendations regarding the static and dynamic voltage control as well as the scientific background, simulation platforms, and validation on sample distribution networks are presented here. The simulation results are provided to support these recommendations.

1.3 How to read this document

The network codes related to two main scenarios of WP3 namely SV_A and SV_B are explained and drafted in D3.9 *Drafting of Ancillary Services and Network codes definitions, V2.* D3.9 updates and replaces D3.8 *Drafting of Ancillary Services and Network codes definitions, V1.* The requirements on communication for both the scenarios can be found in D1.3. It is recommended to the reader to peruse through the voltage scenarios in these documents. The output of D3.9 will be used as the input for **WP6** and **WP7**. Figure 1-1 shows the placement of this deliverable (**D3.9**) in the wider context of **WP3** as well as interlinked work packages of the RESERVE project:

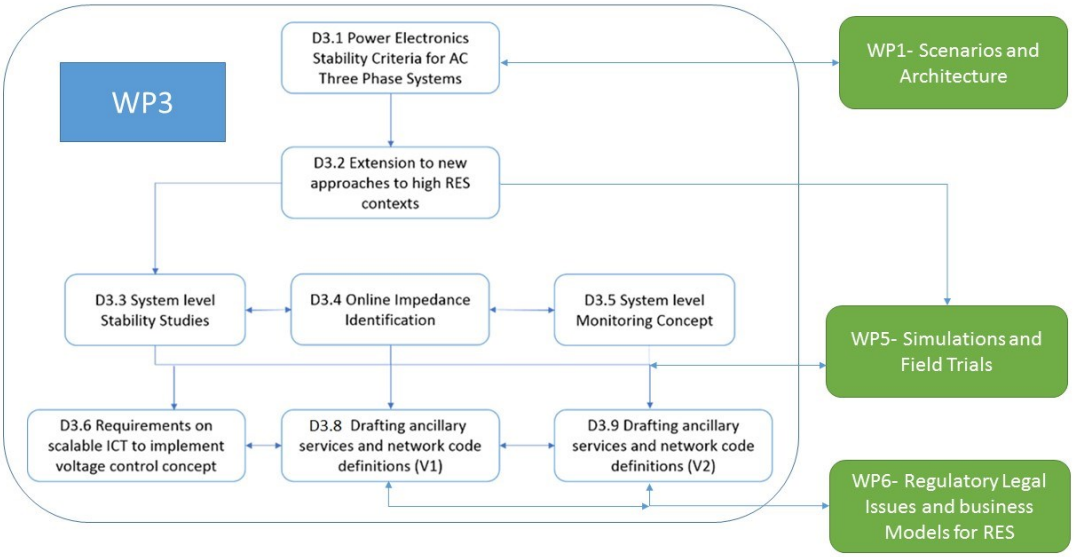

Figure 1-1 Relations between Deliverables in WP3 and other work packages

1.4 Approach used to undertake the Work

The following steps were applied to develop the results reported in this deliverable.

- The foundation of the new approaches to voltage stability and control are expanded upon from **D3.2, D3.3, D3.4, D3.5** and **D3.6** to a simulation environment in **D3.8**.
- System equations governs the performance of the Dynamic Voltage Stability Monitoring technique (to achieve **O2**) and the AVM technique (to achieve **O1**).
- The formulation of both techniques, i.e., AVM and DVSM, is put forward in this deliverable, expanding the application of inverter-based RES units to a case-study (see **D5.3**) context (to achieve **O4**).
- Step-by-step methodologies are developed to outline the replicability of the approach to any distribution feeder context irrespective of the differing inverter-based RES technology.
- Case studies are performed to validate the techniques in using time-domain simulations and time-series power flow (to achieve **O3**). The efficient ICT techniques are required for implementing AVM and DVSM.
- Conclusions are drawn based upon the performance of the voltage control techniques in the simulation environment.

2. Drafting Network code recommendation for DER control considering voltage control strategies

The Network Codes (NC) in many jurisdictions place thresholds and mandatory requirements on the operational envelopes of connected devices including Distributed Energy Resources (DERs). Such requirements include thresholds for the Reactive Power performance of such devices. A number of Specific DER Technologies are subject to power factor requirements including Wind Generators, Solar PV Generators and Storage. These are discussed in greater detail below.

2.1 Power factor requirements for DER technologies

The Renewable Power Production (RPP) shall be equipped with reactive power control functions capable of controlling the reactive power supplied by the RPP at the Point of Connection (POC) as well as a voltage control function capable of controlling the voltage at the POC via orders using set points and gradients for the specified parameters [1]. The reactive power requirements of DERs are different in different network codes. Table 2-1 provides a comparison between different network codes.

Table 2-1 Reactive Power Requirements for DERs

Grid Code	Reactive requirement specified at	Reactive power range (pu)	Equivalent Power factor	Reference
Denmark	Grid Connection Point	-0.33 – 0.33	0.95 – 0.95	[2]
Germany	Grid Connection Point (Transmission Code)	-0.33 – 0.33 -0.33 – 0.41 -0.41 – 0.33	0.95 – 0.95 0.905 – 0.925 0.925 – 0.95	[3]
UK	Grid entry point		0.95 – 0.95	[4]
Ireland	LV side of grid transformer	-0.39 – -0.31	0.92 – 0.95	[5]

In this section the power factor requirements of different inverter based DER will be discussed.

2.1.1 Power factor requirements for Wind technology

There are some general issues regarding the reactive power capability of wind technology as follows:

- The requirements for synchronous machines are specified at the machine terminals
- The relationship between machine capability and capability at the interface point will vary from one installation to another.
- The design implications of different reactive capability requirements are not certain, and will vary between installations, technologies, manufacturers etc.
- The utilisation of the full reactive power capability of a generator located in a weak part of the network may result in unacceptably high voltages near the generation side without impacting significantly on the grid voltage, therefore resulting in unusable reactive capability due to the characteristics of the local network
- Synchronous machines are dynamic reactive power sources, and thus contribute to voltage regulation and voltage stability. Wind farms may depend on static devices (such as capacitors which in addition have voltage squared output dependence) and thus may not deliver the same performance even if they have the same nominal capacity.
- Synchronous machines have an inherent reactive power capability, controlled by excitation control. Over-excitation, delivering capacitive reactive power to the system is normally limited by either exciter current limits or stator current limits. Under-excitation, delivering inductive reactive power, is normally limited by stability considerations. In integrated utilities, the reactive capabilities of individual machines were normally a matter for negotiation internally. Greater capacitive capability could normally be achieved at some cost increase due to the greater alternator and exciter ratings required. On the other hand turbine improvements

leading to increased output could lead to reduced reactive capability if the alternator rating was not also increased.

The Irish Distribution Code specifies power factor requirements for Wind technology with less than 5 MW capacity, these are shown in Figure 2-1 [5].

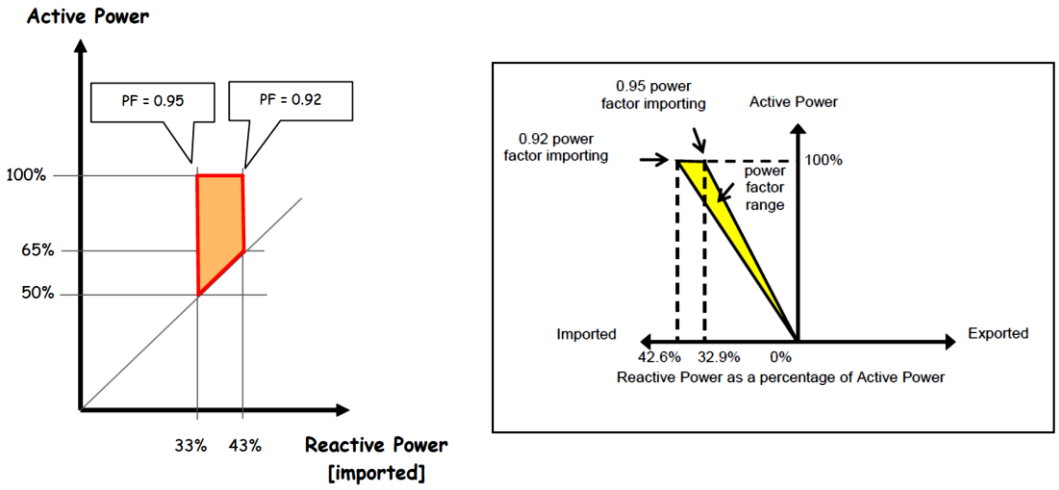

Figure 2-1 Power Factor (PF) requirements for wind technology with less than 5 MW capacity

As can be observed in Figure 2-1, the wind technology is not allowed to inject reactive power to the grid (only lagging power factor is allowed). In general, the reactive power output of inverter based wind technology is limited by several factors which will be discussed here:

- Case a) Reactive power provision for wind technology without considering the thermal limits of the inverter is schematically shown in Figure 2-2. In this figure, every point shows a mathematically simulated operating point (just for demonstration purpose). In this case, the wind turbine can provide reactive power upto the maximum of its reactive capacity without considering its active power.

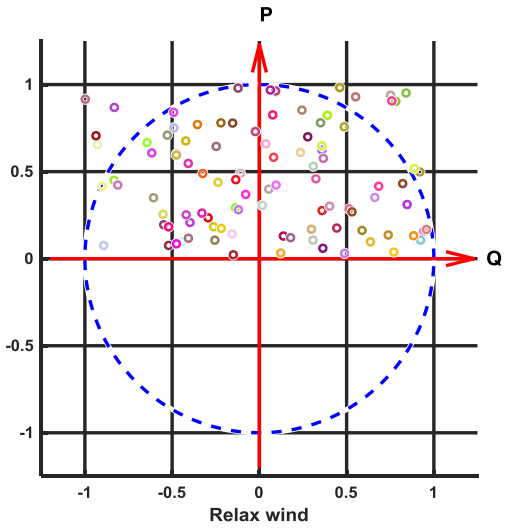

Figure 2-2 Reactive power capability for wind without considering the thermal limits of inverter

The reactive power of the wind in case a) is constrained as given in (2-1):

$$-Q_{wind}^{max} \leq Q_{wind} \leq Q_{wind}^{max} \quad (2\text{-}1)$$

- Case b) Reactive power provision for wind technology with considering the thermal limits of the inverter see Figure 2-3. In this case, wind turbine can provide the reactive upto maximum of it reactive capacity but the reactive power limit is calculated considering the active power output of the wind turbine/

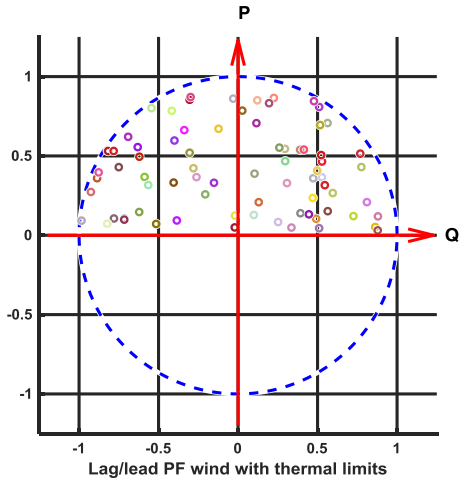

Figure 2-3 Reactive power capability for wind considering the thermal limits of inverter

The reactive power of the wind in case b) is constrained as given in (2-2):

$$\begin{gathered} -Q_{wind}^{max} \leq Q_{wind} \leq Q_{wind}^{max} \\ \sqrt{Q_{wind}^2 + P_{wind}^2} \leq S_{wind}^{max} \end{gathered} \quad (2\text{-}2)$$

- Case c) The wind turbine is limited to provide lagging reactive power only, see Figure 2-4. In this case, the wind turbine is not allowed to provide leading reactive power. In other words, the wind turbine is not allowed to inject reactive power to the grid. This is done to prevent the voltage rise in the distribution network.

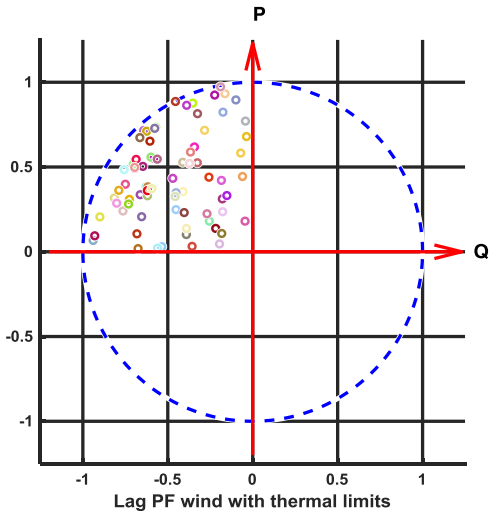

Figure 2-4 Lagging reactive power capability for wind considering the thermal limits of inverter

The reactive power of the wind in case c) is constrained as given in (2-3):

$$\begin{gathered} -Q_{wind}^{max} \leq Q_{wind} \leq Q_{wind}^{max} \\ \sqrt{Q_{wind}^2 + P_{wind}^2} \leq S_{wind}^{max} \\ -Q_{wind}^{max} \leq Q_{wind} \leq 0 \end{gathered} \quad (2\text{-}3)$$

- Case d) the Irish Distribution Code's requirements for reactive power provision by wind technology see Figure 2-5. In this case, the wind turbine is only allowed to provid lagging power factor (absorb reactive power) but within the specified limits as shown in Figure 2-1.

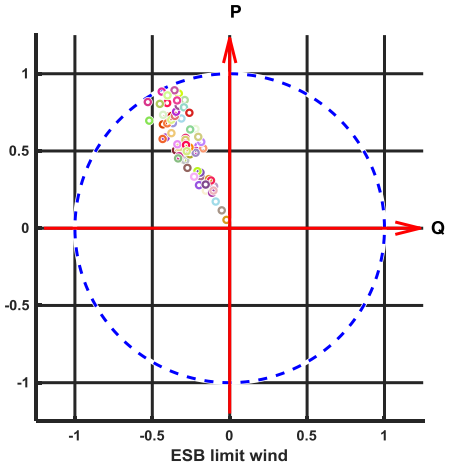

Figure 2-5 Reactive power capability for wind considering the Distribution Code's requirements

The reactive power of the wind in case d) is constrained as given in (2-4):

$$\begin{gathered} -Q_{wind}^{max} \leq Q_{wind} \leq Q_{wind}^{max} \\ \sqrt{Q_{wind}^2 + P_{wind}^2} \leq S_{wind}^{max} \\ -Q_{wind}^{max} \leq Q_{wind} \leq 0 \\ 0.92 \text{ lag} \leq PF_{wind} \leq 0.95 \text{ lag} \end{gathered} \quad (2\text{-}4)$$

- Case e) The proposed reactive power provision of wind technology is shown in Figure 2-6. In this case, the wind turbine is required to provide both lagging and leading power factor within the specified limits which are 0.92 lagging/leading.

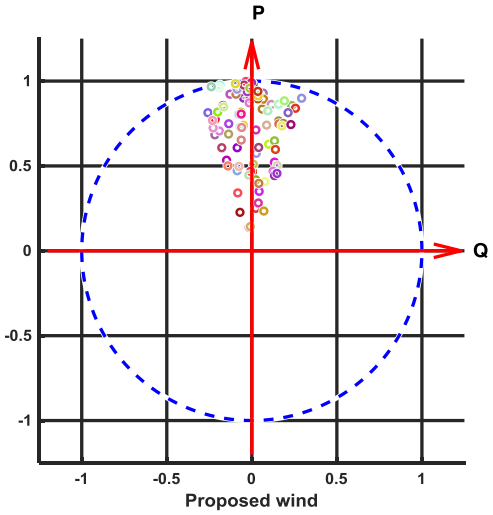

Figure 2-6 Proposed reactive power capability for wind

The reactive power of the wind in case e) is constrained as given in (2-5):

$$-Q_{wind}^{max} \leq Q_{wind} \leq Q_{wind}^{max}$$
$$\sqrt{Q_{wind}^2 + P_{wind}^2} \leq S_{wind}^{max} \quad (2\text{-}5)$$
$$0.92 \text{ lag} \leq PF_{wind} \leq 0.92 \text{ lead}$$

Allowing the wind turbines to have a more flexible range of operation has the following pros and cons:

Pros:

- The capability to inject reactive power to the grid for increasing the voltage level in high demand period
- Some wind technologies can provide reactive power to the grid even at no-wind conditions
- It can reduce the loading of the transformer connecting LV to MV
- Improve the security of supply
- It can delay the need for distribution network development plans

Cons

- The reactive power injection can cause overvoltage issues in low load periods
- Considering the thermal limits of inverter, the active power output of the wind will be more limited
- Allowing leading reactive power support by wind turbines requires more coordination between different flexibilities and resources

2.1.2 Power factor requirements for PV technology

Case a) Reactive power provision for PV technology without considering the thermal limits of the inverter see Figure 2-7.a. In this case, PV can provide the reactive up to the maximum of it reactive capacity without considering its active power. The reactive power of the PV in case a) is constrained as given in (2-6):

$$-Q_{pv}^{max} \leq Q_{pv} \leq Q_{pv}^{max} \quad (2\text{-}6)$$

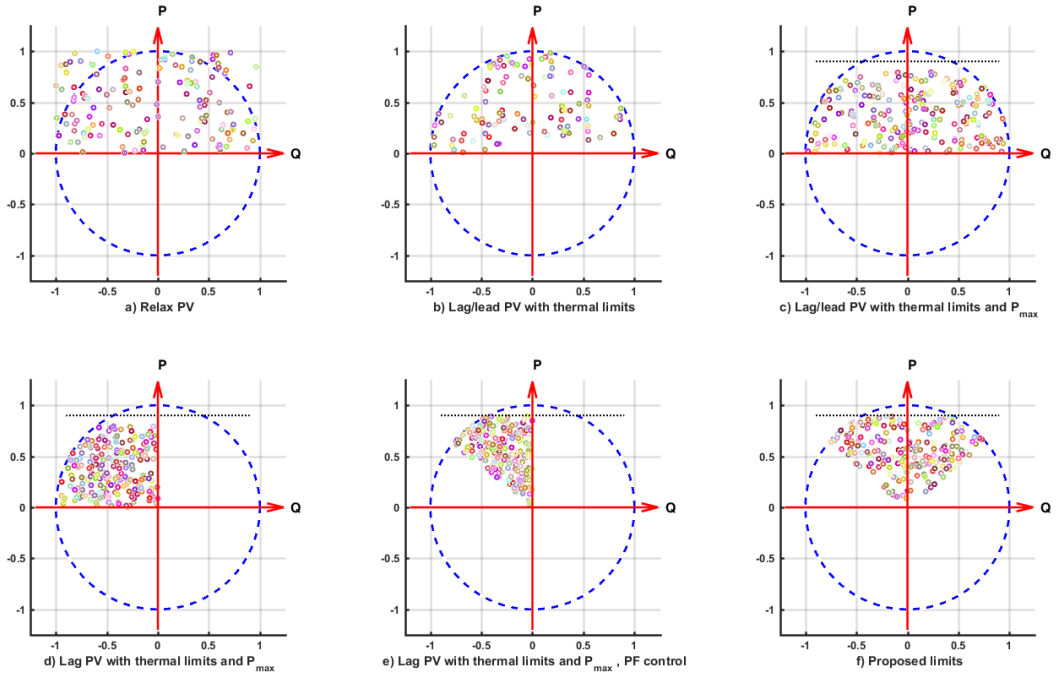

Figure 2-7 Reactive power capability for PV technology

Case b) An inverter attached to a PV generator is not an infinite source or sink of reactive power. Its instantaneous reactive power capability is limited by its fixed apparent power capability S and the variable real power generation P as depicted in Figure 2-7.b In this case, PV can provide the reactive up to the maximum of it reactive capacity without considering its active power. The reactive power of the PV in case b) is constrained as given in (2-7):

$$\begin{aligned} -Q_{pv}^{max} \le\ & Q_{pv} \le\ Q_{pv}^{max} \\ & \sqrt{Q_{pv}^2 + P_{pv}^2} \le S_{pv}^{max} \end{aligned} \tag{2-7}$$

Case c) The PV unit should be operated at an active power output below the rated capacity of the PV. The Solar Plant shall be able to be operated in every possible operating point in the P-Q Diagram for each solar plant size as shown in Figure 2-7.c [6]. The reactive power of the PV in case c) is constrained as given in (2-8):

$$\begin{aligned} -Q_{pv}^{max} \le\ & Q_{pv} \le\ Q_{pv}^{max} \\ & \sqrt{Q_{pv}^2 + P_{pv}^2} \le S_{pv}^{max} \\ & P_{pv} \le 0.9 S_{pv}^{max} \end{aligned} \tag{2-8}$$

Case d) In some network codes, the PV units are only allowed to provide lagging power factor (absorbing reactive power) see Figure 2-7.d. The reactive power of the PV in case d) is constrained as given in (2-9):

$$\begin{aligned} -Q_{pv}^{max} \le\ & Q_{pv} \le\ Q_{pv}^{max} \\ & \sqrt{Q_{pv}^2 + P_{pv}^2} \le S_{pv}^{max} \\ & -Q_{pv}^{max} \le\ Q_{pv} \le 0 \\ & 0 \le\ P_{pv} \le 0.9 S_{pv}^{max} \end{aligned} \tag{2-9}$$

Case e) In some network codes, there are extra constraints on PF that a PV unit can provide see Figure 2-7.e. The reactive power of the PV in in this case is constrained as given in (2-10):

$$
\begin{gathered}
-Q_{pv}^{max} \leq Q_{pv} \leq Q_{pv}^{max} \\
\sqrt{Q_{pv}^2 + P_{pv}^2} \leq S_{pv}^{max} \\
-Q_{pv}^{max} \leq Q_{pv} \leq 0 \\
0 \leq P_{pv} \leq 0.9 S_{pv}^{max} \\
0.92 \text{ lag} \leq PF_{pv} \leq 1
\end{gathered}
\tag{2-10}
$$

Case f) The proposed reactive power capability curve for PV technology is shown in Figure 2-7.f. The PV unit must be able to control reactive power at the Grid Connection Point in a range of 0.92 lagging to 0.92 leading at maximum active power and according to (2-11) inspired by [7]:

$$
\begin{gathered}
-Q_{pv}^{max} \leq Q_{pv} \leq Q_{pv}^{max} \\
\sqrt{Q_{pv}^2 + P_{pv}^2} \leq S_{pv}^{max} \\
-Q_{pv}^{max} \leq Q_{pv} \leq 0 \\
0 \leq P_{pv} \leq 0.9 S_{pv}^{max} \\
0.92 \text{ lag} \leq PF_{pv} \leq 0.92 \text{ lead}
\end{gathered}
\tag{2-11}
$$

2.1.3 Power factor requirements for electric storage systems

The electric energy storage technologies like batteries and Vehicle-to-Grid (V2G) can not only inject active power but also they can absorb active power. This is unlike PV and wind technology behaviour in which they can just inject active power to the grid. The reactive power output of an inverter based storage technology is limited by several technical factors which will be discussed here.

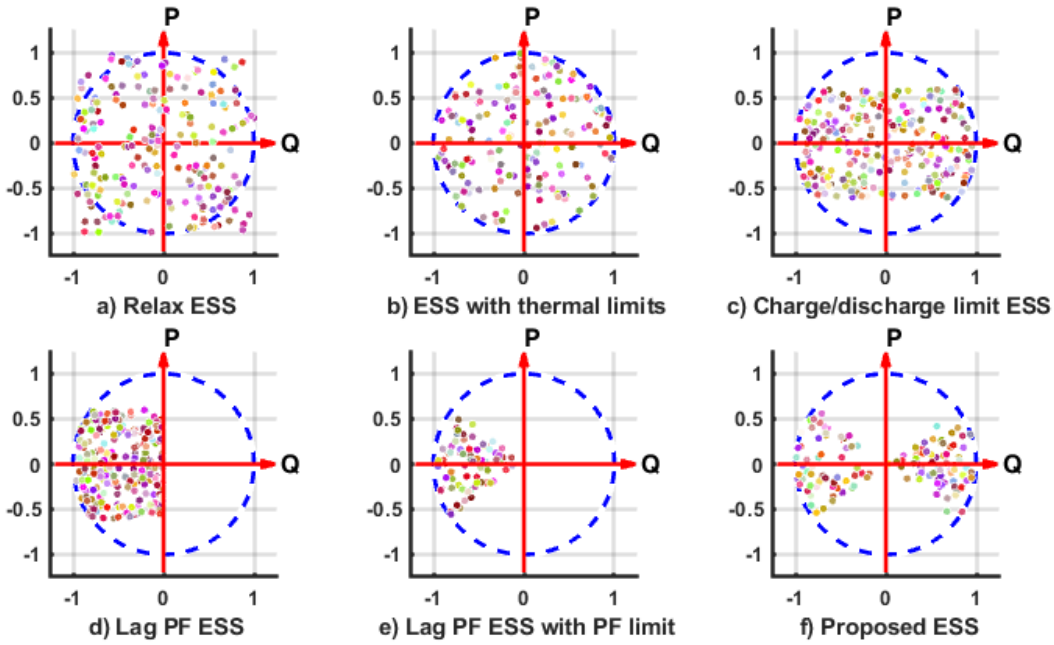

Figure 2-8 Reactive power capability for electric energy storage technologies

Case a) In this case, the ESS can provide reactive/reactive power up to its inverter capacity. The active power also changes within its max range. The reactive power capability curve is shown in Figure 2-8.a. The reactive power of the ESS in this case is constrained as given in (2-12):

$$-Q_{ESS}^{max} \leq Q_{ESS} \leq Q_{ESS}^{max}$$
$$-S_{ESS}^{max} \leq P_{ESS} \leq S_{ESS}^{max} \quad (2\text{-}12)$$

Case b) In this case, an additional constraint is added which is the thermal capacity of the unit. The resulting reactive power capability curve for ESS is shown in Figure 2-8.b. The reactive power of the ESS in this case is constrained as given in (2-13):

$$-Q_{ESS}^{max} \leq Q_{ESS} \leq Q_{ESS}^{max}$$
$$-S_{ESS}^{max} \leq P_{ESS} \leq S_{ESS}^{max} \quad (2\text{-}13)$$
$$\sqrt{Q_{ESS}^2 + P_{ESS}^2} \leq S_{ESS}^{max}$$

Case c) In this case, the charging and discharging limits are taken into account. The resulting reactive power capability curve for ESS is shown in Figure 2-8.c. The reactive power of the ESS in this case is constrained as given in (2-14):

$$-Q_{ESS}^{max} \leq Q_{ESS} \leq +Q_{ESS}^{max}$$
$$-P_{ESS}^{max} \leq P_{ESS} \leq P_{ESS}^{max} \quad (2\text{-}14)$$
$$\sqrt{Q_{ESS}^2 + P_{ESS}^2} \leq S_{ESS}^{max}$$

Case d) In this case, the constraints are similar to case c but the reactive power is limited to the lagging PF. The resulting reactive power capability curve for ESS is shown in Figure 2-8.d according to **(2-15**):

$$-Q_{ESS}^{max} \leq Q_{ESS} \leq 0$$
$$-P_{ESS}^{max} \leq P_{ESS} \leq P_{ESS}^{max} \quad (2\text{-}15)$$
$$\sqrt{Q_{ESS}^2 + P_{ESS}^2} \leq S_{ESS}^{max}$$

Case e) In this case, an additional constraint is added which is controlling the reactive power within a specific range. The resulting reactive power capability curve for ESS is shown in Figure 2-8.e. The ESS must be able to control reactive power at the Grid Connection Point in a range of 0.92 lagging to unity PF according to (2-16):

$$-Q_{ESS}^{max} \leq Q_{ESS} \leq 0$$
$$-P_{ESS}^{max} \leq P_{ESS} \leq P_{ESS}^{max} \quad (2\text{-}16)$$
$$\sqrt{Q_{ESS}^2 + P_{ESS}^2} \leq S_{ESS}^{max}$$
$$0.92 \text{ lag} \leq PF_{ESS} \leq 0.92 \text{ lead}$$

Case f) The proposed reactive power curve for ESS is shown in Figure 2-8.f. The ESS must be able to control reactive power at the Grid Connection Point in a range of 0.92 lagging to 0.92 leading according to (2-17) [8]:

$$-Q_{ESS}^{max} \leq Q_{ESS} \leq +Q_{ESS}^{max}$$
$$-P_{ESS}^{max} \leq P_{ESS} \leq P_{ESS}^{max} \quad (2\text{-}17)$$
$$\sqrt{Q_{ESS}^2 + P_{ESS}^2} \leq S_{ESS}^{max}$$
$$0.92 \text{ lag} \leq PF_{ESS} \leq 0.92 \text{ lead}$$

2.2 Voltage Control and operating conditions in the presence of DERs

The calculated voltage rise due to the DER's connection must not cause voltage outside the permitted limits. The nominal voltages at distribution systems are given in Table 2-2.

Table 2-2 Distribution nominal voltages (Irish System)

Level	Voltage range
Low voltage (LV)	230V – phase to neutral 400V – phase to neutral
Medium voltage (LV)	10 kV 20 kV
High voltage (LV)	38 kV 110 kV

The DSO should operate the distribution system in a way that the voltage at the supply terminal as defined in EN 50160 [9], complies with that standard. The voltage range tolerance shall be 230V ±10%. The resulting voltage at different points on the system depends on several factors but at the connection point can be expected to be in accordance with Table 2-3 under steady state and normal operating conditions [5].

Table 2-3 Operating voltage range

Nominal voltage	Maximum voltage	Minimum voltage
230 V	253 V	207
400 V	440 V	360
10 kV	11.1 kV	Variable according to operating condition
20 kV	22.1 kV	
38 kV	43 kV	
110 kV	120 kV	

The voltage regulation control will follow the requirements presented by [10] which is shown in Figure 2-9.

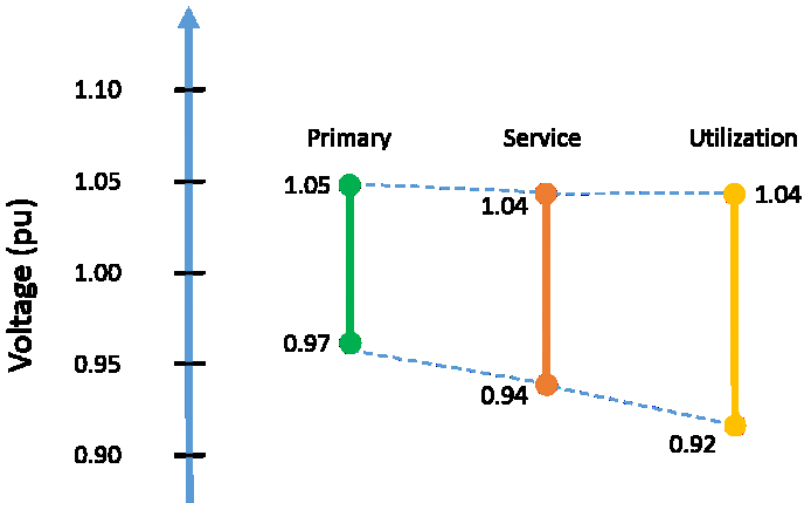

Figure 2-9 Voltage regulation control requirements

The primary voltage refers to the voltage at the point of primary side of the step down transformer at the customer side. The service voltage means the voltage at the customer's meter, or the load side of the Point of Common Coupling (PCC). The utilization voltage refers to the voltage at the point of use where the outlet equipment is plugged in.

2.2.1 Voltage rise (Existing):

2.2.1.1 Steady-state voltage rise criteria (Available in the current Irish NC)

The connection of embedded generators to the distribution network may impact on the DSO's ability to regulate network voltages. For this reason, DSO requires embedded generating systems to control reactive power output, within their capability, to maintain the point of connection voltage to an agreed target or operate at an agreed power factor such that voltage variations are maintained within prescribed limits. The DSOs shall be able to monitor both active and reactive power generation by the RPPs at POC point of connection [1].

The overvoltage is one of the main reasons for limiting the capacity (active power) of non-dispatchable DG, such as PV, that can be connected to a low voltage (LV) distribution system. During high PV generation and low load periods, there is a possibility of reverse power flow, and consequently voltage rise, in the LV feeder. In general, to address overvoltage issues one can:

- Reduce the secondary LV transformer voltage adjusting the tap;
- Allow the DGs to absorb reactive power
- Install auto-transformers/voltage regulators;
- Increase the conductors size, reducing line impedances
- Store the power surplus for later use
- Curtail the power of DER units.

The voltage rise due to distributed generators must not exceed +2% (MV) and +3% (LV) of the nominal system voltage [7].

2.2.1.2 Active power control

The DER system must be capable of reducing its active power output in cases of danger for a proper system operation. These cases include the following:

- Potential congestions and equipment overloading,
- Imminent danger of islanding operation,
- Endangerment for static or dynamic system stability,
- Over frequency
- Maintenance work.

Other rules used for design of connection and potential network reinforcement are [11]:

- if not available, the minimal load on the feeder is considered at 20% of the peak load.
- if not available the tan φ of the consumers on the feeder is considered to be 0.4.
- in LV, a maximum gradient of 2% of the voltage for 1 kW of additional load or generation is allowed at a given point.
- in LV, 1.5% of voltage loss is considered in the connection (between the DER and the connection point on the network).

The MV voltage planning uses the adjustability of the reference voltage at the secondary of the HV/MV transformer. It is based on the voltage profile of MV feeders connected to the same HV/MV transformer.

The majority of distribution networks bulk substation transformers are fitted with OLTC facilities and will automatically act to restore network voltage levels within minutes [1].

The MV voltage is maintained utilising the tap changers flexibility in the HV/MV substation and dynamically adapt tap position in a range usually of about [±15%] around the nominal setting.

LV voltage adjustment also uses tap changers of transformers MV/LV. The position of the tap changers can be changed manually with three settings (+0%, +2.5%, +5% against the nominal setting) [11].

In addition, Line Drop Compensation (LDC) controls may also be used to regulate the network voltage at a location downstream of the bulk substation. These controls are commonly used to regulate network voltages and maximise transfer capacity to customers.

The inverter must disconnect within 3 seconds when the average voltage for a 10 minute period exceeds the maximum nominal operating voltage [1].

2.2.2 Voltage control requirements in grid codes (Existing)

The voltage control requirements are expressed in a variety of ways in grid codes. The issues specified can include:

- The ability to receive a set point (which may be local or remote)
- Range of set points
- Droop settings
- Time to change a set point
- Transient response to step changes

The requirements in various grid codes are summarised in Table 2-4, and are discussed in further detail below.
The UK Grid Code requires continuous steady state control of voltage at the grid entry point. The controller must be capable of the following

- The slope must be adjustable over a range of 2% to 7%.
- Deviations from set point to be corrected within 5s.
- The time to implement a new set point or slope does not appear to be stated.
- The response to a step change to commence within 0.2s, with 90% of the plant capability to be produced within 1s.
- The settling time must be less than 2s, with peak to peak reactive power oscillations no more than 5% by that time.

The Irish Grid Code is similar albeit less specific. It requires a similar response to that of a synchronous generator's automatic voltage regulator. The voltage set point is at the HV side of the interface transformer, which is normally also the connection point. The slope must be adjustable over a range of 2% to 10%. A change to the voltage set point must be capable of being received automatically and of being implemented within 20s. 90% of the steady state response to a step change in set point or voltage must be achieved within 1s.

Table 2-4 Voltage control requirements

Grid Code	Reactive requirement specified at	Specified set point	Droop setting	Transient response	Set point changes	Reference
Denmark	Reactive Power Control Power Factor Control Voltage Control (> 25 MW)		Required		10s	[2]
Germany	Reactive Power Control Power Factor Control Voltage Control			Immediate	1 min	[3]
UK		95%-105%	2%-7%	90% within 1s		[4]
Ireland	Voltage regulation similar to AVR	HV side of grid transformer	1%-10%	90% within 1s	20 s	[5]

In Denmark, Germany and Spain there is provision for power factor control, reactive power control or voltage control. The German Transmission Code states only that the generator voltage control must take immediate action in the case of voltage changes. A new set point must be implemented

within 1 minute. In Denmark, set point changes must be implemented within 10s. There is provision for a droop setting. In Spain, the slope can range between 0 and 25 (MVARr p.u. / Voltage deviation p.u.); the entire response to a change must be achieved within 1 minute.

Alberta requires a continuously-variable, continuously-acting, closed loop control voltage regulation system. The set point can range from 95% to 105%, and the droop 0-10%. Reactive current compensation may be required. 95% of the response to a step change must be achieved between 0.1s to 1s after change. Québec also requires a droop setting between 0 and 10%. The Onshore Non-Synchronous Generating Unit shall provide continuous steady state control of the voltage at the Onshore Grid Entry Point with a Set point Voltage and Slope characteristic as illustrated in Figure 2-10 [4].

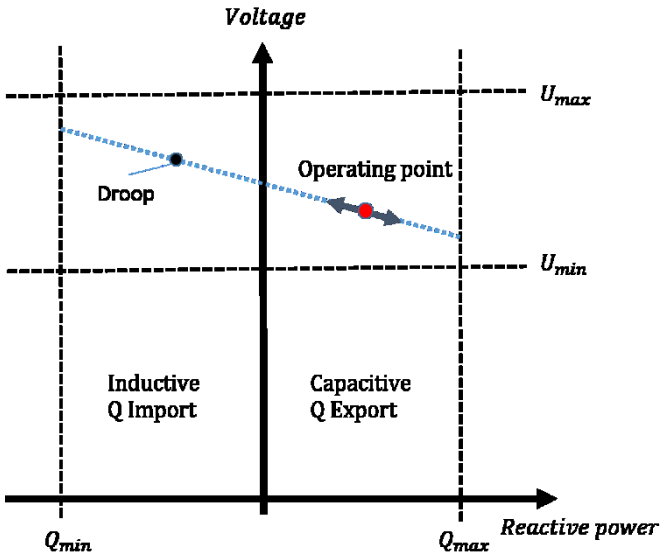

Figure 2-10 Setpoint Voltage and Slope characteristic

2.3 Influence of variation of network characteristics on AVM

A resilient active voltage management is proposed. One of the main factors that affects the Volt-var curves in a three-phase unbalanced distribution system is the system configuration, i.e., the network configuration and availability of the system controllable devices. It is quite probable that in operation of a distribution system, the system configuration is changed due to the electrical faults, scheduled maintenance, forced outages of the system components and also operation strategies. These may drastically change the critical parameters in the VVCs assigned to each inverter-based DER. Otherwise, the AVM technique may not be effective in different operating conditions and contingencies. In this chapter, the effects of the network configuration and also the availability of the system controllable devices on the proposed AVM algorithm are analysed. The impedance identification technique is used as an option to develop a resilient Volt-var optimisation scheme. The simulation studies given in this chapter show that by adaptively updating the VVCs according to the system configuration, the values of the objective functions will be improved.

2.3.1 Data Required in Simulations of AVM strategies

2.3.1.1 Network characteristics

Network configuration should be supplied as one of the main inputs in order to extract the Volt-var control scheme, i.e., the VVCs. Since the networks are usually unbalanced in low-voltage distribution systems, it is necessary to supply the three-phase diagram of the system including the transformer phasor group, load type (single- of three-phase), load connection type (delta or star), grounding type (grounded or ungrounded) as shown in **Figure 2-11**.

Line characteristics should also be provided as an important input data to the proposed decentralised AVM algorithm. Additionally, the line resistances, self-reactance of each phase and mutual reactances between different phases should be provided.

If there is any type of fixed reactive power compensators (such as capacitor banks) installed across the system network, the technical characteristics of these compensators should be provided in order to extract the VVCs.

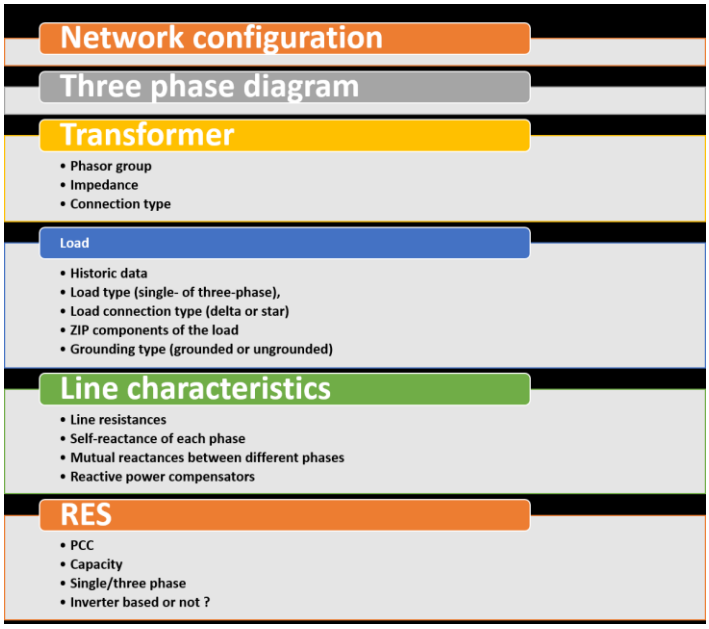

Figure 2-11 Data Required in Offline Simulations to Find the AVM strategies

2.3.1.2 Load model

The historical load levels at each load point or at least the historical data on the total load level should be supplied as well as the number of customers, load types and load connection at each load point. A change in the load levels at various load points may drastically change the voltage profile and can change the control action required as shown in **Figure 2-11**.

In LV networks, the consideration of *load to voltage sensitivity* is of utmost importance. The voltage sensitivity is an outcome of the physical infrastructure that the network embodies but it is also dependent on the generation and load composition. A bottom-up demand model [12] is used here to construct a representative demand profile of any amount of customers on an LV feeder. This model epitomizes occupancy patterns and behavioural characteristics of the customer to provide a load composition that gives an accurate representation of the devices assumed to be drawing current. Thus, this style of model has the advantage of also including the representative ZIP composition of the customer premises. More information in this regard can be found in **D3.2**. Here, it is necessary to supply the historical load to voltage sensitivity factors.

2.3.1.3 Inverter characteristics

Maximum capacity of the inverters should be declared. If there are other limitations in operation of these inverters they should also be provided. These practical limitations depend on the inverter type, e.g., solar PV inverters and battery storage inverters. These limitations should be determined to ensure the safe operation of the inverter itself and also to restrict the undesired impacts of the operation of each specific type of inverter on the power quality of the system costumers.

The inverter type (solar, battery… single- or three-phase), connection type (star or delta) and other configuration information of the system inverters should be provided as shown in **Figure 2-11**. It should be noted that some types of inverters cannot be applied to solve/mitigate some specific problems in a certain type of distribution system. **Table** 2-5 shows the objectives that can be selected to be followed according to the type of the inverters and also the network. In the active voltage management of low voltage distribution systems, the main objective depends on the system needs and also availability of the controllable devices that can effectively satisfy

such objectives. In such systems, availability of renewable energy resources and other controllable inverter-interfaced devices enables the system operator to control the load point voltages more effectively to achieve a variety range of objectives. In this project, three main objectives are considered for the active voltage management in futuristic low voltage distribution systems. These objectives are presented in **Table** 2-5.

Table 2-5 Objective menu

Code	Objective	Requirements	Three phase Network	Single phase Network
1	Voltage unbalance improvement	Single-phase inverter	✓	X
2	Loss reduction	Both Single/three-phase inverters	✓	✓
3	Improvement of voltage deviation ($V_{desired}$=1 pu.)	Both Single/three-phase inverters	✓	✓

Historical data on the energy generation of RESs should also be provided to develop the scenarios of RESs' power production. It is very important that the proposed method embodies a prognosis of the future operating conditions based on the historical data that should be provided as an important part of the impute data for the proposed AVM algorithm.

2.3.1.4 Power and voltage modes of operation for Inverter-interfaced devices

Most of controllable inverters are operated under power control mode. i.e., the value of active and reactive power injections are set by the system operator. Some other controllable inverters are operated under voltage control mode. The operation mode of each inverter should be determined in order to develop the proper voltage strategy that can be applied to each specific inverter. Moreover, under both of these operation modes, the inverter limitations should be taken into account (see **D3.3**).

The active voltage management includes different control modes for the inverter-based resources to optimise their performance depending on whether the generator is connected to the grid, or is in island mode. Therefore, they can be set to maintain the voltage (voltage control mode), the PF (power factor control mode) or the reactive power (power control mode).

In this chapter, the extracted VVCs are applied to find the optimal reactive power set-points in power control mode of operation. In the process of extracting the VVCs, an optimal voltage is found for each inverter. It should be noted that the optimal voltages can be considered as the voltage set-points in the voltage control mode of operation for these inverters. If the inverters follow these voltage set-points in the voltage control mode of operation, the results will be the same as those that are obtained in power control model of operation where the inverters are tasked with following the reactive power levels that are found using the extracted VVCs. In fact, in both control modes of operation, the inverters should try to follow the optimal voltages as accurate as possible based on the operational limitations which should be considered for each type of inverters.

2.3.1.5 Operator's goals

Different objectives can be considered for voltage control in low-voltage distribution system (**Table** 2-5), e.g., minimisation of voltage unbalance, minimisation of active power losses and minimisation of active and reactive power purchase cost. The voltage control objective should be declared by the system operator.

Selecting the proper objective function depends widely on the issues faced that the distribution system operator is faced with and also the type and capacity of controllable devices that can be controlled to achieve a specific objective. As an example, in a low voltage distribution system with only one small single phase battery inverter installed on phase *a*, there is not enough control capacity to improve the average value of the phase voltages at system three-phase load point. **Table** 2-5 gives an insight into the types of the objectives that can be considered in different circumstances.

2.3.1.6 Voltage at points of common coupling for RESs

At each connection point, the value of 3-phase voltage should be measured (before finding the optimal reactive power support of each inverter) and transferred to the local control unit (see **Figure 2-12**). For single phase controllable inverters the data on the voltage levels of other phases may be unavailable. For these inverters there is no other choice except for measuring the single-phase voltage and developing the control strategy based on this measurement.

2.3.1.7 Active and reactive power injection of the inverters

The capacity of each inverter is limited by the maximum current that the device switches can interrupt or the thermal current limit specified by the manufacturer and also by the maximum inverse bias voltage of the switches or the maximum voltage level that the device insulation can tolerate in steady state condition [13].

In the steady state studies of power systems, these limitations are usually modelled by a single constraint, i.e., the apparent power injected by this inverter cannot be higher than the maximum allowable apparent power which is always referred to as the inverter capacity. In **D3.3**, it has been discussed how to consider this limitation in AVM algorithm. There may be some other limitations that depend on the inverter type. The next subsection briefly discusses these limitations. More information can be found in **D3.3**.

2.3.1.8 Practical limitations

For some PV units, it is necessary to consider the maximum power angle (regarding minimum permissible power factor) to avoid high harmonic distortions. Such limitation imposes new upper bound for the change in the reactive power support which should be treated in the same way as the upper bound regarding the maximum capacity constraint. Fortunately, in most of low-voltage distribution systems, the harmonic limitations are not very tight. However, if there is any limitation in the operation of system inverters, these limitations should be considered in developing the voltage control strategy which determines the reactive power support of each inverter especially in futuristic distribution network with high penetration of RES.

For different systems, if there are such limitations, they should be declared to be considered in extraction of the VVCs and also in the final function which is developed for online application of the proposed VVO based on the extracted VVCs (see **Figure 2-12**).

2.3.1.9 Network impedance viewed by the inverter from the point of common coupling

In the project definition, the impedance identification technique can be considered as an option to develop a more accurate and effective VVO scheme. In this chapter a VVO framework which apply this technique to find out whether or not such technique can be applied.

In the decentralized control system, it is assumed that the local control agent has no information about the other controllable devices installed at other connection points. The main goal of measuring the system impedance at each connection point ($Z^{network}$) is to identify or approximate the characteristics of the system, e.g., system configurations and also the availability of the inverter-interfaced controllable devices installed at other connection points in this system (see **Figure 2-12**).

Usually, the small systems with one or two inverter based controllable devices have fixed configurations and therefore, the impedance identification technique [14] is not applied on these systems. Moreover, the practical requirements of applying the impedance identification technique are not yet completely available in any practical low-voltage distribution system. Therefore, in order to accomplish the items determined for Task 3.4 in this work package, this technique is implemented in this chapter where the simulations are conducted based on measuring the network impedance viewed from the connection point of the inverters to see whether or not this technique can be applied to improve the effectiveness of the proposed VVO framework developed as a part of SV_B voltage control plan. A real size distribution system will be considered to test this technique.

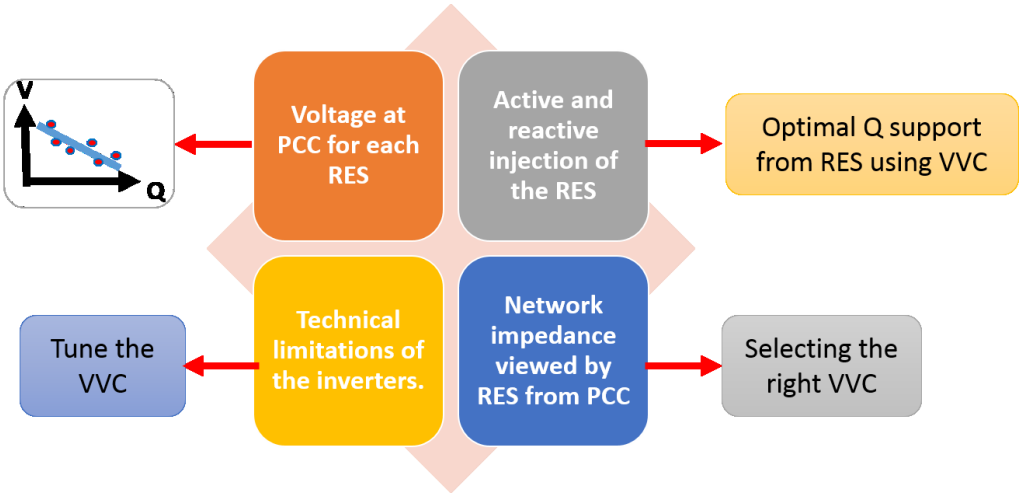

Figure 2-12 Data Requirement in Online Application

2.3.2 Resilient AVM to deal with different contingencies

The basic proposed active voltage management is a decentralized algorithm for active voltage management to maintain the steady state voltages in the presence of different inverter based RES technologies. The proposed technique controls the provision of reactive power from these units using an optimisation method.

An offline network analysis is conducted as a centralised solution which is briefly explained in this section. More details of the basic decentralised AVM algorithm can be found in **D3.3** and **D3.3**. The method of obtaining and applying the Volt-var Curves (VVCs) for voltage control is outlined below and depicted in Figure 2-13:

- Stage 1: determines the optimal voltage across all scenarios that minimises the voltage unbalance of the feeder, or other objectives of interest, considering unlimited reactive power support for all RESs.
- Stage II: determines the closest possible voltage deviation from optimal in each scenario, constraining the reactive power of the RES units to within representatively realistic bounds.
- Stage III: the voltage levels without any changes in the reactive power injections of the controllable devices, i.e., base voltages, are found.
- Stage IV: to conclude the offline-procedure the resulting reactive power set-points (Stage II) are plotted against the resulting voltage set-points (Stage III) to determine the Volt-var curves for each RES system.
- In application mode, for each inverter, the voltage is measured at PCC and the value of the change in the reactive power injection is found using the regarding VVC. The value of the final reactive power injection of this inverter is found according to its capacity and other operational constraints.

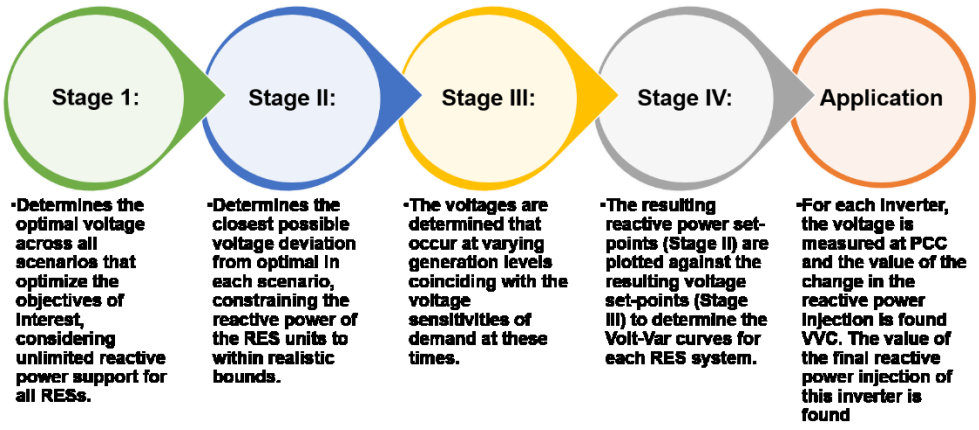

Figure 2-13 Method of obtaining and applying the VVCs for voltage control

In most of the practical applications, a simple power factor limit, e.g., power factor>0.95 lag, is still being used as the industry common engineering practice for reactive power control of the inverter based controllable devices. In this subsection, first, it has been discussed how these new operational constraints (which are mostly proposed for safe operation of RESs as well as achieving higher levels of power quality) affect the voltage controllability in low voltage distribution systems enabled with different types of controllable devices comparing to the industry common practice (power factor limitations).

The proposed AVM in **D3.2** and **D3.3** is based on the fact that all inverter-based RES units are in normal operation and the Thevenin model of the network seen from the PCC of each RES remain unchanged. As it is expected in reality, some network topology might change due to the failure of some components which alters the basic assumptions of the proposed AVM. This chapter intends to propose a Resilient Active Voltage Management (RAVM) to remain robust against possible RES failure events.

2.3.3 Impacts of network characteristics on AVM

In futuristic distribution networks, there might exist several RES technologies at different PCCs. The Thevenin equivalent of the network seen by each individual RES is different and depends on the network characteristics and also the behaviour of other RES in the network [15] as shown in **Figure 2-14**.

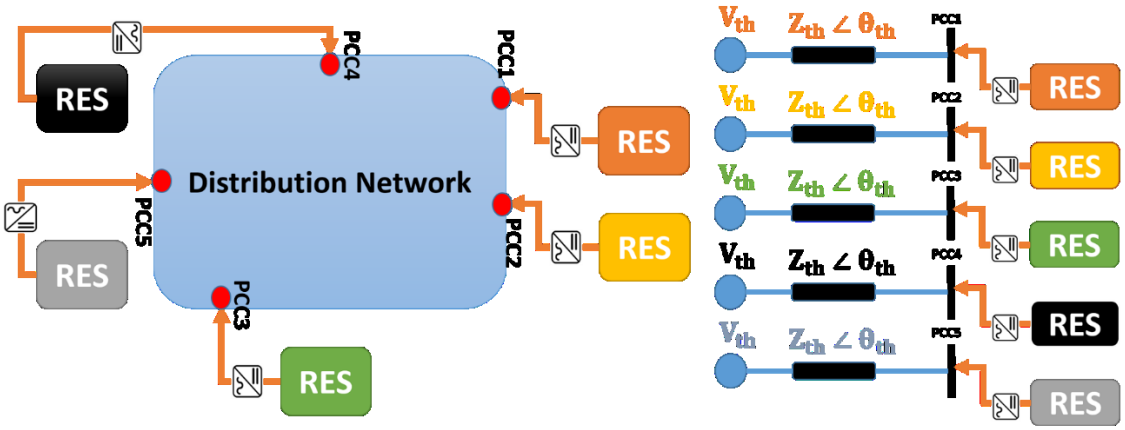

Figure 2-14 Schematic of network seen by each individual RES

The Thevenin network seen by each RES is dependent on several parameters such as those as described in **Figure 2-15**.

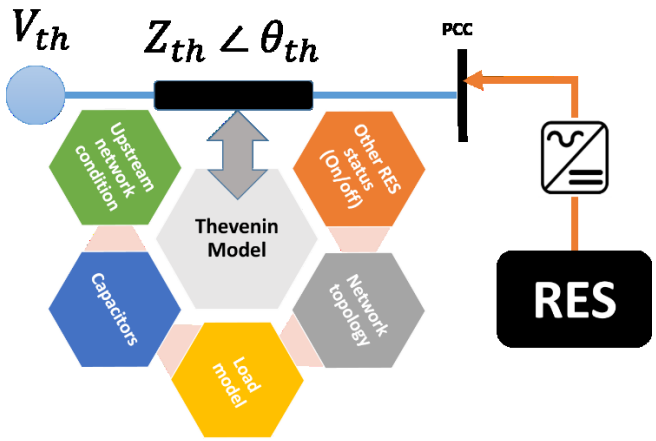

Figure 2-15 Factors influencing the Thevenin network equivalent seen by each RES from PCC

The impact of network parameters as well as the demand characteristics on VVC are already captured in operating scenarios described in **D3.2** and **D3.3**.

2.3.4 Network contingencies

The VVC of each individual RES is obtained and used for active voltage management as described in **D3.3** and **D3.5**. The idea of VVC is based on the fact that the equivalent Thevenin model of the network seen from PCC of each RES does not change. In reality, many factors might cause changing the equivalent Thevenin model seen by each RES. This will deteriorate the effectiveness of the designed AVM. The influence of the RES/inverter failure of AVM performance is shown in **Figure 2-16**.

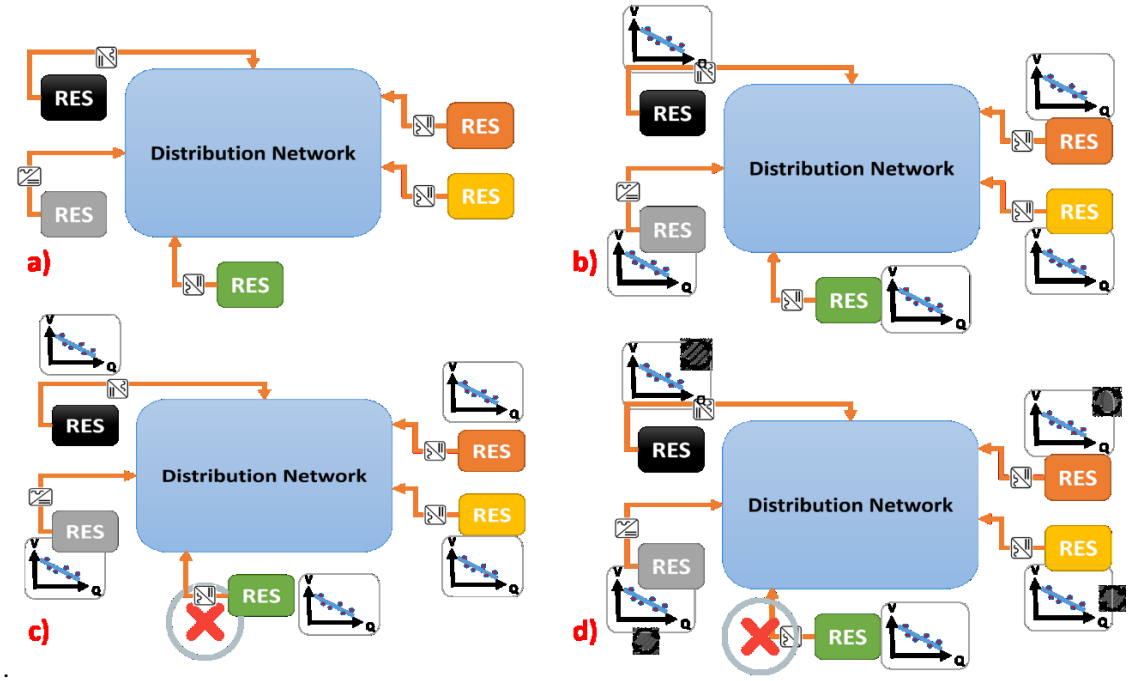

Figure 2-16 Influence of the inverter/RES failure on AVM performance

- Figure 2-16-a) Shows the futuristic distribution network with several inverter based RES connected to the grid. These technologies can be of PV, wind, storage or any inverter based energy resources.
- Figure 2-16-b) Shows the same futuristic distribution network that for each individual RES, a VVC is tuned and optimised for the selected objective function using the technique described in **D3.2**.
- Figure 2-16-c) Shows the case when there is a contingency on one of the RES units. In this case, the pre-tuned VVC may not able to provide the required performance. This is due to the fact the Thevenin parameters of each RES (see Figure 2-14) are changed and the VVC is no longer valid for the updated network topology
- Figure 2-16-d) In this case, if there is any contingency on any of the RES,
  - Initially, the contingency is identified for each RES using a local impedance identification technique (see Section **D3.5**)
  - the VVCs for the rest of them will be updated to capture the changes in the network topology.

So the DSO needs an adaptive and resilient AVM technique to remain robust against the contingencies that might happen to the inverter based RES units. The framework for VVC extraction in resilient AVM method is shown in **Figure 2-17**.

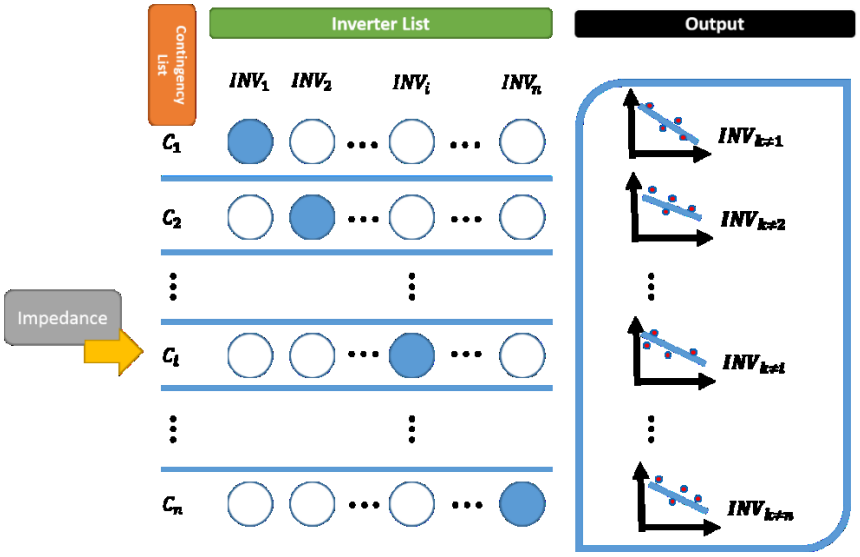

Figure 2-17 Schematic resilient VVC determination for AVM

The following assumptions are taken into account to obtain the resilient set of VVCs:

- The only contingency considered in this framework is the failure of the inverter based RES units
- Only single contingencies are captured in this framework since the probability of simultaneous contingencies with higher orders (two or more components fail at the same time is a very rare event)
- Assuming that there are 'n' RES units in the grid, the VVC extraction is repeated n times.
- At contingency row *i*, it is assumed that the inverter at RES *i* is failed and is not able to inject power to the grid. The VVCs for the rest of the units are optimised.

Once the VVCs shown in **Figure 2-17** is found then the utilization of the RAVM is straight forward. The algorithm described in Section 2, is used to find the impedance seen from PCC of each RES. This impedance can indicate that which row of **Figure 2-17** should be used for selecting the appropriate VVC.

2.4 System level AVM

2.4.1 Architecture

The effectiveness of the voltage control strategy widely depends on the accuracy of the system model which is used to extract such a strategy in the online applications. As decentralized approaches rely only on local measurements for system identification, the effectiveness of the control strategy may be compromised. On the other hand, centralized approaches suffer delay issues, low speed, communication errors due to contamination of measurement and command signals in communication channels, lack of enough measurements and some other issues.

The round-trip time of a complete cycle from the inverter to the point of calculation and back is important. The quicker the measurement and the required change can be communicated the more accurate and effective the control action. A longer delay between the instance of measuring the voltage level at PCC and the time of applying the new setting of reactive power injection for inverters of the controllable devices leads to less effective results. The delay includes both the measurement and the actuation delays that widely exist in real systems. For a centralized control system, this delay is higher which reduces the effectiveness of the control actions. In a decentralized control, this delay is lower. However, even a small reduction in this time delay can be a great help.

In this section, the structure of a hierarchical active voltage management algorithm is defined, where the decentralized (local) controllers try to solve the voltage problems and the higher level (system level) control keeps the local system identification results as accurate as possible. Under such a setup, the control strategies are quickly extracted by the local control systems to meet the real-time requirements of active voltage management in the current low voltage distribution

systems and the system model applied in the local control systems is kept up-to-date by the system level control to mitigate the potential errors. Using the proposed method developed in **D3.4**, the parameters of the local AVM algorithm can be updated according to the network configuration and also the availability of the inverter-based controllable devices.

In **D3.2** and **D3.3**, the proposed local active voltage management algorithm was discussed. The focus was on the application of Volt-var Curves (VVCs) for determining the reactive power supports of the inverter-based controllable devices in an unbalanced low voltage distribution system. After application of VVCs and finding the new settings of each inverter, it is quite possible that more corrections are required according to the new set of PCC voltages. A supervised closed-loop control is proposed here to achieve a near optimal reactive power dispatch between the system controllable devices for better voltage control. Regarding this supervised control, the other task of the system level control is to initiate the control process to reach a balanced state.

This chapter also tackles another important subject. Considering the high penetration level of the RES in LV distribution systems, there may be some opportunities to control the load point voltages more effectively using these high control capacities. In this chapter, a framework is developed to consider different objectives at the same time in the proposed method for AVM. This leads to the exploitation of the system control capacity. The voltage control objective(s) should be determined by the system level control according to the system needs and control capacity.

2.4.2 Local Measurements

The data requirements for local (decentralized) control were discussed in **D3.4**. Here we summarize these data in the following list, then the data requirements for system level control will be explained.

The Data required for decentralized AVM algorithm is described as follows:

- Network configuration (the three phase diagram)
- Line characteristics
- Fixed reactive power compensators
- The historical load levels and load model parameters (ZIP coefficients) at each load point.
- Maximum capacity of the inverters
- Inverter type, connection type (star or delta).
- Historical data on the energy generation of RESs.
- Inverter mode of operation (Power control mode or voltage control mode)
- Operator Objectives such as minimisation of voltage deviation from a desirable value, minimisation of voltage unbalance, minimisation of active power losses and so on.
- Inverter impedance as a function of frequency (viewed at the connection point of each inverter).
- Voltage at inverter connection point
- Active and reactive power injection of the inverters before developing the voltage control strategy.
- Additional limitations of the inverters, such as maximum power angle (regarding minimum permissible power factor).
- Network impedance viewed by the inverter from the connection point.

In this chapter, a supervised decentralized control approach will be discussed. In the unsupervised decentralized approach presented in **D3.2**, **D3.3** and **D3.4**, first the voltages are measured at PCCs. Based on these voltages and using VCCs, the value of the change in the reactive power support of all inverters will be determined. However, for two reasons the final voltage set at PCCs may not match the optimal voltages or target voltage set. The first reason is that the operational constraints of the inverters for each type of control devices (see **D3.3**) may restrict the voltage control capability of the set of inverter-based controllable devices installed across the network. The second reason is that the VVCs are obtained using a linear regression technique which gives an approximately optimal reactive power setting. There would be some unpredicted states for which the final voltages (after applying the new control settings) would never match the target voltages.

A supervised control is able to solve the problem while keeping the decentralized structure of the decentralized control system. This supervised control framework benefits the advantages of both centralized and decentralized control systems. In this sub-section, the data that should be passed from the local control system to the central control unit and vice versa will be discussed. The next sub-section discusses this supervised closed-loop AVM algorithm.

The data which should be communicated from the central control unit to each local control system are listed below:

- Network configuration
- Availability of the system controllable devices
- The objectives that the local control should seek
- Control commands (when a balanced state has not yet been reached)

Regarding the objectives that may be considered by the DSO, a discussion will be provided later in this chapter. The main important change concerning **D3.3**, is that in this section, the basic foundations of the multi-objective active voltage management algorithm is developed to better exploit the control capacity available in the system. In this way, the operator's objectives are better satisfied in improving the service quality.

It should be noted that according to the framework provided in **D3.4**, the local control system of each RES is able to approximate the network configuration and also deduce the availability of the controllable devices by tracking the system impedance viewed from the regarding PCC. This fast local system identification approach enables the local control system to make the decision based on the last updated characteristics of the system. However, in the case that the data provided by the local system identification unit is not accurate enough, the network configuration and also the availability of the system controllable devices will be communicated from the central control unit to the local control systems.

The data which should be communicated from each local control system to the central control unit are listed below:

- Target voltage
- Upper and lower bounds on the reactive power support that can be provide by this controllable device (according to operational constraints of the regarding converter)
- Last measured voltage at PCC
- Current reactive power injection at PCC

2.4.3 Monitoring and Decentralized AVM

In the future low voltage grids, with multiple inverter-based sources connected, voltage regulation may become a critical task. The potential exists for inverter interfaced sources to be deployed to regulate the voltage at the point of common coupling (PCC) of each inverter-based controllable device. The PCC voltage regulation is attainable with inverter interfaced sources by dynamically controlling the amount of reactive power injected into the power distribution grid by individual systems.

In **D3.2, D3.3,** and **D3.4** a framework was developed for local voltage management based on the local measurements and Volt-var curves. This framework proposed a static voltage control in which the reactive power injections of the controllable devices were found to achieve a certain objective. The performance of the proposed decentralized voltage control in improving the operator objectives was proven in D3.3. However, after applying this framework it is quite possible that further corrections are required since a balanced state may not be reached. In this section, a closed-loop control is proposed to deal with this issue. This control structure dynamically controls the voltage at PCC of the system inverter based controllable devices.

2.4.4 Supervised System Level Voltage Management

In **D3.4**, the plant models of the PCC voltage controller of the inverter-based devices were derived considering both reactance and resistance of the network to which these devices are connected. Different inverter-based controllable devices, i.e., PV, V2G, battery and any other types of controllable systems were evaluated to identify a suitable compensator for the open-loop PCC voltage controller to regulate the PCC voltage at a given reference voltage in the voltage control mode of operation or to find the reactive power compensator of the controllable devices. Simulation studies in **D3.2**, **D3.3**, **D3.4** and experimental verification reported in **D5.2** confirm that the theoretical approach taken to derive the control plant model of the PCC voltage controller is effective and the procedure that is followed to design the controller is robust. The control design procedures illustrated in the current research leads to a PCC voltage control system with acceptable dynamic and steady-state performance.

In this chapter, a supervised closed-loop controller is proposed to regulate the PCC voltage of the inverter-based RES systems that is connected to a single-phase or three-phase power distribution

feeder (with a relatively high R to X ratio for the impedance seen from the PCC of each controllable inverter).

Based on the simulations conducted in **D3.2** to **D3.4**, the proposed voltage control technique based on VVCs is able to improve the system operation and to better satisfy the DSO's objectives. However, after application of VCCs to find the new reactive power injections of the controllable devices, it is quite possible that we do not achieve the optimal voltages. In order to elaborate on the sides of the issue, it should be noted that though by applying the VVCs for optimisation of the reactive power dispatch, the performance metrics will be improved (compared to the fixed power factor assumption and uncontrolled dispatch), the results are not globally optimal. Actually, the globally optimal results cannot be achieved using any decentralized control system. Therefore, the results of the proposed AVM algorithm can be further improved by a new round of applying the VVCs for obtaining the new reactive power setting for the system controllable devices, based on the new voltages achieved after applying the results of the previous round of voltage control based the proposed local AVM algorithm. In other words, after first round of applying the VVCs to find the optimal reactive power injection of all inverters, the set of voltage measurements will be updated. It is quite possible that according to these new voltage levels, further corrections are required.

Each inverter can start a new round of voltage control based on the available voltage measurement and the regarding VVC. However, it is possible that without a proper supervision, such actions lead to the fluctuation of the reactive power settings of the system controllable devices. In case of weak networks, this may even lead to an uncontrolled situation which would never converge to a stable situation. This indicates the need of applying a supervised closed loop voltage control based on the prosed local active voltage management using the VVCs extracted in the offline **system level** studies.

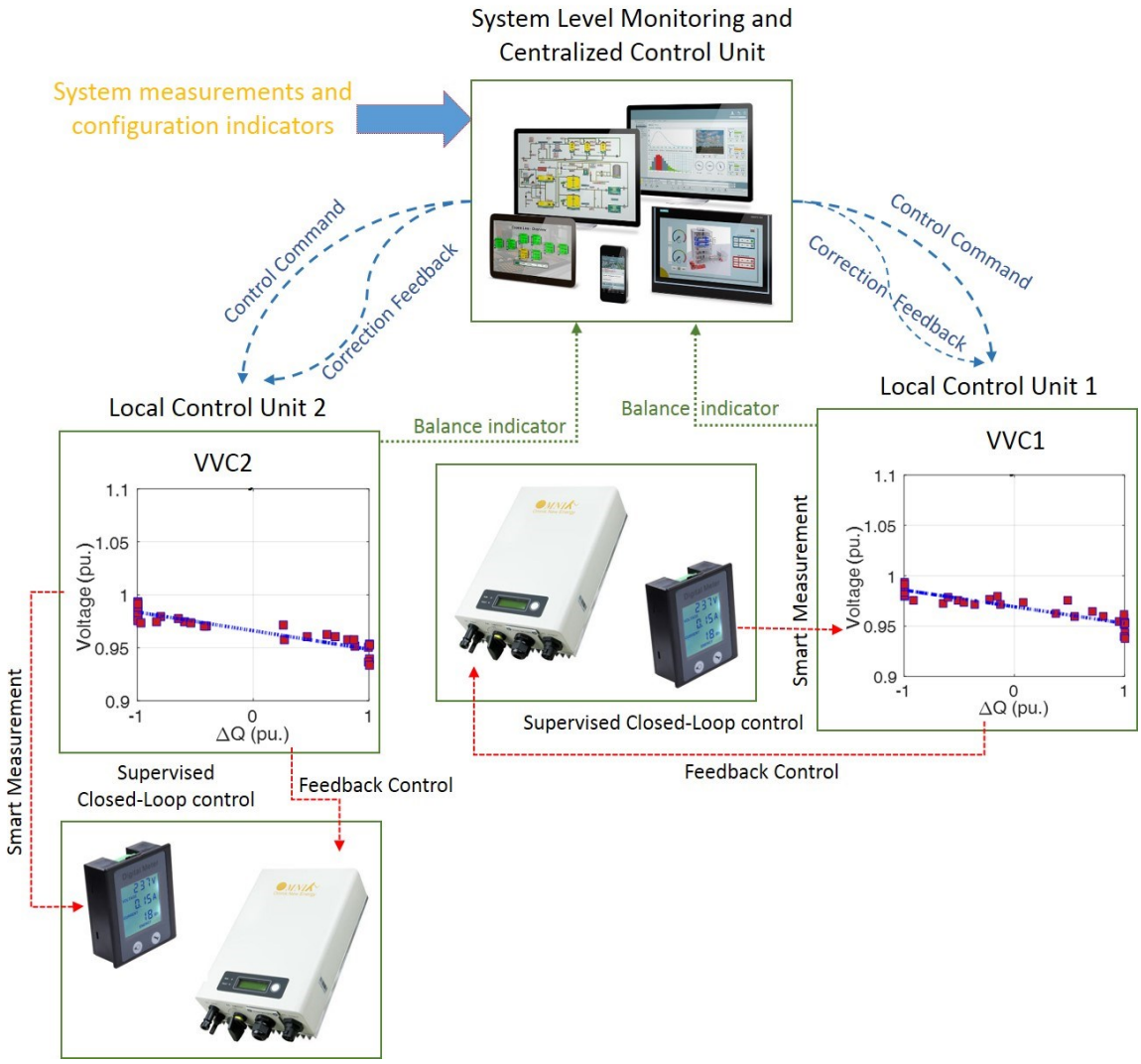

Figure 2-18 Proposed structure for supervised AVM algorithm

The balance points of each VCC are, $Q=Q^{max}$, $Q=Q^{min}$ and of course $V=c$ which is approximately equal to the target voltage of the regarding inverter. This indicates that after a successful application of the VVCs for the active voltage management in a low voltage distribution system, the reactive power or voltage settings at the PCC of **all** inverter-based controllable devices should be set at one of these balance points, signifying the fact that the required reactive power support is optimally dispatched between the system controllable devices to achieve a predefined system level objective or there is no other way to further optimise these settings due to the practical limitations on the reactive power supports that can be provided by each inverter, e.g., capacity limit. More discussions regarding these practical limitations that depend on the type of controllable devices under study can be found in **D3.3** and also **D3.8**.

Based on this discussion, the remaining part of this subsection is dedicated to provide a summary of the proposed supervised closed-loop decentralized active voltage management algorithm. Figure 2-18 presents a schematic diagram of the proposed supervised AVM algorithm.

2.4.4.1 Local control system

1) System identification:

1-1) Identify the network topology and controllers' availability according to the impedance measured at the PCC of the regarding inverter periodically (see **D3.4**).

1-2) Keep the identified model up-to-date.

1-3) Verify the identified model according to the data received from the system level central control unit.

2) Real-time control:

2-1) Wait for the control command from central control unit or initiate a new periodical round of voltage control

2-2) Measure the voltage at PCC when a new control command is received or at the instance of the periodical control routine.

2-3) Use the proper VCC according to the system characteristics identified in steps 1-3 and also the objective that is dictated by the central control unit to be followed. As discussed in D3.3, if some of the inverters are working under voltage control mode of operation, they should be tasked with following their target voltages (which also depend on the network configuration, availability of the other inverters and more importantly the system level objective for active voltage management).

2-4) Communicate the balance state to the central control unit. In this stage, the reactive power injection, new voltage level, minimum and maximum allowable reactive power injection and target voltage are communicated.

2.4.4.2 Central control unit

1) System level analysis

1-1) Identify the network configuration and availability of the controllable devices.

1-2) Decide on the system level objective to be followed by the local control systems.

2) Real-time control

2-1) Analyse the data received from the local control systems.

2-2) Initiate the new control command if a balanced point has not been reached yet.

Stop sending the control commands if the control settings of the controllable devices are not significantly changed for two consecutive control rounds or the average distance of the PCC voltages from the target voltages is increasing (to avoid fluctuation of the PCC voltages around the target voltages).

2.4.5 How to coordinate decentralized controllers

The low voltage distribution system which is used here to showcase the supervised closed-loop AVM technique, and extract the VVCs for a set of inverter-based controllable devices in a multi-objective framework, is a radial LV feeder with 85 nodes situated in Ireland which was also used in **D3.3**. The required input data can be found [16]–[19]. Similar to **D3.3**, in this chapter, it is assumed that at the head of the feeder in the multi-scenario case, a separate feeder connection off the transformer supplies further 85 customers. This system was fully introduced in **D3.3**. In this chapter, it is assumed that the controllable devices are 9 V2G systems installed at different locations across this network. The batteries of Electric Vehicles (EVs) have a considerable potential not only to provide energy for the locomotion of EVs, but also to dynamically interact with the low voltage electricity grids.

Similar to **D3.3**, it has been assumed that these inverters have the bidirectional reactive power exchange capability, but the active power can only be absorbed by these inverters. Some computer simulations were conducted in **D3.3** and the VVCs were obtained for this test system.

Figure 2-19 (a) and (b) show the target voltages for minimisation of the voltage unbalance and loss minimisation, respectively. For the sake of brevity, only the target voltages are depicted. The slopes of the VVCs can be found in **D3.3** for both objectives. As can be seen, the target voltages are higher considering minimisation of the voltage unbalances as the objective comparing to the target voltages found for loss minimisation. The reason lies under the fact that with the lower voltages the active and reactive demands are lower at different load points due to the voltage-dependent nature of the system loads. These lower demands cause lower line currents which in turn lead to lower power loss.

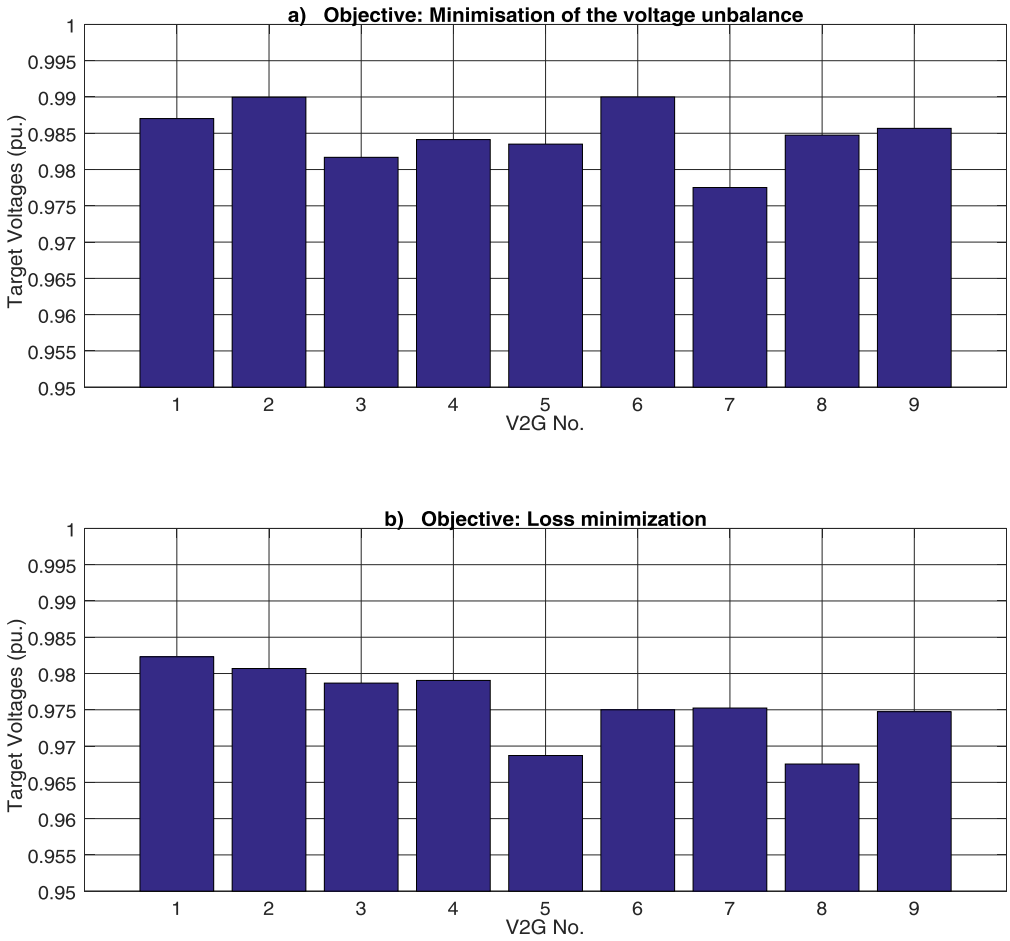

Figure 2-19 target voltages with minimisation of the voltage unbalance (a) and loss minimisation (b) as the system level objectives

In this sub-section, the performance of the proposed supervised AVM algorithm is analysed. As proposed in subsection 2.4.4, the central control system sends control commands and receives the balance status of the local control systems. This central control unit stops sending the control commands if the control settings of the controllable devices are not significantly changed for two consecutive control rounds or the average distance of the PCC voltages from the target voltages begin to increase. This helps to avoid fluctuation of the PCC voltages around the target voltages. Here, this control structure is applied and the average voltage deviation (AVD) from the target voltages is monitored to analyse the efficiency of the proposed voltage control algorithm. Further information regarding this algorithm can be found in subsection 2.4.4.

To calculate the value of AVD after each round of control, a three-phase power flow is first conducted to find the voltage at PCC of each inverter i (V_i) after applying the reactive power setting, proposed by the VVC of this inverter. The distance between the target voltage and the new voltage level of this inverter (V_i^{opt}-V_i) is then calculated. The mean square error of the voltages at all PCCs is considered as AVD. This index is monitored in two studies (for minimisation of the voltages unbalance and loss minimisation as the system objectives) until one of the stopping criteria is met.

For the most probable operation scenario in the operation of the sample system of this subsection (see D3.3), the proposed centralized closed-loop local active voltage management is applied to find the optimal setting of the V2G systems. The actual operational constraints are considered to limit the reactive power support that can be provided by each V2G system (see **D3.3**). The AVD is depicted in **Figure** 2-20 and **Figure** 2-21 for consecutive rounds of control for minimisation of the voltage unbalance and loss minimisation, respectively. For the first study, the central control system stops sending the control command after 5 rounds of control since after the fifth round of applying VVCs the begins to increase. After applying the final reactive power control strategies the voltage of no inverter matches the regarding target voltage and 4 inverters are supplying the

maximum allowable reactive power due to their regarding operational limitations. In the second study, the central control unit stops sending control commands after 4 iterations since all the inverters reach a balanced condition (see subsection 2.4.4), i.e., one of the PCC voltages reaches the regarding target voltage, 4 inverters cannot provide any power support due to operational constraints and their active power consumption levels and other inverters are absorbing the maximum reactive power possible (due to their operational constraints) to reduce the value of the AVD. As can be seen, the value of AVD indexed is improved for both cases, signifying the efficiency of the proposed supervised closed-loop AVM algorithm.

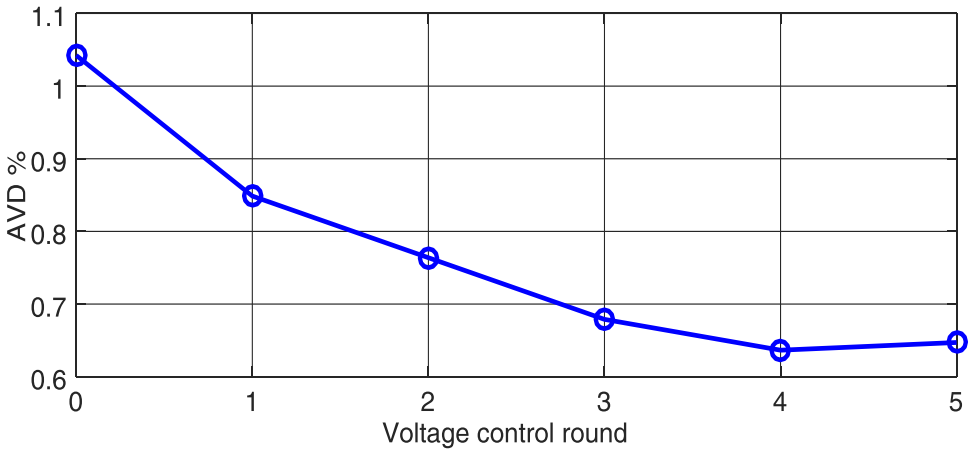

Figure 2-20 Average voltage deviation from the target voltages in consecutive rounds of control, objective: minimisation of the voltage unbalance.

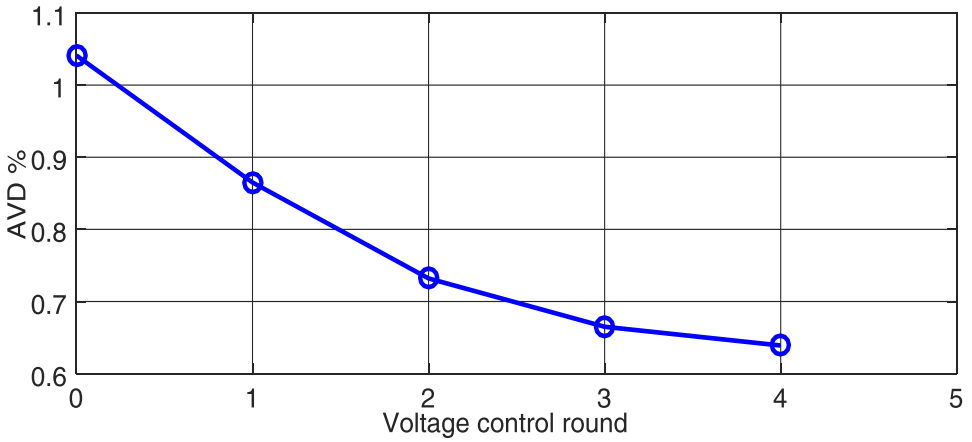

Figure 2-21 Average voltage deviation from the target voltages in consecutive rounds of control, objective: loss minimisation.

2.4.6 Multi-agent active voltage management

In the active voltage management of low voltage distribution systems, the main objective depends on the system needs and also the availability of the controllable devices that can effectively satisfy such objectives. In these systems, the availability of DERs and other controllable inverter-interfaced devices, enable the system operator to control the load point voltages more effectively to achieve a variety of objectives. In this project, three main objectives are considered for the active voltage management in futuristic low voltage distribution systems. These objectives are presented in Table 2-6.

Table 2-6 Objective menu

Code	Objective
1	Voltage unbalance improvement
2	Loss reduction
3	Improvement of voltage deviation ($V_{desired}$=1 pu.)
4	Multi-objective AVM

This section extends the existing AVM methodology presented in **D3.2**. The objectives of the active voltage management depend on the system needs and also the availability of the controllable devices that can effectively satisfy such objectives. In a low voltage distribution network with high penetration of RES and other controllable inverter-interfaced devices, there may be some opportunities to control the load point voltages more effectively using these high control capacity. Here, it has been tried to develop a framework to consider different objectives at the same time in the proposed method for active voltage management. Sometimes these objectives are incomparable and even opposing. Thus, the application of an efficient multi-criteria decision-making technique is proposed. A multi-objective active voltage management is developed to extend the works accomplished in **D3.2**. The proposed multi-objective framework considers needs and priorities of the distribution system operator and satisfies these objectives simultaneously.

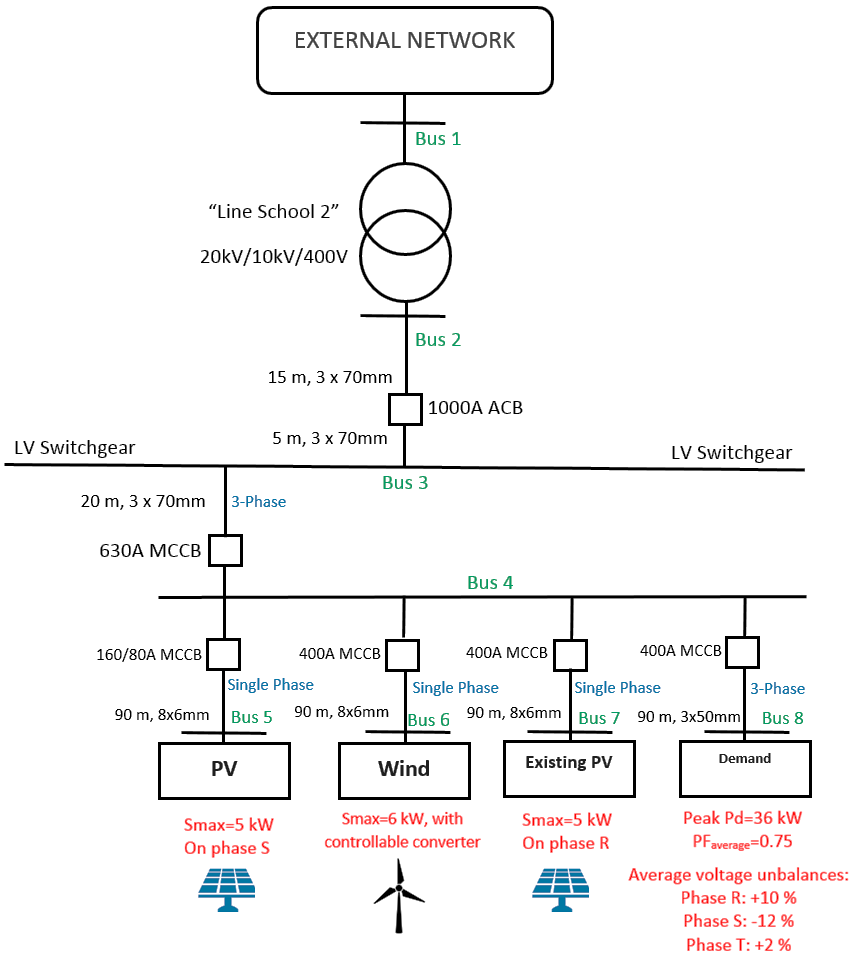

Figure 2-22 Simple low voltage distribution system for analysing the effects of various objectives on each other

A very simple example is considered here to explain how the available reactive power support capacity in low voltage networks can be exploited to satisfy more than only one objective. This simple low voltage distribution system is presented in **Figure** 2-22. This is a simplified system based on a real system in Portlaoise, Ireland. Useful data are also presented in this figure. Let's focus on the single scenario to be able to present the voltage profiles in different studies. **Table** 2-7 presents the active and reactive demands on different phases, ZIP load characteristics (see deliverable **D3.2**, **Section 3.2**), active power production of each PV and active production of wind turbine, in this scenario.

Table 2-7 Single scenario data for the simple example presented in Figure 2-22

Active power demand at bus 8 (kW), phase R/T/S	9.55/7.22/8.65
Reactive power demand at bus 8 (kVAR), phase R/T/S	4.63/3.50/4.19
Load factor at bus 8	70%
Load Z coefficient at bus 8	0.4
Load I coefficient at bus 8	0.2
Load P coefficient at bus 8	0.4
Active power production of new PV (kW)	0
Active power production of existing PV (kW)	0
Active power production of wind turbine (kW)	0

In this simple example, the optimal voltages have been obtained considering the voltage unbalance minimisation as the only objective. In order to analyse the effectiveness of the proposed method for optimising the voltage unbalance in the first scenario (Table 2-7), the voltages of all three phases have been depicted in **Figure** 2-23. These voltages are also depicted in **Figure** 2-24 considering, with the fixed power factor criterion for the operation of all inverters of the available RESs. As can be seen, the proposed algorithm has effectively reduced the voltage unbalance at the load point, i.e., bus 8 of this small low voltage distribution system. The optimal value of voltage unbalance in this scenario is 0. The value of voltage unbalance for common industry practice, i.e., Power Factor (*PF*)=0.95 is 0.35%.

However, as can be seen, as a result of applying the optimal set-points (reactive power injected by the system inverters) found considering voltage unbalance minimisation as the objective of the active voltage management algorithm, the average voltage deviation of three phases has increased, i.e., the voltages at load point are more deviated from 1 pu., which is not desirable. Quantitative results show that, with this objective, the voltage deviation is 2.4 for optimal control plan. For the fixed power factor strategy (*PF*=0.95), the value of total voltage deviation is 2.2%. The load level is not very high in this scenario. With higher load levels, this problem is more severe due to higher values of the voltage drop across the network lines.

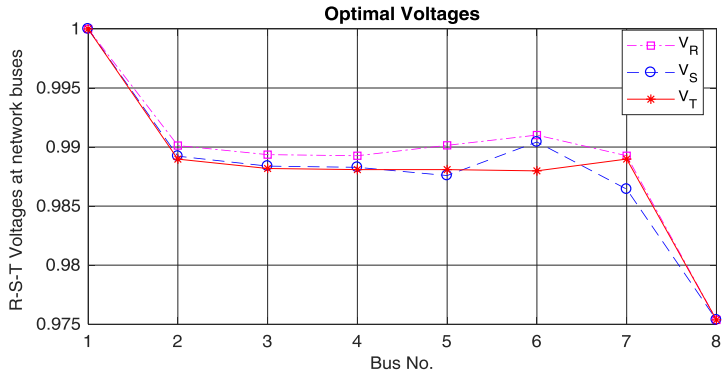

Figure 2-23 Optimal voltage levels at system buses, single-objective (minimisation of voltage unbalance).

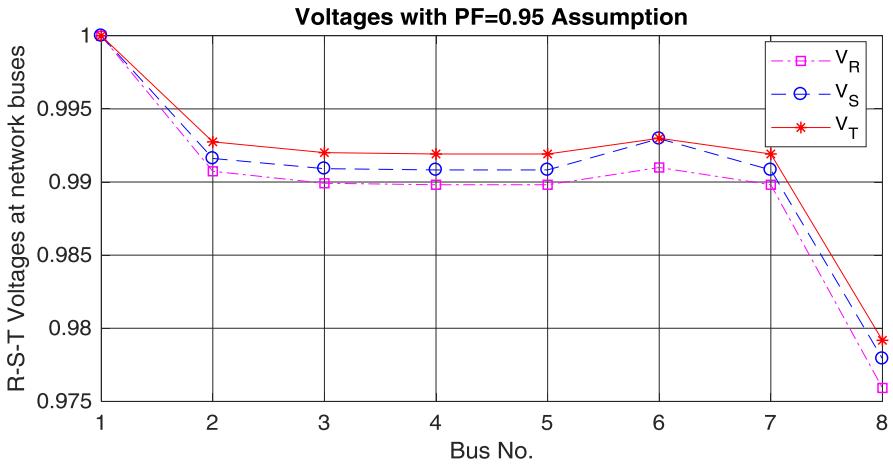

Figure 2-24 Voltage levels at system buses, fixed power factor criterion for reactive power support (PF=0.95).

In a separate study, the objective is changed to minimisation of the voltage deviations from 1 pu. **Figure** 2-25 shows the voltage profiles for each phase at the load point (bus 8 in Figure 2-22). Comparing this figure to the voltage levels presented in Figure 2-23 and Figure 2-24, it is obvious that the voltage deviation has been improved. The value of voltage deviation is 1.4% in this study. However, with the optimal reactive power control plan extracted in this study, the voltage unbalance is about 0.38% which is even higher than the voltage unbalance associated to the fixed power factor strategy (*PF*=0.95).

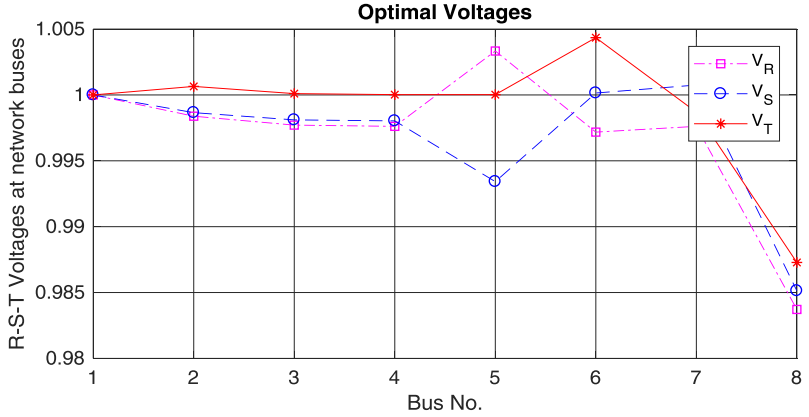

Figure 2-25 Optimal voltage levels at system buses, single-objective (minimisation of average voltage deviation).

Looking at the results obtained for this simple example, one can say that with this high control capacity (three controllable RESs), there may be some opportunities to control the load point voltages more effectively. Here, it has been tried to develop a framework to consider both objectives at the same time in the proposed method for active voltage management. Looking at these objectives, it is obvious that they are incomparable and may be opposing. This indicates the fact that the regarding objective functions cannot be summed up to give a single objective function. Therefore, the application of an effective multi-criteria decision making (MCDM) method is inevitable. This method should be able to compare the values of these objective functions for a proposed decision.

Here, fuzzy multi-objective decision making (FMODM) method is applied [20]-[21]. This method is briefly introduced here. A more detailed discussion is provided in **D3.5**. FMODM belongs to a wide category of the MCDM approaches which are called outranking methods. In contrast to the other methods, the outranking methods have the characteristic of allowing incomparability between alternatives. This characteristic is important in situations where some alternatives cannot be compared for one or another reason.

As explained in **D3.5**, in the fuzzy domain, the degree of satisfaction of each objective is specified by a value between 0 and 1 (signifying the worst and best possible objective function values). In this method, firstly, the best and worst values of each objective function should be found. A single-objective optimisation was conducted to find the optimal set-points of the network inverters to find the best value of each objective function. In order to find the worst value of this objective function, the value of this objective function is calculated without applying any reactive power support.

According to the proposed multi-objective framework and the single objective studies on this simple low voltage distribution system, the best and worst values of the first objective function (voltage unbalance) is 0 and 0.35%, respectively. The best and worst values of the second objective function are also 1.4 and 2.2%, respectively. The membership functions of the first and second objectives are presented in **Figure** 2-26. As can be seen, the degree of satisfaction of the first and second objectives increases monotonically as the value of each objective function decreases from Obj^{max} to Obj^{min}.

For each solution vector (including the value of the reactive power injection of all inverters). The values of these objective functions, i.e., voltage unbalance and voltage deviation objective functions, are calculated according to the explanations provided in deliverable **D3.2**. The values of membership functions of voltage unbalance and voltage deviation problems ($\mu_1(X)$ and $\mu_2(X)$) are found next using the membership function provided in **Figure** 2-26.

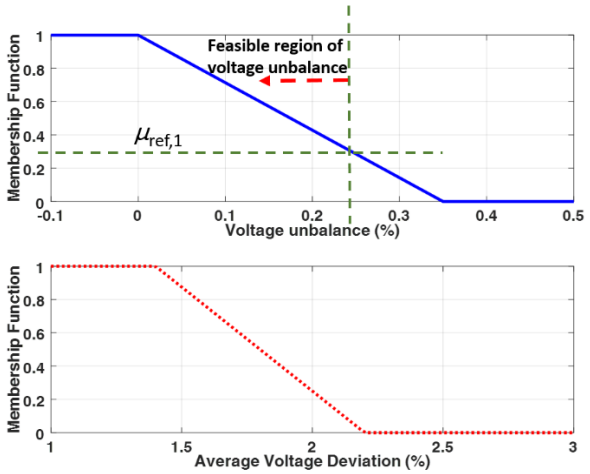

Figure 2-26 Membership functions of the problem objectives (minimisation of voltage unbalance and minimisation of average voltage deviation).

The final fitness function is provided in **(3.18)**. The optimisation tries to maximize this fitness function.

$$\max_{X}\left\{\mu_1(X)+\mu_2(X)-p_1(X)-p_2(X)\right\} \qquad \textbf{(3.18)}$$

$$p_i(X) = \begin{cases} W.(\mu_{\text{ref},i}(X) - \mu_i(X)) & \mu_{\text{ref},i}(X) > \mu_i(X) \\ 0 & \text{otherwise} \end{cases} \quad \textbf{(3.19)}$$

To define a more controllable significance level for these objectives, after extracting these membership functions, the decision-maker is asked to specify the minimum achievement degree of each membership function, i.e., reference membership function μ_{ref}, which takes the real values between 0 and 1. Higher values of this parameter show more importance, and hence give more weight to the regarding objective. In this system, in order to give the same importance level to both objectives (minimisation of voltage unbalance and minimisation of average voltage deviation), μ_{ref} is assumed to be 0.4 for both objectives. The value of reference membership function introduces a constraint on the value of each objective function as depicted in **Figure** 2-26 for the first objective (minimisation of voltage unbalance). The optimisation algorithm tries to satisfy these minimum allowable membership function constraints as the soft optimisation constraints by forming a penalty function, i.e., p_i in equation **(3.19)**, for each constraint and appending this constraint to the objective function using a big *M* constant. The value of both *M* constants is assumed to be 100 signifying a constraint violation tolerant of 0.02 (see **D3.5**).

Using this membership functions and applying the multi-objective fuzzy optimisation technique, a solution is achieved that satisfies both objectives as much as possible. The three-phase voltage levels at all network buses are depicted in **Figure** 2-27. As can be seen, both voltage unbalance and voltage deviation have been improved simultaneously compared to the results presented in **Figure** 2-24 for the system with fixed power factor strategy (PF=0.95) for reactive power support. The values of these objective functions are 0.22% and 1.67%, respectively.

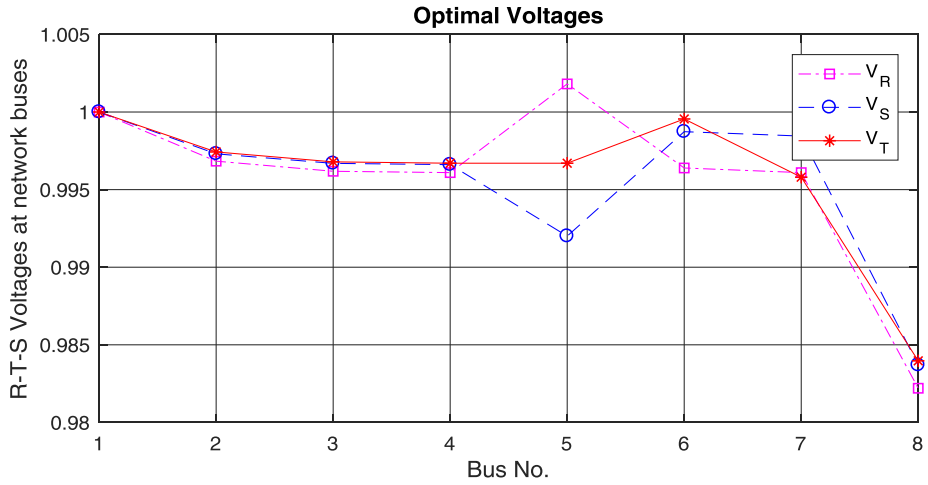

Figure 2-27 Optimal voltage levels at system buses, multi-objective (simultaneous minimisation of voltage unbalance and average voltage deviation).

For a week-long period, the active and reactive demands and other required data have been extracted for this system. These data can be found in **D3.3**. VVCs are extracted for the multi-objective case where two important objectives from the system operator's point of view, i.e., voltage unbalance minimisation as the first objective and active power loss minimisation as the second objective are considered to be improved simultaneously. This framework enables the system operator to consider any different (and probably opposing objectives) simultaneously.

The potential of incorporating V2G systems, i.e., the batteries of EVs and inverters of the charging stations (with bidirectional reactive power exchange capability) is investigated in the low voltage distribution network introduced in this subsection. As mentioned before, it has been assumed that the system operator is interested in simultaneous minimisation of the voltage unbalance at all the load points and energy loss to increase the power quality of the low voltage consumers connected to this test system and to reduce the system cost, respectively.

As explained in **D3.3**, in the first step the optimal voltage levels should be found for all V2G inverters. These voltages are referred to as the target voltages and in this subsection, the inverters should follow these voltages to simultaneously minimise the voltage unbalance index and power loss. The second stage in the offline calculations determines the optimal reactive

power injections of V2G systems in each scenario that lead to the closest voltage levels to those obtained for V2G inverters in the first stage. The second stage in the offline calculations considers the capacity constraint as the only limitation on the operation of the V2G systems connected to this sample system. In order to analyse the effectiveness of the proposed voltage management algorithm, the actual limitations of these systems are taken into account when these VVCs are applied to find the reactive power injection of each inverter in the online studies.

In Stage 3, the voltages of all inverters are found in each scenario considering no reactive power injection for the network inverters. The VVCs are extracted by applying a linear regression technique on all the (voltage)-(reactive power injection) pairs found in the third and second stages, respectively. For more discussion see **D3.2** and **D3.3**.

2.5 Volt-var curve based reactive power control (proposed)

The active voltage management of LV distribution network can use different flexibilities such as capacitor switching [22], demand response [23] and reactive power management of inverter based DERs [24]. The idea of using Volt-var capability of inverter-based RES was described in **D3.2.** The Volt-var curve active voltage management (AVM) concept is successfully put to trial in **WP5**.

2.5.1 Active voltage management

The AVM technique is a decentralised approach to voltage control for maintaining steady state voltage in the presence of RES. The technique capitalises on the inverter-based RES units by engaging with the provision of reactive power from these units.
The AVM technique consists of a multi-scenario three-phase AC OPF analysis of RES connections on LV feeders. An offline network analysis takes place, which is a centralised solution that determines:

- an optimal voltage set-point for each point of RES connection
- the range of expected voltages anticipated at the point of connection
- the spread of reactive power set-points that would render the RES connection capable of achieving the voltage target
- objective governed Volt-var curves for online decentral deployment

The output of this **offline** network analysis is a prescribed Volt-var curve per RES connection determined while fulfilling a single objective of the network operator. The procedure can be repeated to satisfy any objective of the DSO that can be formulated within feasible conditions of an AC OPF. In the field, and in further time-series simulation, these Volt-var curves dictate the voltage control at each point of connection of a RES by utilising the inverter capabilities. The only required input for corrective action to take place is the voltage magnitude measurement local to the RES unit. The input-output procedure of Volt-var curves is depicted in Figure 2-28.

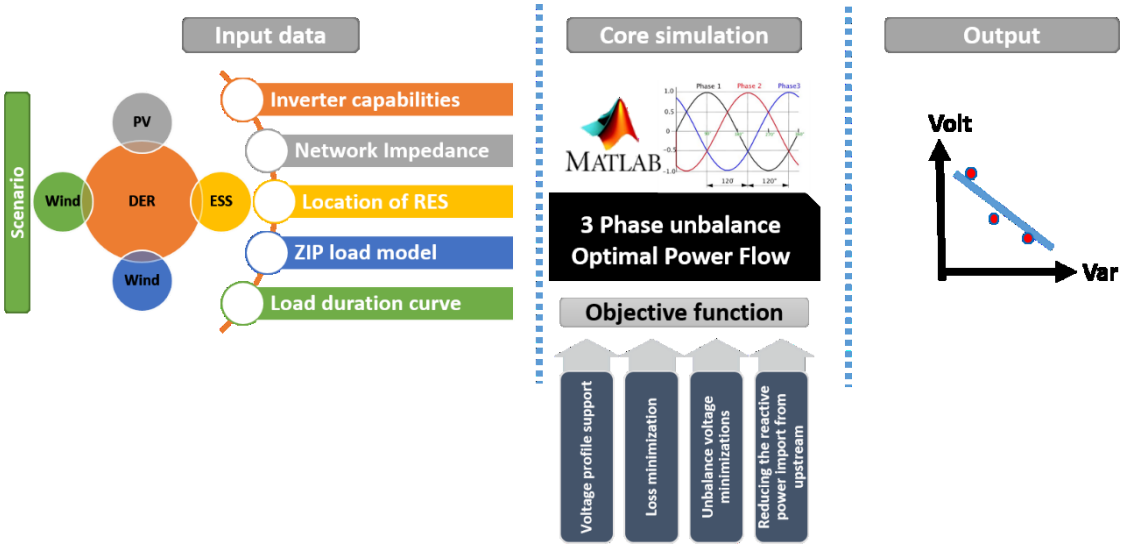

Figure 2-28 Input-Output of Volt-var curve determination procedure

The network topology, impedance information and the active and reactive power settings of demand customers and scenarios of RES alike are constituting the input data for Volt-var determination. This data is fed into a three phase unbalanced OPF and the optimal VVCs are found based on the selected objective function. The possible objective functions are:

- Active power loss minimization
- Voltage unbalance minimization in three phase networks
- Voltage profile improvement
- Minimizing the need for importing the reactive power from upstream network

The centralised voltage control scheme is shown in Figure 2-29.

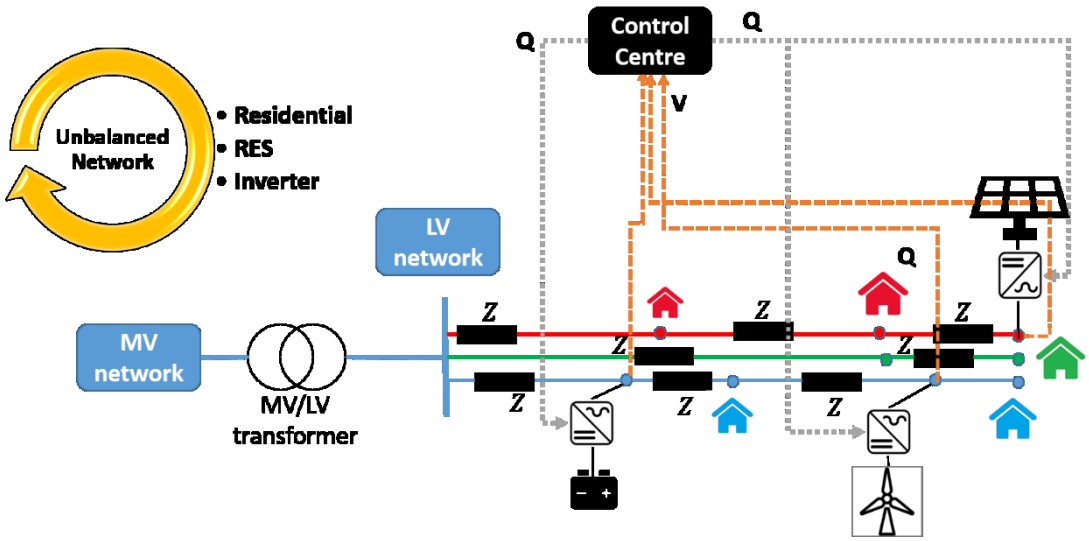

Figure 2-29 Centralised voltage control

The decentralised voltage control scheme for active voltage management is shown in Figure 2-30.

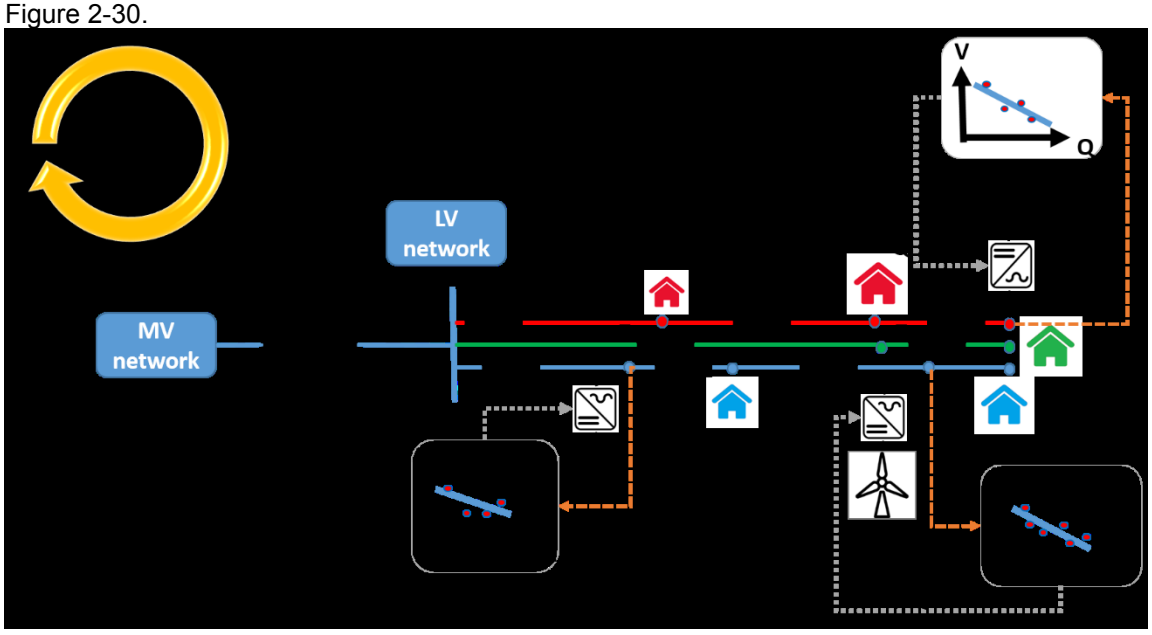

Figure 2-30 Decentralised Volt-var curve based voltage control

The local voltage at the connection point is measured and will be sent to the VVC. Based on the VVC the optimal Q setting will be sent back to the inverter.

2.5.2 Determination of the Volt-var curves

A four stage multi-scenario analysis, building on the work of [24], is used to investigate the Volt-var curves that arise from differing objectives of the DSO. This database is fed to the 3-OPF tool in **Stages I – IV** for the formation of the Volt-var curves as shown in Figure 2-31. Each stage is described as follows:

- Stage I – Optimal voltage setting

The purpose of Stage I is to ascertain the single optimal voltage at the terminals of the RES connection that optimises the object function across the multi-scenario case study. At this stage, the reactive power resource available from the inverter technology is left unconstrained. The optimal **voltage magnitude** setting found for each RES is passed to Stage II of the analysis.

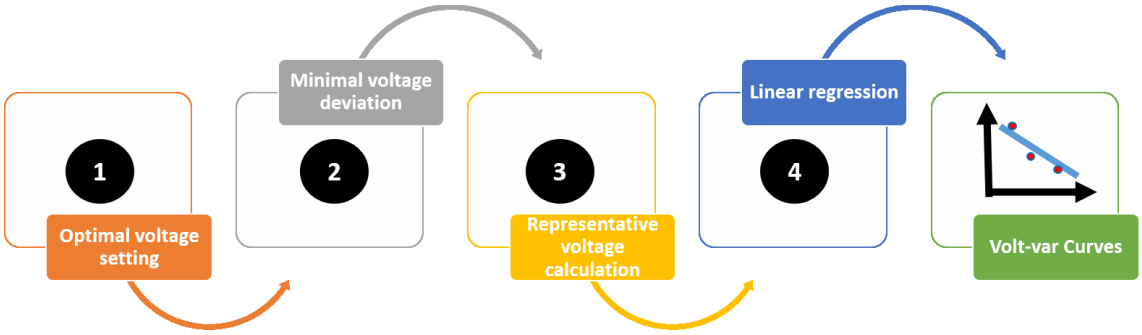

Figure 2-31 Four stages of VVC determination

- Stage II – Optimizing the objective function

Taking the voltage target output from Stage I, Stage II determines, for every scenario, the minimal possible voltage deviation from optimal.

The new objective minimises the difference in the sum of squares between the optimal target voltage and the best possible voltage achievable by utilising the available reactive power. For Stage II of the analysis, the reactive power constraints of the RES are implemented. In the case of inverter capabilities of a PV, there is a limitation in the amount of reactive power resource the device can provide, directly proportional to the active power output. The technical constraints of the inverters are implemented in the 3-OPF tool and the optimisation procedure is run once for each inverter-based RES connection to be fitted with a Volt-var curve. The **reactive power set-points** of Stage II, obtained for each RES, are stored to be used as one of two inputs to Stage IV.

- Stage III – Representative voltage calculation

In Stage III, straightforward power flow solutions are obtained, with the RES constrained to operate at unity power factor. No optimisation is performed in this examination of the scenarios. The aim here is to examine the resulting voltages, should no reactive power be injected or absorbed at the location of RES. This analysis gives an indication of the representative voltages that may exist at varying generation levels coinciding with the voltage sensitivities of demand at these times. The resulting **voltage magnitudes**, observed in each scenario, at the terminals of the RES units are the second and final input required to calculate the Volt-var curves, in Stage IV.

- Stage IV – Formulation of Volt-var curves using linear regression

In Stage IV, the resulting reactive power set-points of Stage II and voltage set-points of Stage III, obtained for each RES under examination, are inspected to be formulated into a Volt-var curve. Figure 2-32 shows an example of a Volt-var curve. As seen the orientation of the Volt-var curve should exhibit a negative slope and the intercept of the curve should match the optimal voltage set-point for the RES unit. The **slope** and **intercept** are the two characteristics to be determined from this offline analysis.

The intercept, C, of the Volt-var plots should, in theory, match the exact voltage found for the RES systems in Stage I of this procedure. The slope of these curves (m , coefficient of $\mathrm{Q_{RES}}$) guide the RES unit to control their absorption/injection of reactive power based on the

monitored voltage at their terminals. Employing a linear regression analysis to the voltage and reactive power set-points, calculates the slope and intercept for each RES system. This formulates the relationship between the voltage observed at the terminals of the RES system, V_{RES}, to a reactive power output Q_{RES}, of the form seen in equation (3.1).

$$V_{RES} = mQ_{RES} + c \tag{3.1}$$

Recall, that in achieving the voltage, determined in Stage I, the RES units are providing sufficient reactive power to support, and achieve, the objective of the DSO; in this case the minimisation of voltage unbalance. Hence, the instructions can be relayed in a decentralized manner for online-implementation of the AVM technique.

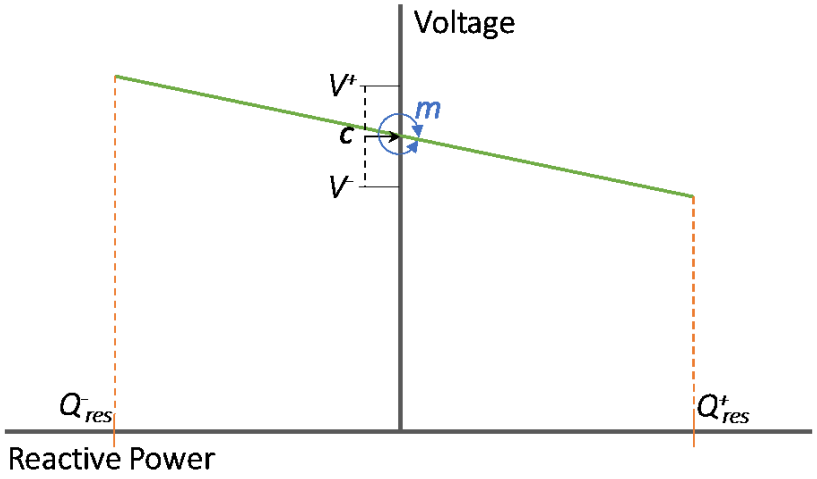

Figure 2-32 Sample VVC showing orientation and bounds of voltage and reactive power

To summarise the procedure involved in producing the Volt-var curves the following flow-chart of Figure 2-33 is provided.

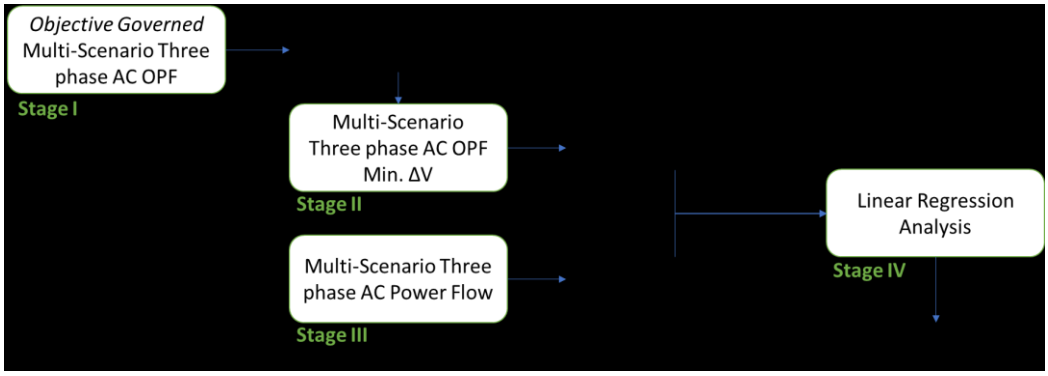

Figure 2-33 Procedure to determine objective governed VVC using the 3φ-OPF tool

- Stage I determines the optimal voltage across all scenarios that minimises the voltage unbalance of the feeder, or other objectives of interest.
- Stage II then determines the closest possible voltage deviation from optimal in each scenario, constraining the reactive power of the RES units to within representatively realistic bounds.
- In Stage III, the voltages are determined that occur at varying generation levels coinciding with the voltage sensitivities of demand at these times.

- Finally, to conclude the offline-procedure the resulting reactive power set-points (Stage II) are plotted against the resulting voltage set-points (Stage III) to determine the Volt-var curves for each RES system.

The AVM technique reduces the offline centralised analysis to an online and decentral deployment through the means of optimally chosen Volt-var curves, giving a practical means to facilitate the objectives of the DSO by managing the voltages on distribution systems.

2.5.3 Irish Field Trials for VVC

The field trials of the proposed VVC based reactive power support of inverter based RES are being performed specially on the following sites:

- Active voltage management (SV_B) for Trial site RES-PV-NTC-0
- Active voltage management (SV_B) for Trial site RES-BAT-FIRE-0
- Active voltage management (SV_B) for Trial site RES-V2G-LEOP-0

2.5.3.1 Network codes validated in these Trials

- NC.3 Distribution system – voltage control
- NC.14 Decentralized voltage control
- NC.15 Requirements for new behaviour of RES inverters
- NC.18 Leading power factor

2.5.3.2 Methodology

The inverter will be operated in grid connected mode. Figure 2-34 Summarizes the trial procedure.

- The voltage at the connection point of each (PPC) is measured and the measured value is transferred to the local control unit.
- After receiving the required data, each local control unit finds the applicable change in the reactive power injection of regarding inverter.
- The new reactive set-point of this inverter is transferred to the inverter to change the reactive power support accordingly.
- The new setting is applied
- The voltage at the connection point of each (PPC) is measured and the measured to check if the desired objective is satisfied or not.
- Save the data for future analysis

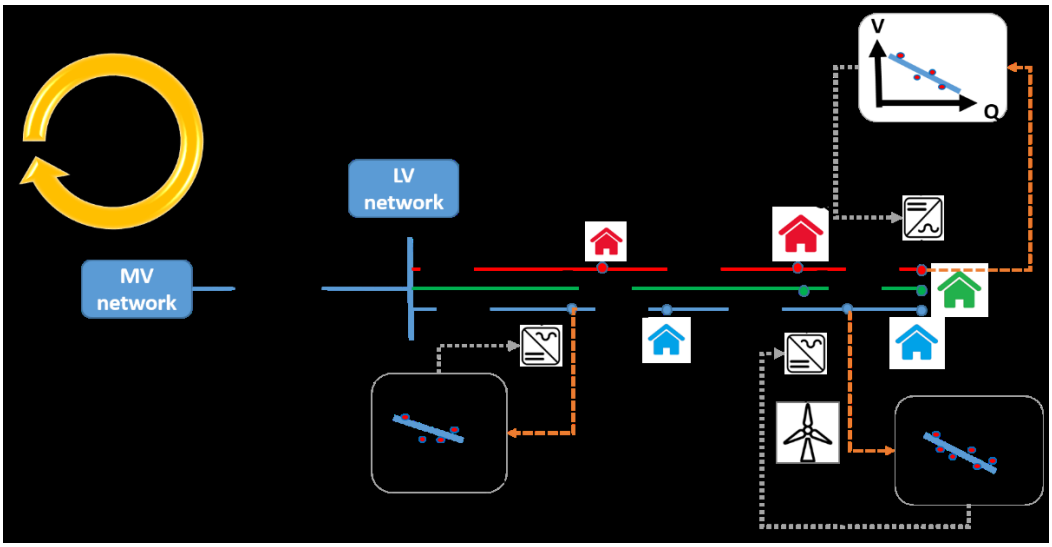

Figure 2-34 Summary of the trial procedure for VVC

2.6 Conclusion

This chapter proposes the network codes from the outcome of the technical work of scenario SV_B Static Voltage Stability assessment. A set of network codes are proposed covering various aspects of the scenario from a DSO perspective and from that of the RES inverter. The proposed power factor and reactive power support requirements for different technologies including wind, PV and energy storage technologies are presented. Few of the simulations are already completed and the results are presented in this chapter. The remaining simulation and trials will be performed in last 12 months of the project.

The 4 most important network codes identified which are relevant to SV_B are provided below:

- NC.3 Distribution system – voltage control
- NC.14 Decentralized voltage control
- NC.15 Requirements for new behaviour of RES inverters
- NC.18 Leading power factor

3. Drafting Network code recommendation from power electronic stability criteria and online system monitoring perspective

Based on the current distribution system architecture, analyses were done on both steady state and dynamic voltage stability considering influence of high RES within this project. The results of which are covered in earlier deliverables such as D3.2 and D3.3. In order to solve these problems, RESERVE addresses modification in network codes and proposes the implementation of decentralised voltage control solution which are ICT driven. These new voltage control techniques developed in RESERVE also require modifications and introduction of new network codes. This chapter covers the network codes and ancillary services proposed in RESERVE and showcases the offline, real-time simulation and hardware results pertaining to the validation and testing of the proposed network codes.

Deliverable D6.1 provides a wish list of network codes in Table 2. The important network codes considered relevant for SV_A are:

- NC. 14 Decentralised voltage control
- NC. 18 Leading power factor operation
- NC. 17 Dynamic stability margins
- NC. 15 Requirements for new behaviour of RES inverters
- NC. 16 New requirements for perturbations injected from RES inverter

3.1 Recommended Network Codes

3.1.1 Control of Power-Electronic based Active Distribution Grids

3.1.1.1 NC.14: Decentralised Voltage Control

The state-of-the-art voltage regulation concept in LVAC grids is based upon centralised control. The SSAU regulates the LVAC feeder voltage through changing the tap positions in the On-Load Tap Changing (OLTC) Transformers and by switching ON and OFF capacitor banks to regulate reactive power flow, thereby controlling the bus voltage. With the rise in inverter-based RES units, the dynamic interactions among large number of power electronic converters might lead to unstable modes or oscillatory modes in the feeder voltage profile. Therefore, we recommend the practice of decentralised voltage control for the DSO. The underlying ideology is that the large number inverter-based RES units in the LV grid is considered as degrees of freedom for control.

3.1.1.2 NC.18: Leading Power Factor Operation

The work done with the scenarios SV_A and SV_B would demand the RES inverters to operate with a leading power factor at times for providing grid voltage support. In the present scenario, the power factor is operated with only a lagging power factor in certain DSOs. Hence this WP will provide recommendations to modify the grid code to include leading power factor. The implementation of Virtual Output Impedance (VOI) control enables dynamic injection or absorption of reactive power based on the amount of voltage overshoot or undershoot. Thus, under dynamic conditions, the power factor of the inverter can be leading or lagging more than the specification in existing grid codes.

3.1.2 Monitoring techniques for DSOs for Power-Electronic based Active Distribution Grids

3.1.2.1 NC.17: Dynamic Stability Margins

With large number RES inverters in the LVAC grids, we envision a virtual impedance based decentralised control. For accessing the grid voltage stability, a stability monitoring algorithm is developed which is placed in the SSAU. The stability of such a dynamic system is assessed through dynamic stability margins such as gain and phase margins. In the current grid codes, there is no such definitions found. Hence for the futuristic grids, we propose the inclusion of dynamic stability margin definitions. Additionally, we envision through our work to determine minimum dynamic stability margin limits or thresholds that the system must possess.

3.1.3 New generation of Power-Electronic converters

3.1.3.1 NC.15: Requirements for new behaviour of RES inverters

In the context of decentralised control, the control command received from a tertiary level or from a Microgrid operator might be set-points for real and reactive power in a conventional sense. However, the methods developed in RESERVE, envisions a case where the higher control level might modify the closed-loop behaviour of inverter. By behavioural we mean the control parameters themselves. The examples pertaining to WP3 are presented as follows:

- The Dynamic Voltage Stability Monitoring (DVSM) (SV_A) functionality which resides in the SSAU would send control commands back to the VOI controller, which will in turn modify the control parameters of the inverter to achieve the set-point impedance. Hence, the behavioural of inverters are modified here and since the SSAU sends these commands, the DSO grid codes must allow it.
- The Active Voltage Management (AVM) (SV_B) technique modifies the Volt-var curves of the RES inverter. Hence the concept of Volt-var curve definition for house RES inverters must be included into the grid codes.

3.1.3.2 NC.16: New requirements for the perturbations injected from RES inverters

Grid codes should be formed related to the injection of white noise signal into the grid voltage for a short duration. The white noise signals, otherwise known as Pseudo Random Binary Sequence (PRBS) is generated in the control loop of the inverter, where the duty cycle or current/voltage reference are perturbed. This induces perturbations on the output voltage and current of the inverter for impedance measurement. In WP3, we will determine the magnitude of perturbation required for accurate determination of impedance and injection time period that is required for the noise injection and propose them for new grid codes.

3.2 Specification of Dynamic Voltage Stability Criteria

Generalizing a grid code for dynamic voltage stability which defines minimum gain and phase margin can be difficult. This problem is analogues to defining minimum system inertia which again cannot be generalised for all networks. Sensitivity of a grid towards harmonic instability depends on many factors such as:

- Cable length and cable impedance between various active sources (RES integrated PV inverters)
- Installed capacity of active sources and active loads (contant power loads) in the network
- Bandwidth of controllers and PLLs of active sources and load
- Strength of the medium voltage grid to which the LV network is connected

Exemplary simulation results of the measurement of grid behaving passively is illustrated in Figure 3-1, where the measurement of impedance is based on the WSI concept used in the device which is explained in Section 3.6. For a passive network, the characteristic loci obtained is strictly on the right of the imaginary axis. Introduction of active sources changes this passive behaviour the characteristic loci penetrates the left side of the Nyquist plot. Figure 3-2shows the characteristic impedance of a network consisting of active elements. A low value of phase margin can be critical for a system with low damping than for a system with high damping. Furthermore, a direct correlation is not observed between the above mentioned 4 factors and a critical point where system can become unstable. Enforcing converters to behave passively for a wide range of frequencies can ensure passivity at most nodes in the grid.

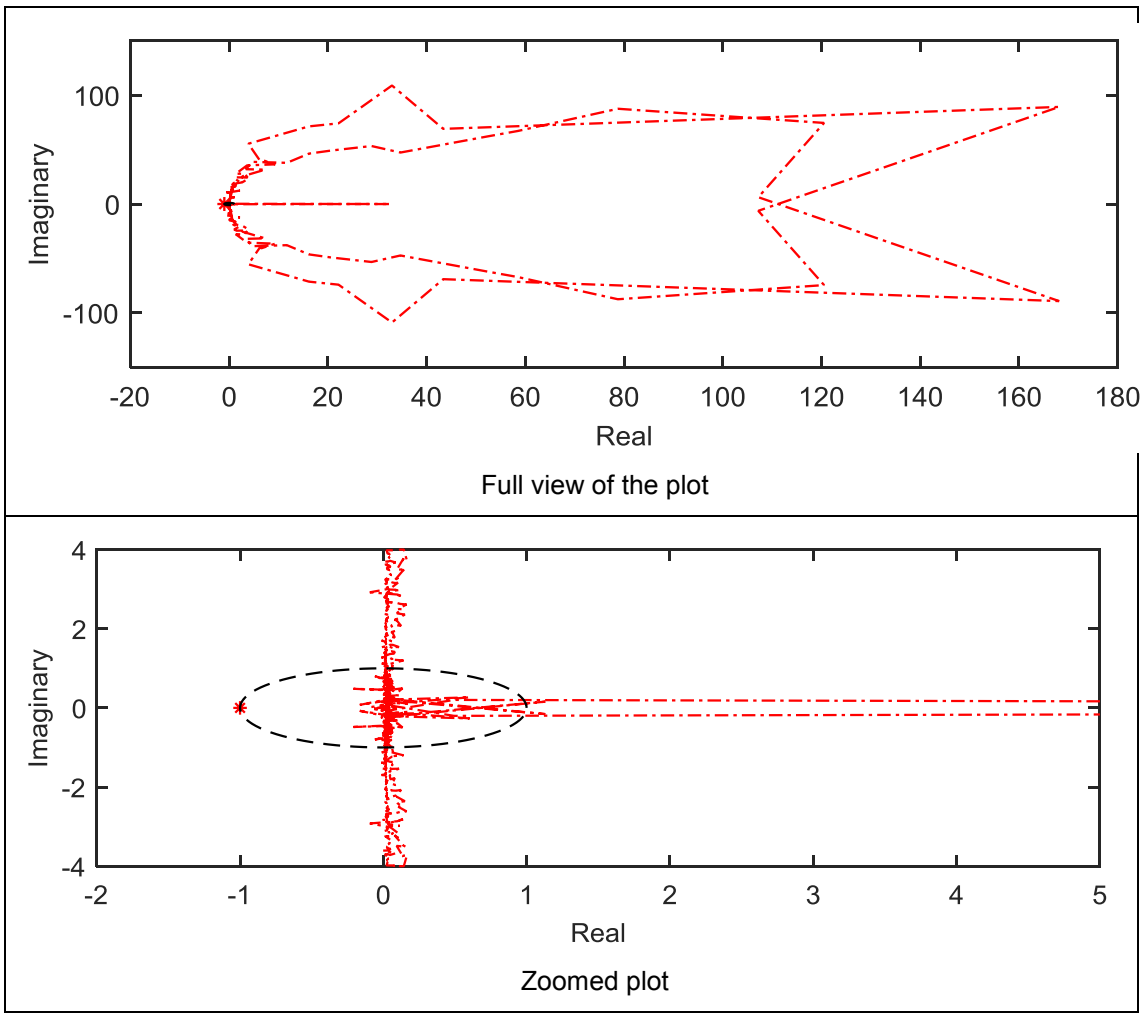

Figure 3-1 Characteristic loci of return ratio matrix for a network exhibiting passivity

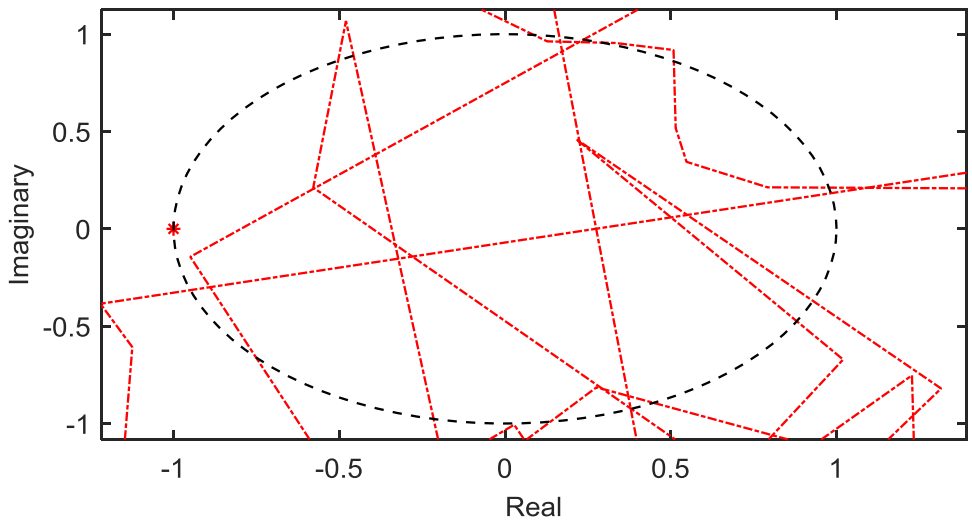

Figure 3-2 Characteristic loci of return ratio matrix for an active network

The simulation and frequency domain stability analysis of Irish distribution network based on the Generalized Nyquist Criterion is already provided in **D3.3**.

3.2.1 Remarks on Passivity Enforcement

Recently, passivity-based control approaches have been gaining importance in control of grid-integrated converters [25], [26]. Passivity property ensures that the system has enough damping to neglect oscillations on the output for a wide range of frequencies. Passivity approach is a non-linear control approach based on energy shaping philosophy and it could be applied to converters and expanded in a bottom-up manner to larger grids and Microgrids [27]. It is well established that parallel interconnection of such passive system results in an overall system which is also passive.

Power electronic converters and active loads in the grid (which are also power electronic driven systems) are connected in parallel to the bus. Considering that when parallel interconnection of such sub-system results in a passive system, then large signal stability can be achieved.

Grid codes can be imposed on grid connected converter manufactures to design converter loops which ensure passivity up to a certain range of frequency where active interactions might occur [25]. This method would lead to passive interconnection of subsystems and would be an optimal approach towards large integration of RES.

3.3 Requirements for Perturbations Injected from RES inverters

3.3.1 Requirements for PRBS injection

PRBS can be injected either at the duty cycle/control signal or at the reference signal. Injecting at the reference signal can get directly filtered by the controller of the inverter. Thus, it is beneficial to superimpose the PRBS signal onto the duty cycle/control signal. The number of shift register bits should be chosen such that the spectrum of PRBS is identical to that of white noise. In order to measure until 25 kHz, a 11-bit shift register is sufficient, and the resultant spectrum is shown in Figure 3-3.

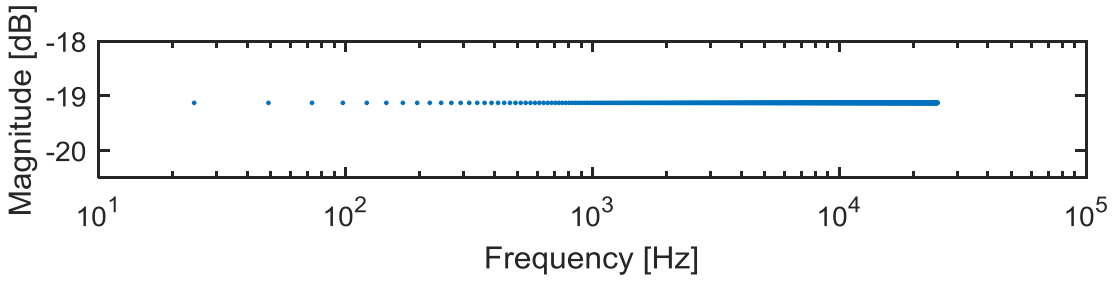

Figure 3-3 PRBS spectrum for 11-bit shift register

The measurement time period is related to noise injection frequency f_{inj}, number of PRBS shift register bits (N) and number of periods of PRBS injection (M). The time period of PRBS injection is given by (**3-1**). The number of shift register bits is the most important factor that decides the white noise approximation of the PRBS. Higher the bits, higher is the closeness of the PRBS spectrum to that of white noise. Therefore, based on the required frequency, the number of bits N needs to be chosen. Periods of the PRBS signal depends on the required resolution in frequency.

The amount of perturbation required in the control voltage before down scaling is typically 1% to 3% of grid voltage. In the experiments performed in RESERVE, the perturbations did not exceed this limit and successful extraction of impedance was demonstrated in both offline and real time simulations and through hardware prototype.

$T_m = M(2^N - 1)/f_{inj}$	(3-1)

3.3.2 Specification of Noise Injection Requirements for grid-forming and grid-feeding RES Inverters

The impedance measurement technique when applied to inverters increases the distortion in the output current for a short duration of time. All the various distribution grid codes cover the aspect of total harmonic distortion (THD), which is a measure of the net harmonic content in the signal. THD is the sum of distortions in the power injected at higher order harmonic frequencies to the power in the fundamental frequency of 50 Hz.

The Irish distribution code DCC6.8.3 covers the total harmonic distortion aspects for a 400 V LV grid. Grid tied inverters have a maximum allowable THD level of 2 percent [28]. As shown from Figure 3-4, THD levels in grid tied inverter may exceed for a short duration when PRBS is injected. For an injection time period of 40 ms in the D axis and Q axis respectively, the THD levels exceed may briefly for a time period of around 50 ms. THD level violation with such a small magnitude, for such a short period of time will not cause any harmonic instability issues in the grid. Therefore, grid codes need to be modified for supporting such new generation of inverters with PRBS noise injection capabilities and impedance measurement devices such as the proposed device in Section 3.5.2. RESERVE proposes the implementation of **NC. 16 New requirements for perturbations injected from RES inverter**. Such a grid code should contain the information of worst case THD during the measurement process, maximum time for which nominal THD level can be exceeded at the time of measurement and percentage of perturbation caused in the bus voltage due to PRBS injection. Time domain simulation results are included in Section A.1 and experimentally verified using the proposed impedance measurement device in Section 3.6.

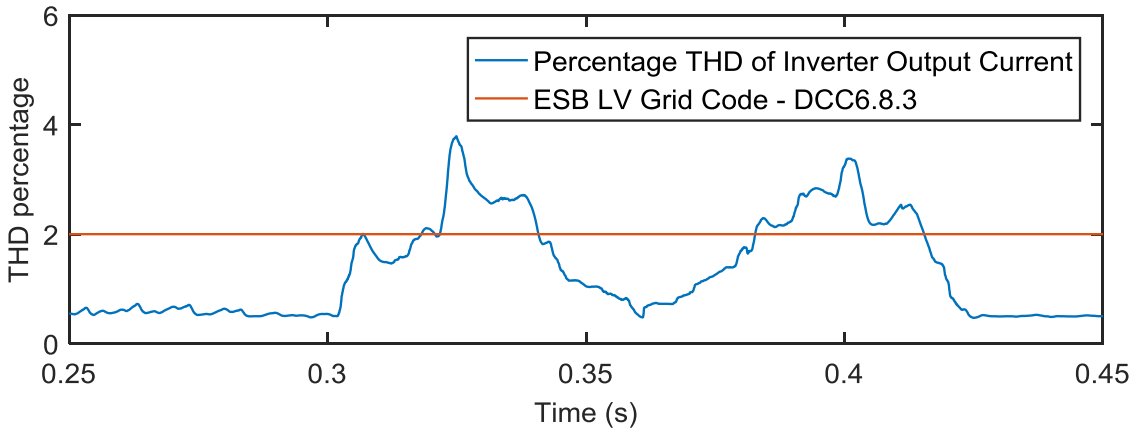

Figure 3-4 Total harmonic distortion during PRBS injection

3.4 Adaptive Virtual Output Impedance based Control for Distribution Grids

The measured grid impedance model is augmented into the closed loop model of the inverter to formulate a generalized plant model. This generalized plant model is dependent on the grid impedance and weighting functions which are used for tuning. The Virtual Output Impedance (VOI) controller is designed by considering objectives in the frequency domain such as modifying the low, high frequency behavior and suppression of resonance peaks. The Dynamic Voltage Stability Monitoring (DVSM) was defined and specified in **D3.5**, where the VOI control algorithm was also defined. Here we present a flowchart of the VOI approach when used with DVSM technique as shown in Figure 3-5.

Step 1: SSAU requests the inverter to do the impedance measurement. Inverter measures the grid impedance. Inverter controller calculates the inverter output impedance using the analytical formulas defined in **D3.5**. Inverter sends its own impedance and grid impedance to SSAU.

Step 2: SSAU calculates the VOI controller using predefined weighting functions

Step 3: Stability is evaluated through GNC at SSAU

Step 4: Criteria such as passivity or minimum stability margin can be adopted and check if the defined stability condition is satisfied.

Step 5: If the stability margins are satisfied, then the SSAU sends the VOI coefficients back to the inverter. If not satisfied, then the weighting functions are changed and algorithm in SSAU goes to back to **Step 2**. This adaptive loop process cannot run for a long time. Therefore, a predefined wait time is defined. Once the time expires, the grid impedance data is not reliable since the grid conditions may have changed. SSAU commands the inverter to perform a new measurement.

The frequency domain stability analysis based on GNC, when the weighting function parameters are changed is presented in Annex A.3. Results of the real-time simulation is provided in Annex A.4.

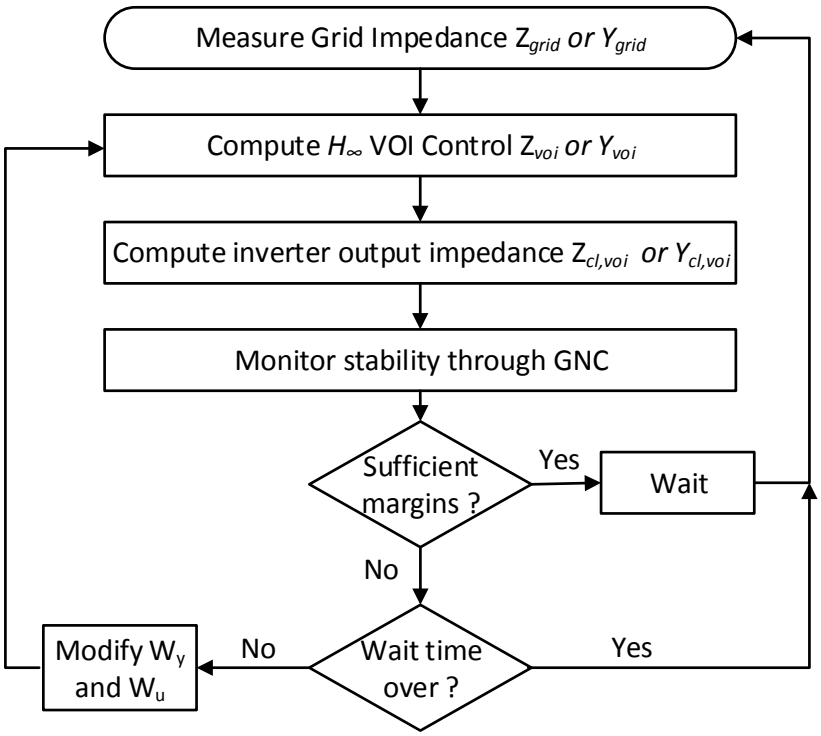

Figure 3-5 DVSM with adaptive VOI control algorithm [29]

Thus, the proposed framework requires new grid codes such as **NC.14: Decentralized Voltage Control**, which allows the DSO operator to do monitoring of inverter, wherein the inverters provides an ancillary service of providing support towards dynamic voltage stability. Furthermore, the way dynamic stability is achieved requires the re-shaping of inverter output impedance. Thus, grid codes need to allow inverters to play such new roles in the grid. Hence, RESERVE proposes **NC.15: Requirements for new behaviour of RES inverters**.

3.5 Stability Monitoring Device for Low and Medium Voltage Networks

Deliverable D3.8 describe the low power inverter developed in RESERVE with WSI functionality. Further investigation revealed the possibility of modifying the device operation and functionality so that the device can serve as an impedance-based stability monitoring device. As mentioned D3.4 and D3.8, the concepts proposed in RESERVE can be integrated into existing inverters through modifications in software or there is possibility to develop new devices that support the grid operation under high RES penetration.

A Wideband Grid-Impedance (WFZ) measurement device is proposed to enable real-time impedance measurement in a non-invasive manner with high plug-and-play capability. A patent is pending for RWTH for the invention of the WFZ device [30].

Within the context of RESERVE, the proposed device enables the measurement of the grid impedance at arbitrary locations in the grid, thus allowing the grid operator to monitor grid stability online. One option is that the device calculates the local stability margins within the device itself. Alternatively, by using wireless communications links, the device transmits the measured grid impedance to the SSAU. The following sections explain the state-of-the-art, device description and application.

3.5.1 State-of-the-Art

3.5.1.1 Method A – Network Analyser

The device terminals Lx and Ly are connected to the power circuit where the impedance needs to be measured. The network analyser performs a sinusoidal frequency sweep from the specified minimum and maximum frequency up to which the grid WFI needs to be measured. This signal is amplified by the power amplifier which requires an external DC power supply. The amplified sinusoidal signals are injected into the system via an isolation transformer. The output current V_{ix} and output voltage V_x are recorded to compute the impedance.

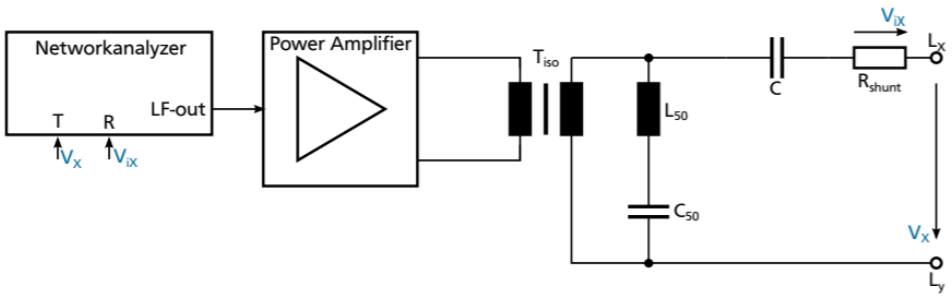

Figure 3-6 Network Analyser [31]

3.5.1.2 Method B – Dynamic Load Switching

The single-phase version of the device is shown in Figure 3-7. It consists of a single-phase diode full bridge rectifier for single phase applications and a three-phase diode full bridge rectifier for three phase applications. At the DC side of the rectifier, a resistive load RL is in series with an IGBT. In parallel to the IGBT, an RC snubber is present formed by the passive elements Rs and Cs.

The switch S, in Figure 3-7 is switched ON and OFF through wave-package technique or inter-harmonic technique. By doing so, the load resistance is switched ON and OFF which introduces large disturbances. By measuring the large deviations in the voltage and currents, the impedance at **only** 50 Hz is calculated.

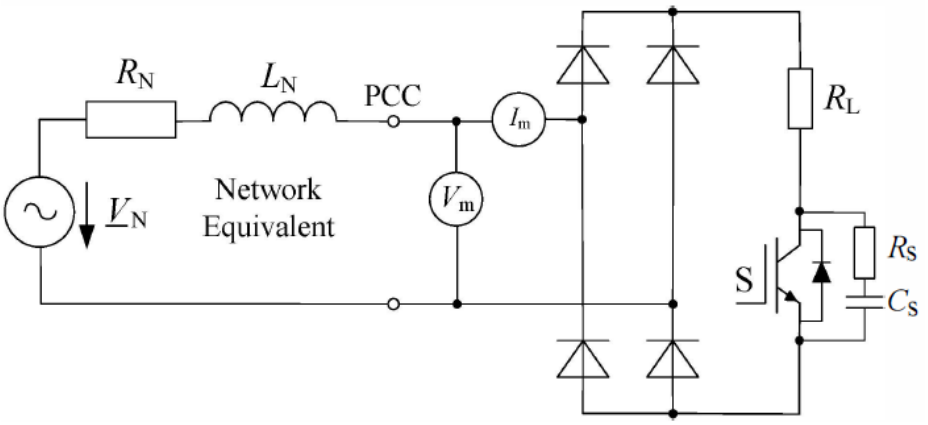

Figure 3-7 Dynamic Load Switching [32], [33]

3.5.1.3 Disadvantages of Network Analyser (Method A)

- The method uses network analyzer for generation of frequency sweep of sinusoidal excitation signal. These signals are amplified by the power amplifier and injected into the power circuit through the high frequency transformer. The requirement of power transformer and power amplifier increases the cost and weight.
- The device requires a power supply to operate power amplifier.
- Due to the above points, the device is not suitable for plug-play

- In a frequency sweep process, the grid is injected with 1 sinusoidal frequency at a given time. This is highly undesirable since the frequency sweep process is time taking and the grid impedance can possibly change before completion of frequency sweep.
- Due to the above reason, devices incorporating frequency sweep technique is not suitable for real-time grid impedance measurement. Devices using white noise injection such as PRBS and MLBS are suited for real-time grid impedance measurement.
- Another disadvantage is the inability to incorporate this device within existing inverters.

3.5.1.4 Disadvantages of Dynamic Load Switching (Method B)

- Measurement of impedance is done only at 50 Hz. Such a device is not suitable for futuristic distribution grids. Due to high penetration of power electronics, a wide band of frequencies are needing to be considered to adjudge stability. It is not only the 50 Hz impedance that impacts stability as in a classical power system
- Method B switches ON and OFF a resistive load through an IGBT switch. This method introduces significant transient disturbance into the system. This method is not a small-signal method as the proposed invention
- Highly lossy. Unlike the proposed , where there is only a capacitor to store energy in the DC link; method B uses a load resistor which is switched through an IGBT switch. Energy drawn from the grid is lost in the resistor as heat energy.
- Cannot be used to compute dynamic stability margins which is the crucial diagnostic tool required for futuristic grids.
- Cannot be integrated into existing inverters.

3.5.2 WFZ Device Description

3.5.2.1 Setup

The new device proposed is shown in Figure 3-8 within the encapsulated box, where the hardware part is highlighted in yellow and the software part is highlighted in green. The device consists of a 3-phase converter with B6C topology and power electronic switches can be realized with either IGBTs or MOSFETs based on the voltage level and carrier switching frequency. The DC side of the converter consist of a negative temperature coefficient (NTC) resistor, relay and a DC link capacitor. The AC side consists of a LCL filter and a relay. In the software side, a controller which could either be conventional current control or non-linear control synthesizes the control command for the PWM block which controls the switching of the IGBTs. The controller relies on measurement of grid injected current, grid voltage and the voltage of the DC link capacitor.

A wideband system identification (WSI) and information management block interacts with the controller. The WSI block is further enabled with communication to communicate the measured grid impedance data to the Secondary Substation Automation Unit (SSAU) for further monitoring.

3.5.2.2 Method

The DC link capacitor is charged from the grid by closing the DC side relay. The NTC resistor limits the inrush current during start-up. During this period, the B6C bridge is operated as a rectifier. Then, the stored energy is injected back into the grid and the B6C bridge is operated as an inverter. During this time, the WSI block injects PRBS noise signals into the current reference of the inverter for 40ms (2 cycles of fundamental grid voltage). Simultaneously, the voltage and current signals are measured and stored in first-in-first-out (FIFO) buffer. The grid impedance is calculated in frequency domain using fast Fourier transform (FFT) algorithm and system identification technique is applied to get the impedance transfer function. The measurement of impedance can be done either in direct-quadrature (DQ) domain or in sequence domain based on the requirement. The device can then compute stability margins by applying impedance-based stability assessment techniques. The device can communicate the identified grid impedance coefficients and the calculated stability margins to the SSAU, where corrective steps are undertaken.

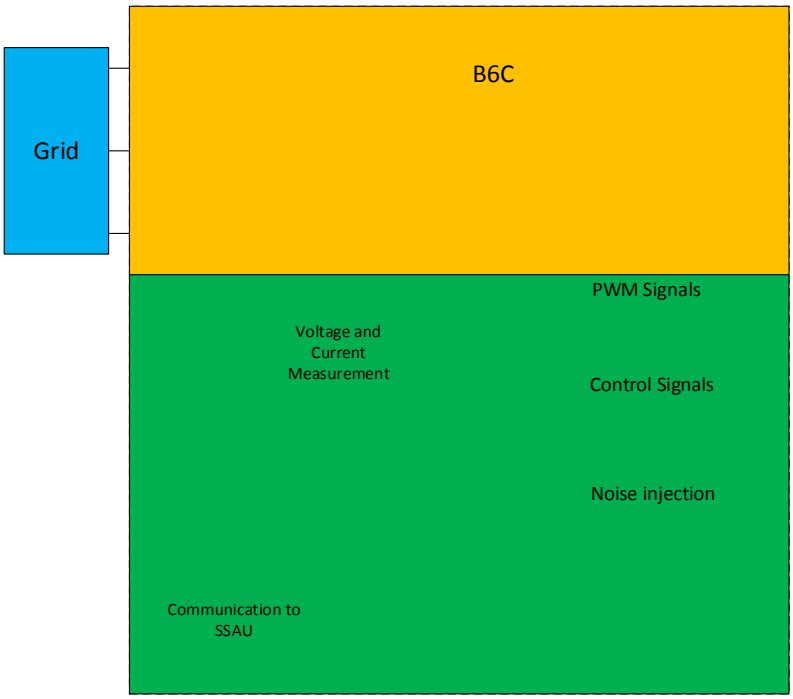

Figure 3-8 Structure of the proposed measurement device (WFZ device)

The proposed device does not require any external power supply since it takes power from the grid and injects back into the grid during measurement. The amount of power consumed is negligible compared to devices which incorporate load switching. The device need not be rated for high power since the goal is to inject small signal perturbations in the grid. As a consequence of the above-mentioned reasons, the device is low cost, low weight and mobile. The envisioned device has high plug-play capability for distribution grid operators to plug the device at any node along the low voltage distribution feeder and measured impedance in real-time and have the stability monitoring executed in real-time. The envisioned device will be equipped with communication capabilities to relay the information to the SSAU. Furthermore, disturbance injected in the grid is negligible since the device is based on WSI concept which is a small-signal technique.

3.5.3 WFZ Device Application

The proposed measurement devices utilize the Wideband System Identification (WSI) technique to measure the grid impedance at the point of common coupling. This technique injects PRBS signal which is superimposed over either the duty cycle, voltage or current reference signals of the device. One of the major applications for which the invented device is intended is shown in Figure 3-9. Consider a low voltage distribution feeder with arbitrary number of buses and let's assume that the stability margins at Bus 6 needs to be monitored as shown in Figure 3-9.

The device is connected at Bus 6 and performs impedance measurement using the WSI block by injecting perturbations in voltage and current. The voltage is measured at the PCC as shown by the red dotted line and the currents are measured on both sides of the red dotted line. Thus, the impedance of two sections of the LV feeder Z_{6L} and Z_{6R} with respect to the PCC can be measured by the proposed device. Based on the impedances Z_{6L} and Z_{6R} that are measured, the stability margins are calculated.

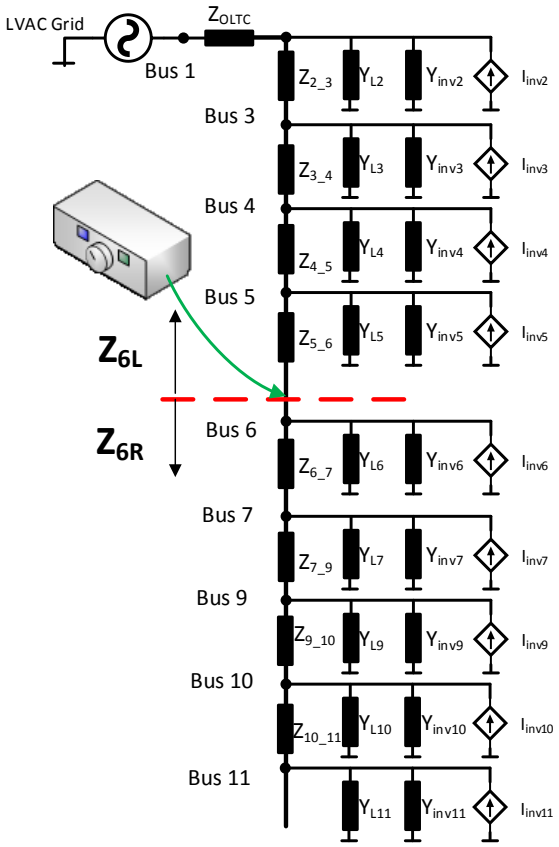

Figure 3-9 Impedance based Stability Monitoring Device

The proposed measurement device enables a non-invasive measurement of the grid impedance at the point of common coupling (PCC) of the device and a measured grid with arbitrary topology and components. This means that no shutdown or interruption of the measured grid section is necessary. The measurement device can be connected at any accessible location in the grid without modifying any existing electrical connections. Furthermore, the grid impedance measurement is performed online, during the normal operation of the grid. Compared to transient methods, where a current pulse is injected, with the proposed device a short duration, minimal perturbation is sufficient to measure the grid impedance. Therefore, the grid impedance measurement can be performed for any operational state of the grid, especially in situations where the grid is heavily loaded.

In practical cases, usually not many options from where to supply a measurement device are available; therefore, most likely the electrical grid to be measured is used. But by doing so, the measurement device influences the grid during the grid impedance measurement process, influencing the measurement result to an unknown extent. For the proposed measurement device, no separate power supply is necessary, since it is self-powered from the measured grid, making the device easy to use in terms of the electrical connections and floating. At the same time, the measurement device does not influence the measured grid substantially during the measurement process, avoiding any significant impact of the measurement device on the identified grid impedance. This is enabled by the DC link capacitor of the measurement device, which is charged by rectification before an impedance measurement is performed. The charging happens slowly, such that the influence on the connected grid, also in heavy load situations, is minimal. During the impedance measurement, only a low power injection from the DC link into the grid takes place, minimizing the effect of the measurement device on the grid and its behaviour at any moment.

Since the proposed device only injects a low power into the measured grid, it is built small and lightweight, allowing the use as a mobile measurement device. Due to the topology of the power section as well as a suitable control and impedance measurement algorithm, the measurement device is flexible in terms of the grid's voltage level (e.g. 230Vrms, 110Vrms) and the number of phases (one, two or three phases). Furthermore, the device enables a grid impedance measurement for AC but also for DC grids. For DC grids, the type of the grid is flexible, e.g. unipolar or bipolar DC grids can be considered.

Due to the non-invasive nature of the measurement device, an automated periodically measurement of the grid impedance is enabled. The measurement results can be stored locally for later use or transmitted to the operator using the device's (wired or wireless) communication capabilities. Furthermore, a communication link allows the remote control of the measurement device.

The proposed measurement device does not continuously measure the grid impedance based on voltage and current measurements, but periodically in user-selected intervals of e.g. 30 seconds or one minute. Therefore, during the time when no grid impedance measurement is performed, the device can be used to monitor the grid's voltage, current and hereby the power quality at the device's point of common coupling with the grid. By using the device's communication capabilities, those additionally obtained measurements can be stored locally and/or transmitted to the grid operator for further processing.

The measured grid impedance is mapped to a transfer function using curve fitting techniques. Thus, the data volume is reduced effectively. For example, for representing the DQ impedance matrices for the two LV feeder sections from the PCC, roughly 100 floating point numbers are required. If the proposed device performs impedance measurement every 30 seconds, then the data volume in Kilo Bytes per second is: 100 coefficients x 8 bytes / (1024 bytes x 30 seconds) = 0.026 kB/s.

Summarizing the above points:

- Light weight
- Low cost
- High plug-play capabilities
- Communication capabilities
- Low data volume
- Highly Non-invasive
- No requirement of external DC power supply for the DC side of the inverter
- Can be integrated into PV inverters and battery inverters. Independent of type of supply in DC side
- Can be integrated into existing STATCOMs in high voltage or medium voltage grids
- Can measure grid impedance from the point of common coupling
- Can measure impedances of the two LV feeder sections as seen by the PCC, if the current measurements of the two sections of LV feeder from the interface node (PCC) is available.
- Can compute dynamic stability margins of the LV feeder at the interface node (PCC).

3.6 Aachen Lab Trial – Grid Forming Mode

A fully programmable, high bandwidth and high switching frequency prototype of the proposed WFZ device is constructed and commissioned as shown in Figure 3-10. A National Instruments Compact-Rio cRIO-9024 hosting a Virtex 5 FPGA is used to implement the software component of the device. A National Instruments NI-9215 and NI-9401 modules are used with cRIO-9024 for enabling high sampling frequency and high speed PWM respectively [34]. The parameters of the built converter are shown in Table 3-1.

Table 3-1 Device Parameters

Converter Parameters	Values
DC Link Voltage	600-750 V
Grid Voltage and Frequency	400 V, 50 Hz
Switching Frequency	50 kHz
Converter Side Choke	2.7 mH, 0.5 Ω
Grid Side Choke	1.8 mH, 0.3 Ω

Filter Capacitance Co	1 μF

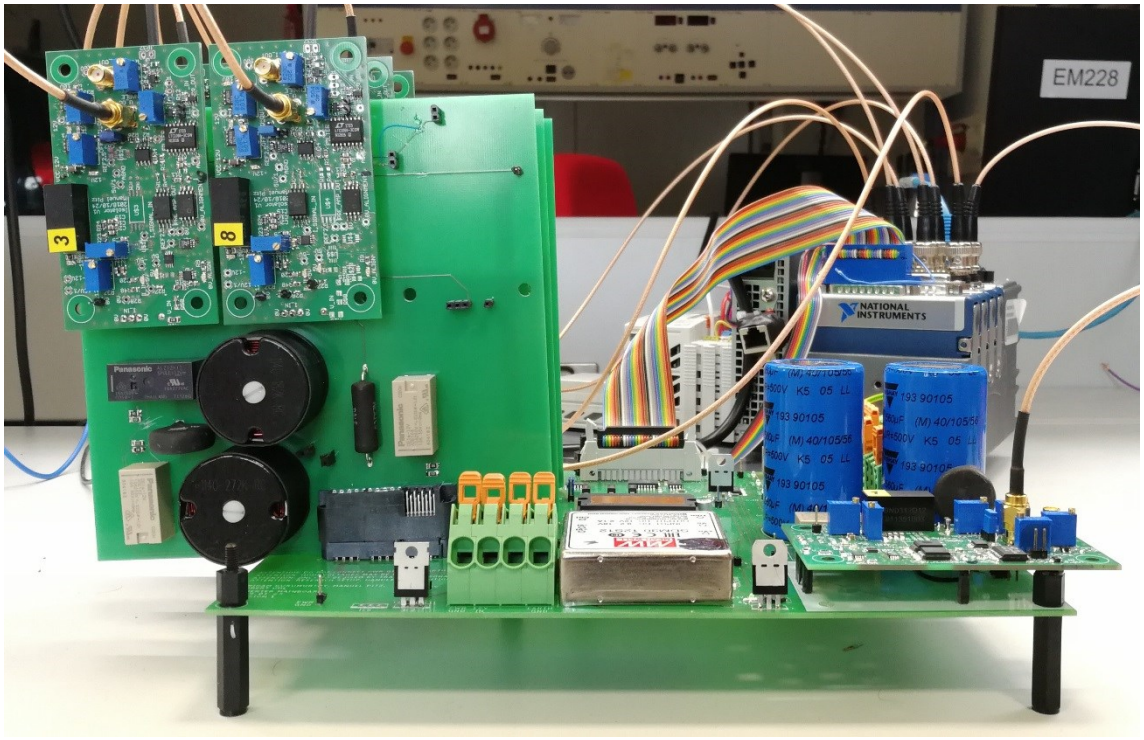

Figure 3-10 Programmable Inverter Prototype – WFZ Device

The WFZ device is operated with a DC Link voltage and it is operated in grid forming mode. A three-phase passive impedance network is sued as the load impedance that needs to measure similar to the simulations performed in Section. The device is operated at 50 kHz and the noise injection is also performed at maximum possible frequency of 50 kHz. Considering a N-bit shift register to generate the noise, we need $2^N - 1$ sample points. In the simulations and experiments, it was found that N=11, is a sufficient choice for obtaining sufficient frequency resolution, thus leading to 2047 sample points. At 50 kHz and N=11 bits, the measurement time period for measuring d-axis impedance is 40.9 ms. Between d-axis and q-axis impedance measurements, a dead-time of 0.02 seconds (1 cycle of power system frequency) is observed for the transients to settle down. Q-axis impedance requires another 40.9 ms. Thus, the total measurement time for measuring DQ impedance matrix is 0.101 s.

Figure 3-11 shows the load current and Figure 3-12 shows the load voltage during the perturbation window of 0.101 s. The obtained d-axis impedance magnitude and phase are plotted in Figure 3-13 and Figure 3-14. In order to validate the obtained measurements, a network analyser is used to make a reference measurement which is denoted by the red curve in Figure 3-13 and Figure 3-14. Strong match is observed between the analytical transfer functions used in Simulations, experimental data of WFZ device and the network analyser.

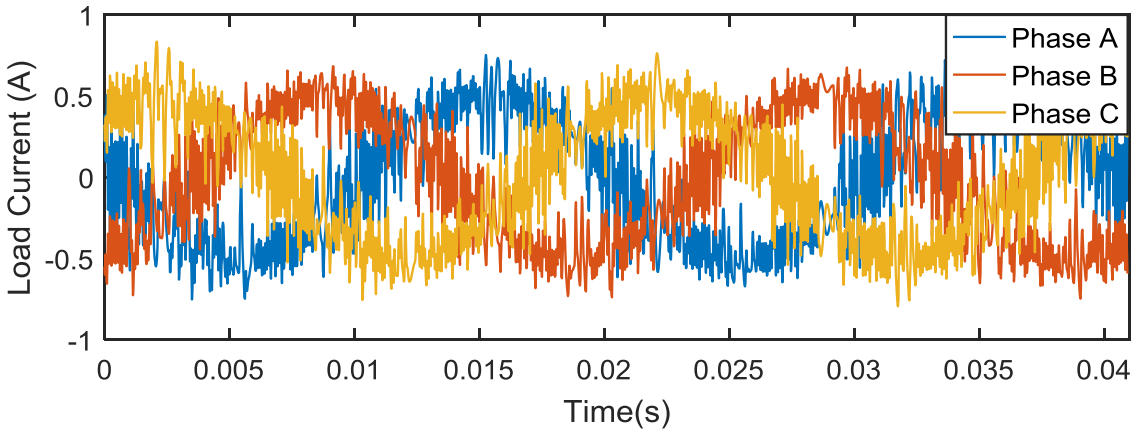

Figure 3-11 Load Current

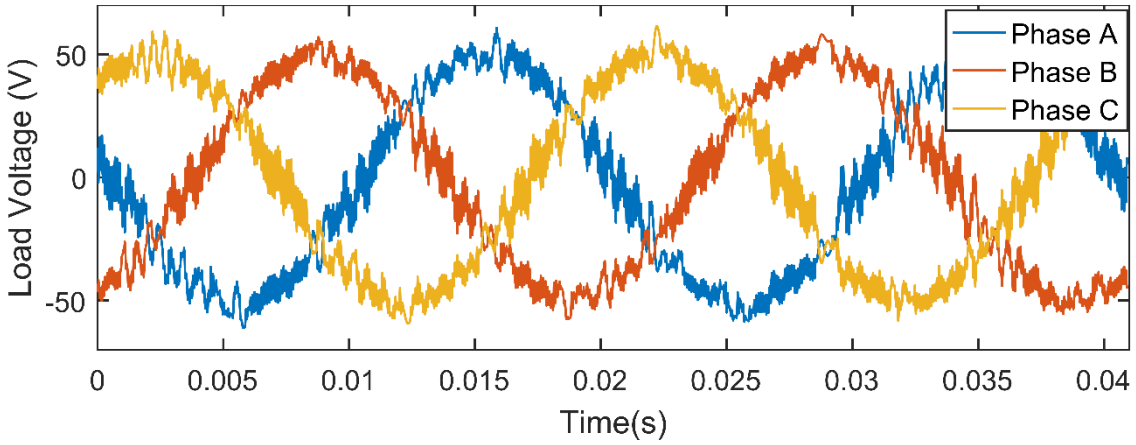

Figure 3-12 Load Voltage

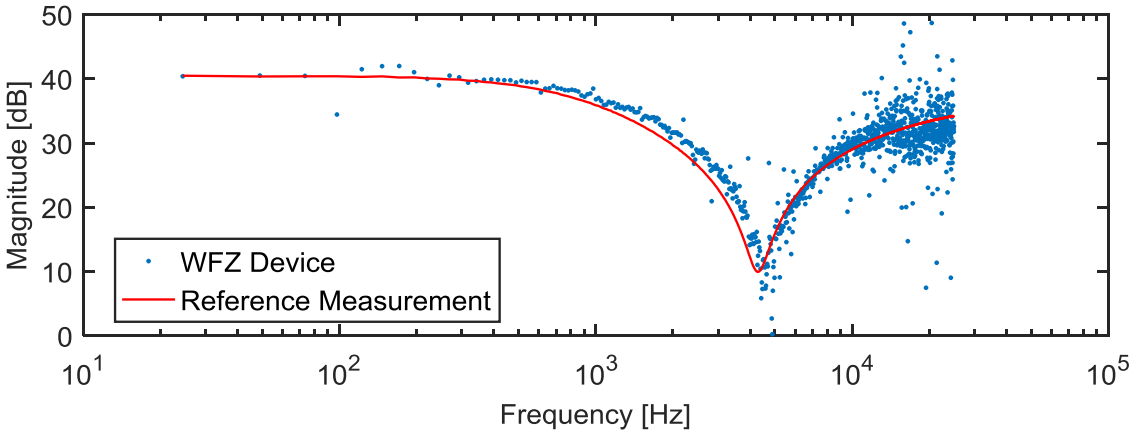

Figure 3-13 D-axis Impedance - Magnitude

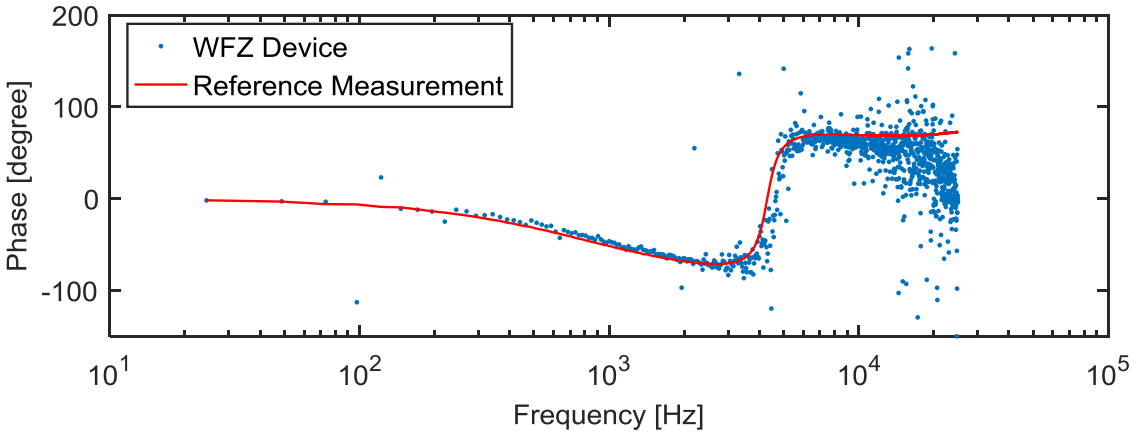

Figure 3-14 D axis Impedance – Phase

Wideband grid impedance measurement is a novel concept for power grids and currently no such wideband frequency grid impedance measurement devices exist in the market. The accuracy of the overall device depends on the accuracy of the voltage, current measurement units and Analog to Digital Converters (ADCs). A wideband grid impedance device is developed within RESERVE project for trialling in Aachen Lab and Irish grid. Details of the device are explained in Section 3.5. Since wideband grid impedance is a complex number defined over a frequency grid, the accuracy of the impedance measurement can be evaluated by complex curve fitting techniques. A known passive networks impedance is first measured using a highly accurate frequency analyser $Z_m(f_i)$ following which the impedance data points obtained from the impedance measurement device $Z_m(f_i)$ can be used to calculate the norm η defined in (3-2**)**. Here N refers to the number of points in the frequency grid.

$$\eta = \frac{1}{N}\sum_{i=1}^{i=N}\left|\frac{Z_m(f_i) - Z_{act}(f_i)}{Z_{act}(f_i)}\right|^2 \quad (3\text{-}2)$$

About 50 experiments are conducted and the impedance deviation norm is calculated to determine the closeness of the measured impedance and reference impedance obtained from a high precision network analyser. Since the proposed device is highly accurate until 10 kHz, the impedance deviation norm is calculated until 10 kHz. The variation of η is presented in Figure 3-15. It can be observed that the device offers high precision since almost all the norm values are close to the mean. Figure 3-16 shows the normalized probability of the norm for the 50 experiments. The mean of the norm is 1.21 and the standard deviation σ is 0.03 which is indicative of high accuracy and precision of the device.

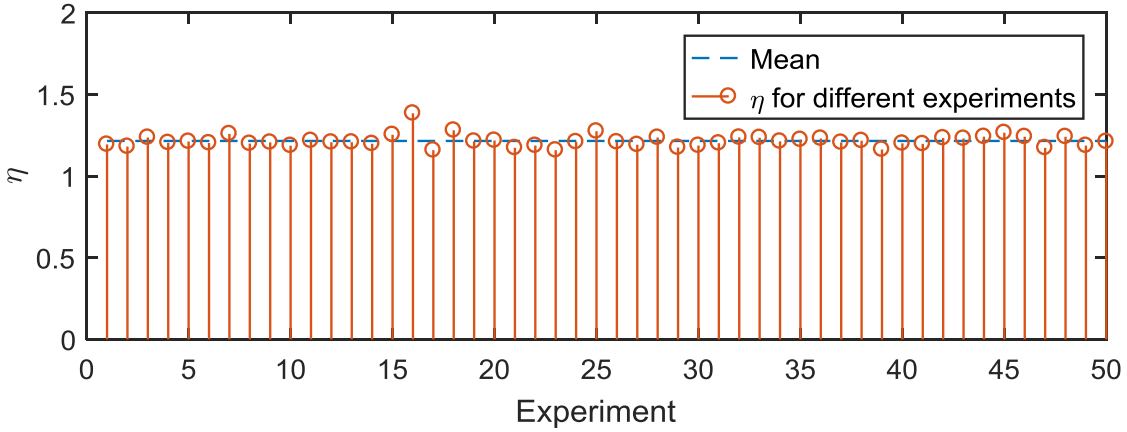

Figure 3-15 Variation of Impedance Deviation Norm

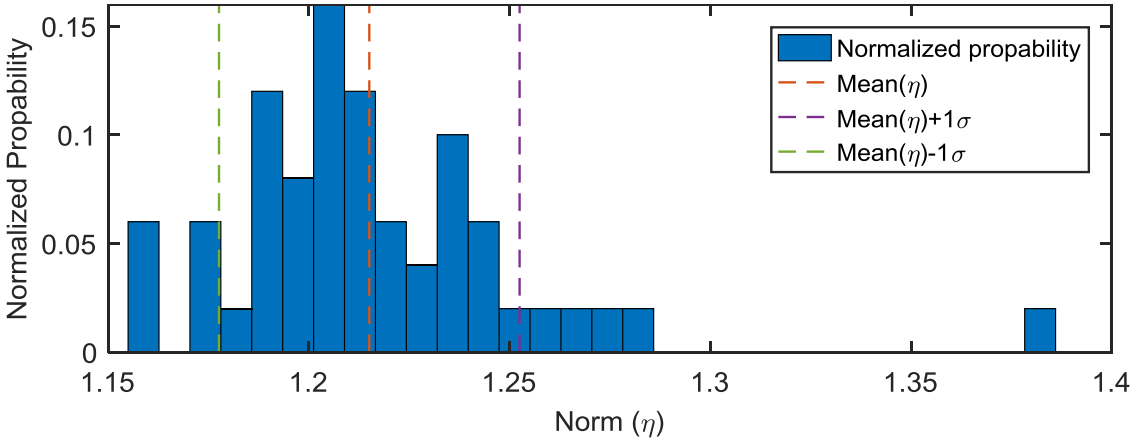

Figure 3-16 Uncertainty evaluation of WFZ device

3.7 Consideration of Solid-State Transformers with DVSM technique – An Outlook

RESERVE proposes decentralised voltage control solution for a power-electronics driven grid mainly considering household PV inverters. Currently, DSOs extensively use OLTCs for voltage regulation, however recent trend in research is towards Solid-State Transformers (SST). The RESERVE approaches are still valid and extendable to SSTs. This section presents an overview on the application of DVSM for SSTs.

3.7.1 Why SSTs would replace OLTCs

The migration towards volatile and distributed energy resources (DERs) enforces the need to have improved interconnection and interaction of LV and MV distribution networks. Currently, OLTCs are used to regulate the LV grid voltage and power flow is unidirectional – from MV to LV side. Dynamics of OLTCs are very slow ranging between 1 to 3 seconds and therefore cannot handle the dynamics arsing due to DERs. Advantages associated with SSTs over OLTCs are listed below:

- Since it is power-electronic based, it enables fast power flow dynamics and possess bidirectional capability
- Significant reduction in both cost and weight
- Can provide provide reactive power support to both MV and LV sides
- Current limiting
- Improved power quality on both MV and LV sides owing to high switching frequerncy since active filtering can be done to grid currents
- Management of storage elemtents or connection to an external DC grid from the DC link of the SST

Thus, due to the numerous inherent and operational advantages, SSTs will mostly likely replace OLTCs. In the subsequent subsections, basic structure and functioning of SST is explained and how the RESERVE approach of VOI control can be applied to SST such that it enables stable interaction between and MV and LV side is briefed.

3.7.2 Description of SST

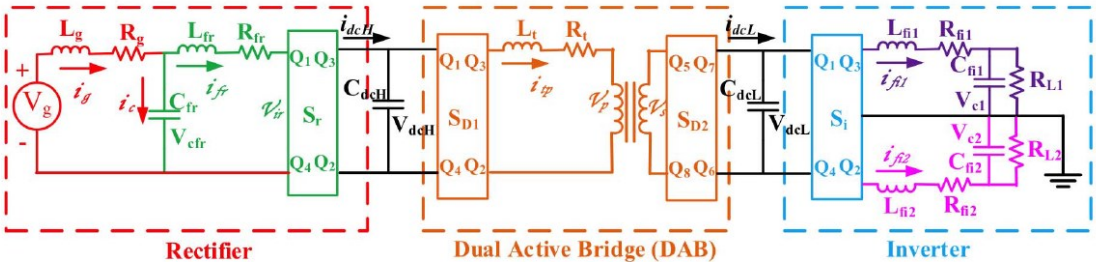

Figure 3-17 Solid State Transformer [26]

SST consists of a rectifier, a DC/DC converter and an Inverter as shown in Figure 3-17. The DC/DC converter in Figure 3-17 is based on the Dual Active Bridge (DAB) topology.

Control Objective of:

- **Rectifier:** Controls the DC output voltage of the rectifier to the desired value, which is also the input side voltage for the DC/DC Converter. Power factor of this converter can be close to 1.
- **DC/DC Converter:** Controls the DC output voltage of the DC/DC converter to the desired value.
- **Inverter:** Controls the AC side line voltage to the desired value of the LV distribution grid.

3.7.3 Extension of proposed VOI approaches for SSTs

Concept: The DVSM technique proposed in RESERVE for RES Inverters can be applied to the rectifier and inverter at the input and output stages of SSTs for controlling and enhancing the interaction between MV and LV side.

Figure 3-18 shows the VOI control technique applied to the rectifier of the SST at the interface node of MV Grid and SST. The controller of SST can use its WSI tool to inject perturbations to the control loop of Rectifier which enables the rectifier to inject bandlimited white noise to the grid. WSI tool can be used to measure the MV side grid impedance $Z_{MV,grid}$. Thus, using the VOI control technique explained in D3.5, the rectifier can modify its impedance to mitigate harmonic instabilities.

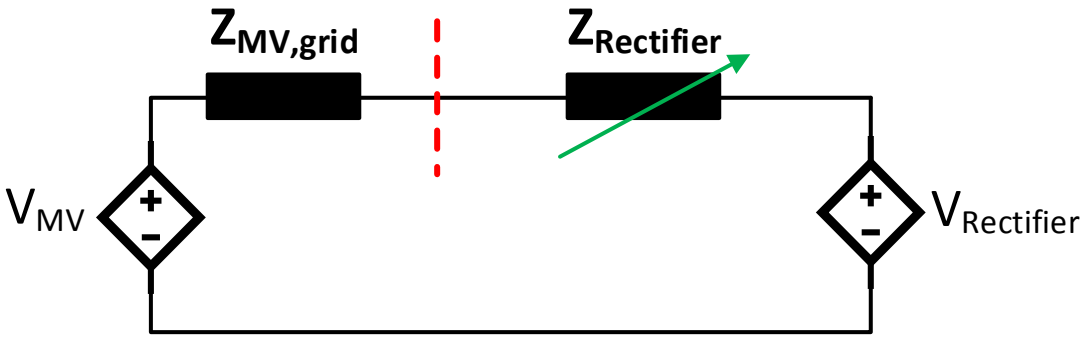

Figure 3-18 VOI applied to Rectifier: MV grid - SST interface

In a similar stability by design approach, the harmonic instabilities at the SST – LV grid interface can be prevented. The inverter can use its WSI tool to measure the low voltage grid impedance (the Thevenin equivalent impedance of the entire LV section) and modify its output impedance by the VOI design approach of D3.5. Figure 3-19 shows the VOI control technique applied to the inverter of SST.

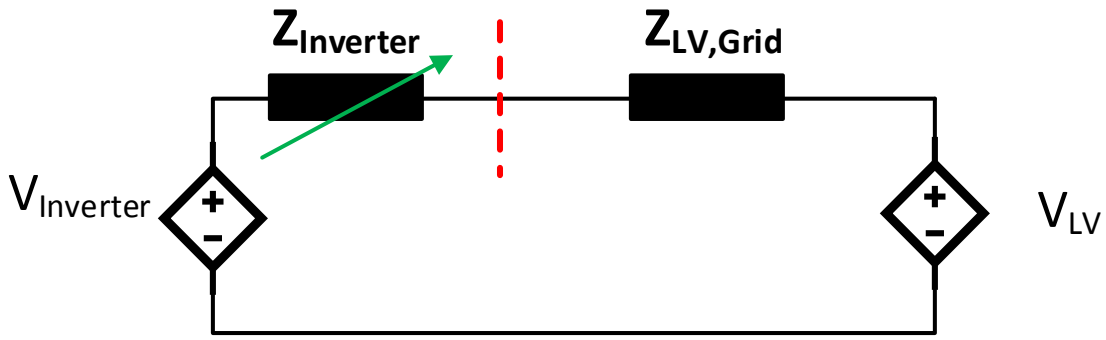

Figure 3-19 VOI applied to Inverter: LV grid - SST interface

Summarising Dynamic Requirements on SSTs

- Bidirectional power transfer capsbility MV ←→ LV
- Reactive Power can be either be absorbed/injected by the Rectifier/Inverter to maintain the desired AC side line voltages on both LV and MV side
- DC/DC Converter topology needs to be bidirectional (eg. Dual Actve Bridge is bidirectional) for enabling bidirectional power transfer. Advantages such as galvanic isolation and high efficiency of the DC/DC converter is highly desirable
- Impedance measurement to be integrated on both Rectifier/Inverter to monitor both the LV side and MV side grid impedances
- Adaptive VOI control concept for both Rectifier and Inverter: to adapt to grid impedance change to actively mitigate harmonic resonance

3.8 Conclusion

This chapter proposes the network codes from the outcome of the technical work of scenario SV_A Dynamic Voltage Stability Monitoring. A set of 5 network codes are proposed covering various aspects of the scenario from a DSO perspective and from that of the RES inverter. We propose a change in the way DSOs operate and monitor the status of the grid. Furthermore, a 5G ICT driven decentralised control of RES inverters is proposed for the inverters. The 5 most important network codes identified which are relevant to SV_A is provided below:

- NC.14 Decentralised Voltage Control
- NC.18 Leading Power Factor Operation
- NC.17 Dynamic Stability Margins
- NC.15 Requirements for new behaviour of RES inverters
- NC.16 New requirements for the perturbations injected from RES inverters

Through the work in RESERVE, a highly programmable inverter prototype is developed which is operated as an impedance measurement. A patent is pending for this invention and a US based company is discussing to build a product based on this device and its concepts.

The RWTH inverter has been successfully operated and trialled in grid connected mode in Aachen lab. The results of the Aachen lab trial and the impending Irish Field Trials will be documented in D5.3.

4. ICT Test/Validations to NC proposed in SV_A and SV_B

4.1 Active Voltage Management in the field

To ascertain the level impact of the AVM on Network Codes in real world implementations, it is important to provide details of the ICT architectures used and challenges faced while deploying and monitoring the AVM and its ancillary services on the Irish trial sites. The following section will discuss the various challenges faced and solutions found when implementing the ICT architecture models defined in D3.6 in the various trial sites and detail the monitoring system developed to observe the AVM implementation so that its impact on the Network Codes could be assessed.

4.1.1 AVM Monitoring Dashboard

Given that the implementation of the AVM is carried out on Low Voltage sections of the grid network the impact of the AVM was difficult to measure due to a lack of visibility from a DSO perspective. This led to the integration of the trial site implementation of the AVM into Servo Live a component of the ESB's cloud-based Servo Platform. Servo Live, in brief, is comprised of a set of cloud based functions that receives, and stores live data from field devices like those used in the implementation AVM. Servo Live has a public domain so it can be accessed as long as the user has an internet connection. The communication protocols it allows are limited to SSH, HTTP, HTTPS and MQTT. This is to restrict bad actors from exploiting potential vulnerabilities of other protocols. SSH requires a user to be white-listed and only server admins can use or need to use this protocol. HTTP traffic is redirected to its more secure form HTTPS which encrypts data in transit between the user and server. MQTT is used to listen for the data being sent between RES devices and AVM execution service, which requires connecting to a password protected message broker that encrypts its payload, similar to how HTTPS encrypts its data. The overall access can be considered highly secure as all the points where the server is publicly accessed have at least user validation or data encryption, if not both in place.

At present there are two type of user that can access Servo Live, a basic user can that access the Servo Live Dashboard via user name and password access via HTTPS and the server admin user that, as stated above will require white listed SSH access to the server. The role of the basic user has primarily read only access that will allow the user configure graph set-up, view data and request data downloads from the application. The role of the server admin user is more centred around the configuration of the system in terms of the configuration of Volt-Var Curves and MQTT endpoints and the deployment of the underlying services that constitute the Servo Live system. These underlying services, Grafana, Nginx, InfluxDB and Subscriber, are responsible for reading and storing data, so it can be accessed by the required system components.

The **Subscriber** service is responsible for collecting the payloads being sent through the MQTT message broker. It currently collects the following information: values sent from RES device, calculated set-point sent from AVM execution service, Volt-Var Curve used for the above calculation and Grid Connection status of RES device (for Battery Sites).

Once collected data is then stored in the **InfluxDB** service. This service is a time-series database, meaning it stores its data in chronological order, making the data easier to graph. The **Grafana** service provides a graphical interface, as seen in Figure 4-1, enabling the visual display of the previously mentioned payload information. Grafana is a software tool with the purpose of displaying values in various ways and has a library of plugins freely available. It's open source so it can be freely downloaded and run on a private server. This service reads in the data from InfluxDB every 10 seconds and updates the graphs accordingly, due to how InfluxDB stores the data it is easy to graph it chronologically. To restrict access to the readings a user is required to login via username and password. Once logged in the user can access the various live feeds for each site and download the data in a CSV format to use for analysis. The **Nginx** service is responsible for making the dashboard accessible via the public internet and ensures that the data is encrypted as it is in transit between user and server. It redirects all HTTP traffic to HTTPS to ensure that the user does not send unencrypted data over the public internet. All HTTPS traffic is directed to the Grafana service, where the user can then log in and view the live readings from the various trial sites. Nginx uses locally hosted TLS certs, which enable the use of HTTPS, the certs are generated with a service known as Certbot which is recognised by most internet browsers. When browsers don't recognise a valid TLS cert it will warn the user that a websites cert is not trustworthy. If a cert is expired or missing, then the browser will warn the user that any information they send to the website will be unencrypted and exposed in transit. With the

implementation of these certs all outgoing and incoming traffic is secured and the user is protected from possible malicious duplicate websites.

Figure 4-1: Servo Live Dashboard

The data that is made available to Servo Live is very much driven by the capabilities of the inverter or measuring device at the trial site and also the configuration of the Subscriber to receive these messages, but if they have been collected they are available for visualisation via read-only configuration on the Servo Live dashboard. To monitor the performance of the AVM and its validation with the NCs, a sample set of values are gathered and displayed such as:

- Voltage readings from the trial site;
- Active Power readings from the trial site;
- Reactive Power readings from the trial site;
- Set Points derived from the Volt VAr curve sent down to the inverter.

4.1.2 Centralised Trial Sites

In D3.6 section 3.1.2.1 we detailed a centralised implementation architecture of the AVM (Figure 4-2) and from an ICT perspective, three out of the six trial sites are considered centralised. The first one to go live was the Kilumney Trial Site and it provided a number of challenges which we had to be able to find solutions to. All three centralised sites involved communicating with a Renewable Battery which belongs to a third-party aggregator company. To communicate with and regulate those batteries, a number of criteria had to be met, which were out of the scope of the original plans.

Originally, it was devised that the set-point would be a relative value -- i.e. the set-point would be a value between +1.0 and -1.0 and the RES device was expected to increase/decrease its reactive power by that amount. However due to certain constraints of the aggregator, an absolute set-point value had to be implemented as the RES device needed a value it can target. Calculating an absolute value involves a more complex algorithm and a variety of energy readings. In addition to the voltage readings, we required Active Power and Reactive Power readings. This was not a major challenge as the aggregator already had access to these readings and could easily add them to the payload, they were sending via MQTT.

With the new set of readings resolved, the revised algorithm provided by UCD was then implemented into the execution service. One additional challenge we faced at this stage was mapping the correct algorithm to each trial site. While the centralised sites required an absolute value, the AVM is also used in the simulation trials which requires a relative set-point.

As each site and simulation has a unique MQTT topic to send data through, we resolved this issue by relating the algorithm to the MQTT topic. Thanks to this particular issue the execution service is now able to facilitate multiple scenarios that require different set-points.

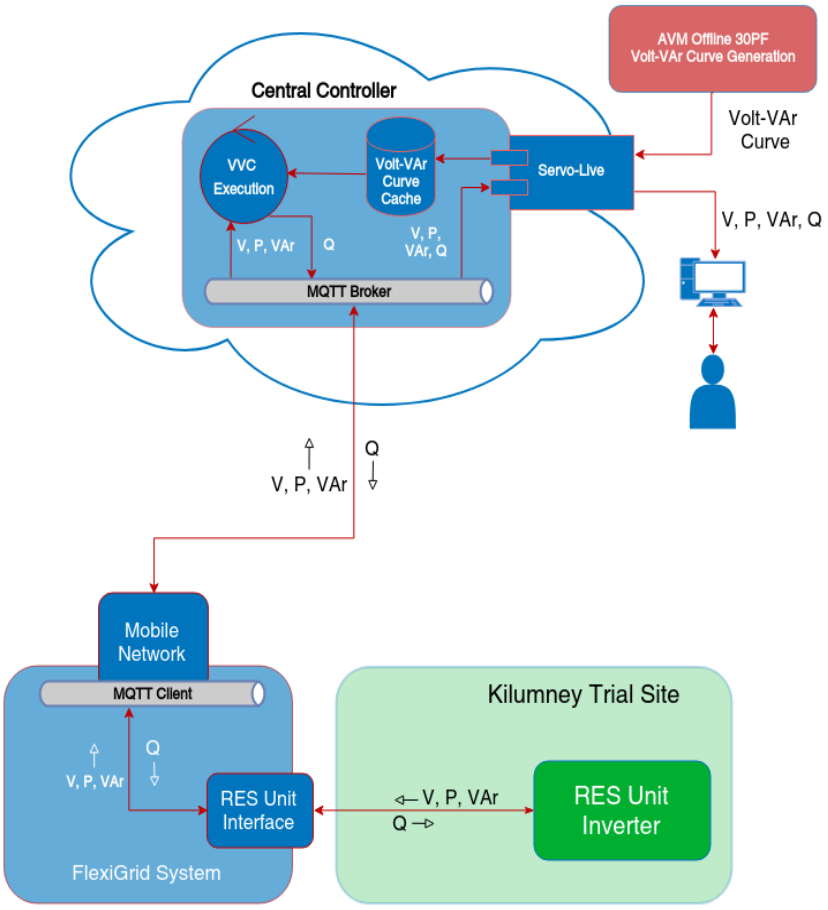

Figure 4-2: Centralised Implementation of the AVM

4.1.3 Decentralised Trial Sites

The remaining three sites are classified as decentralised, detailed ion D3.6 section 3.1.2.2, as all of the voltage management takes place on site and not in a remote server. The RES devices on two sites only require the supply of the volt-var curve as they have more advanced inverters that can self-regulate their voltage output. There is still the need for monitoring the devices output which requires the addition of a device that can read the data and publish to servo-live.

The Vehicle to Grid (V2G) trial site required the most configuration for two main reasons. Unlike the other decentralised sites, the V2G charge point was unable to dynamically regulate its voltage and it has to be provided with a Power Factor value. This was already expected and planned for in the decentralised model detailed in Figure 4-3 so not much was altered.

There were a few additions to ensure the measurements and calculations could be read via the Servo Live dashboard. The AVM execution service is running on the Raspberry Pi but is utilised more as a plug-in instead of running as a fully independent service, making it applicable to wider range of scenarios.

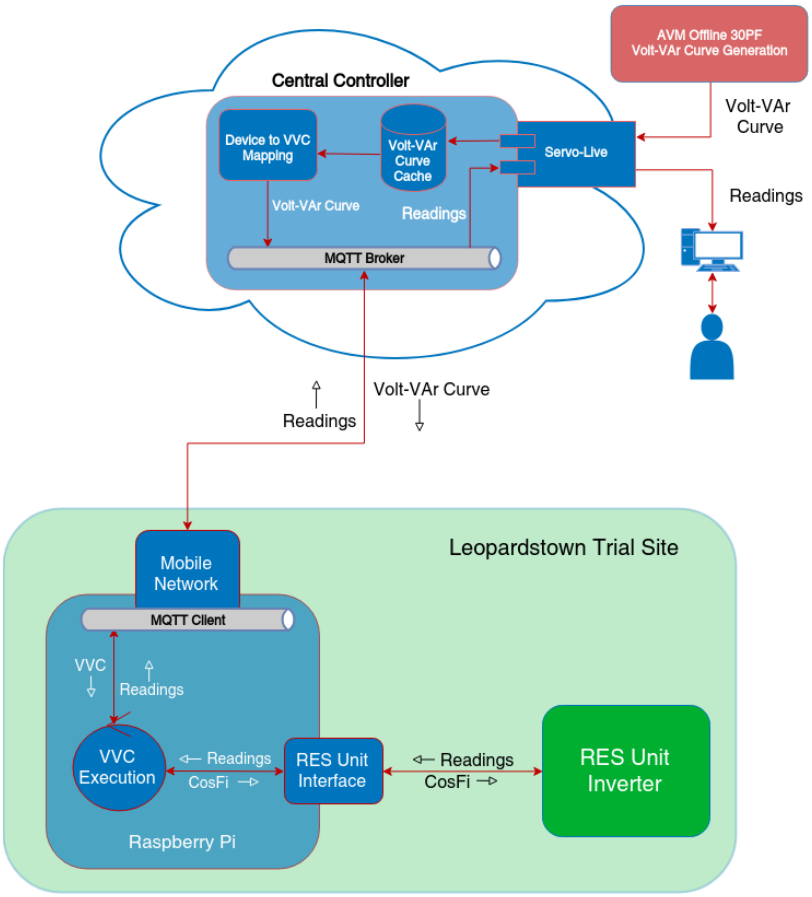

Figure 4-3: Decentralised AVM Implementation

4.1.4 Hybrid Edge Computing Trial Proposal

The Hybrid Mobile Edge Computing architecture, as described in D3.6 section 3.1.2.3 and illustrated in Figure 4-4, is designed to leverage the distributed communications available throughout the electrical network and to leverage mobile edge computing technologies to implement the AVM in a more manageable and scalable way.

While there is no trial site to test this model, the experience gained from the previous trials can help provide a more robust hybrid trial by defining what needs to be included and relevant metrics to test and collect.

Firstly, it is important to have a central location where all relevant parties can view live readings and update VVCs easily for more efficient sets of testing. It allows for discussion between the project members to be clearer and understanding to be clearer as everyone has the same reference point.

As a hybrid model would be dealing with multiple sites, it can manage a variety of RES devices and should accommodate for the individual demands of each device to prove adaptability. With the execution service running on a server directly connected to a 5G base station, it will need scenarios that will require it to perform a variety of calculations such as a relative or absolute set-point or even the Power Factor. It should also be able to send a VVC to either the RES inverter or an edge device such as a Raspberry Pi. If it's able to handle these responsibilities, then its performance should be compared to a more centralised system.

The main reasoning for this model is to provide a solution that is much more scalable than a centralised version. To verify this as a scaling solution the ideal testing scenario involves increasing the load of a centralised model, gather various metrics and then split the same load between two hybrid models, gathering similar metrics. Important metrics to compare would be those laid out in D3.6 like Latency (ms), Packet Load (payload per second), Packet Loss (%), Security (Protocols).

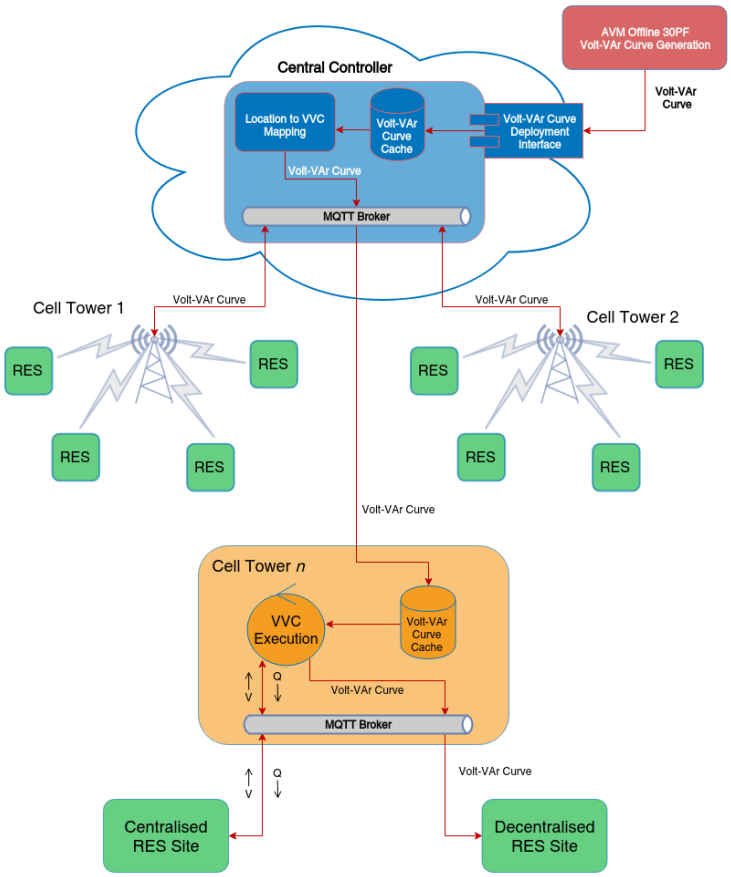

Figure 4-4: Hybrid Mobile Edge Computing AVM Implementation

4.2 5G solutions that should be considered by deployment of the Voltage techniques in Power Networks with high percentage of RESs

This section indicates the 5G solutions that should be considered by deploying of voltage control techniques developed in RESERVE in the power networks with high percentage of RES. These 5G solutions and their applicability to different voltage scenarios are described in further details in Deliverable D3.7.

Providing communications links to new end points in the energy system

Wireless communications systems, such as 5G, will offer cost-effective and easy to deploy solutions to supply communications over shorter distances to connect individual new assets which are part of the voltage management scenario to the mobile network. In a mobile wireless network, it is normal to have a fibre optic cable connecting each base station and antenna to the backbone of the 5G and general communications transmission system. This means that only the distance between the device (communications module or gateway) at the new asset (e.g. an inverter) and the nearest 5G base station antenna is actually communications over the air. Once the signal reaches the base station, it is transmitted further within the 5G and other communications networks to the intended receiver over fixed communications links. Note that receiver can be, e.g., edge cloud hundreds meters away from the device or the central cloud located hundreds of kilometers from the device.

Meeting latency requirements for packet delivery

In some scenarios it might be required that signals are to be transmitted in real time between communications end-points, the device and the receiver (control centre operating the algorithm), with the latency below than 10 ms. This level of latency is within the capabilities of a 5G wireless link with a high level of accuracy (that the packets sent arrive as sent without corruption) and reliability in the communications. Such low latencies could not be achieved with LTE or NBIoT communications features. Once the packets reach a fixed network, such as at the base station which transfer the packets to the mobile backbone transmission network, the determination of the latency in the fixed network connections will depend on the distance travelled and the delays introduction by the processing of packets in mobile and fixed network nodes in the communications path between sender and receiver. The packets are likely to be transferred from the mobile backbone transmission network to the networks of internet providers or communication links providers as part of their communication path to their destination. This delay would need to be investigated for specific solutions in a defined energy system architecture. For voltage control techniques with remote control units located hundreds of kilometres from the devices, such delays could be relevant.

Using edge cloud features to reduce the latency requirements and provide local hosting of algorithms

In order to reduce the requirements on latency over the wireless link, in order that a slower LTE network could be used, and also potentially, to enable hosting of the voltage calculation algorithm close to the assets, 5G Edge Cloud could be included in the architecture of appropriate communications solutions.

Use of communications friendly protocols to maximise the reliability of the communications

In majority of the voltage scenarios, the packets to be transmitted are probably of small size, of the order of magnitude of several hundred kilobits of information. The protocols used by the energy systems should preferably be chosen so that they optimise the efficiency of the use of the wireless communications channel. Examples of commonly used energy protocols which make efficient use of wireless communications channels include Message Queuing Telemetry Transport (MQTT) and Advanced Message Queuing Protocol (AMQP) and other Transmission Control Protocol (TCP) based protocols. Investigations by Ericsson of energy protocols concluded that the use of the Sampled Value protocol is not appropriate as this protocol does not confirm the arrival of packets. Other energy protocols, such as 61850 GOOSE can generate communications problems as it produces bursts of traffic which can suddenly overload wireless channels and cause delays in transmission.

Network Slicing for energy provider control of Quality of Service (QoS) and security features

If the energy provider wants to ensure the quality of service of the communication and the security of the communications on an end to end basis, they could use Network Slicing features of 5G networks to set their own priorities for communications resources reserved for their slice and to use whatever communications security mechanisms they consider appropriate. The 5G networks used could be privately owned by energy providers or could be public 5G networks, or any combination of the two.

Use of public 5G networks without network slicing and public 4G LTE networks

In a public 4/5G network, the bandwidth available is shared between many users without reservation of network resources resulting in the situation that if there is very heavy traffic load on the network, it is possible that network congestion may result in reduced reliability and increased latency of the communications. Complete loss of individual packets is possible in such rare circumstances.

Mobile networks for massive IoT communications

In certain scenarios with not stringent requirements, e.g., if the long geographical distances exist between RESs and central controller, or the latency is not critical (the latency higher than few tenths of miliseconds), 4G, 5G or NBIoT networks can be utilised.

If components requiring communications are in very deep basements (more than 2-3 levels below ground, or in rooms with particularly heavy concrete walls, the penetration of the LTE or NBIoT communications devices may require the deployment of small repeaters, with cabled connections, to ensure reliable communications.

5G networks will also provide excellent communications solutions for such scenarios. Repeaters for the indoor use of 5G spectrum will be introduced to the market in coming years ensuring that 5G will operate in deep basements and in buildings hosting critical infrastructures with reinforced wall

5. Validation and Assessment of Voltage Control in the Field

A core element of the RESERVE project was the validation of the Voltage control techniques developed in the project at various trial sites in Ireland. These trails validated both the Active Voltage Management (AVM) technique and the Virtual Output Impedance (VOIP) technique and where viable the Network Code modifications associated with each. The validation of Network Codes associated with the development and realisation of these control techniques are detailed in this chapter. These comprise (i) Network code recommendations for DER control considering voltage control strategies [associated with Chapter 2 of this document] and (ii) Network code recommendation from power electronic stability criteria and online system monitoring perspective [associated with Chapter 3 of this document].

5.1 Field Trials of Network Code Recommendations for DER Control Considering Voltage Control Strategies

Network code recommendations for DER control considering voltage control strategies were driven by the requirement to accommodate the Active Voltage Management (AVM) control technique developed in the RESERVE project. In contrast to the requirement of the Virtual Output Impedance control technique to develop a new prototype inverter, the Active Voltage Management (AVM) Field Trials can be implemented using existing commercially available inverter technology. Electricity generation and storage technologies are experiencing significant and accelerating demand as the focus on decarbonisation and increased electrification intensifies globally. Many of these new technologies include inverters due to the fact they are coupling DC based devices to external AC networks. This presents a distinct opportunity for the AVM control technique as it can leverage inverter technology that is already being deployed for other purposes without requiring installations purely dedicated to its realisation. Indeed many of the system stability challenges which the AVM technique has been designed to alleviate are themselves exacerbated by a proliferation of new electricity generation and storage installations. Realisation of the AVM technique should both facilitate the installation of these new installations and allow for ever more intensive deployment on existing networks without requiring the level of investment associated with traditional electrical network capacity uprating.

In selecting specific technologies for the AVM Field Trials, it was decided to mix more established technologies such as Solar PV with more cutting edge technologies such as Vehicle 2 Grid chargers. These selections will allow us to compare and contrast the impact of technologies on the effectiveness of the control technique across a range of network configurations located in both rural and urban environments. All AVM trial sites are located in Ireland connected to low voltage distribution networks which are operated by a single Distribution System Operator, ESB Networks. This has allowed for standardised, connection design, and monitoring and will facilitate consistent analysis of network impact.

5.2 Active Voltage Management Filed Trials

In contrast to the requirement of the Virtual Output Impedance control technique to develop a new prototype inverter, the Active Voltage Management (AVM) Field Trials can be implemented using existing commercially available inverter technology. Electricity generation and storage technologies are experiencing significant and accelerating demand as the focus on decarbonisation and increased electrification intensifies globally. Many of these new technologies include inverters due to the fact they are coupling DC based devices to external AC networks. This presents a distinct opportunity for the AVM control technique as it can leverage inverter technology that is already being deployed for other purposes without requiring installations purely dedicated to its realisation. Indeed many of the system stability challenges which the AVM technique has been designed to alleviate are themselves exacerbated by a proliferation of new electricity generation and storage installations. Realisation of the AVM technique should both facilitate the installation of these new installations and allow for ever more intensive deployment on existing networks without requiring the level of investment associated with traditional electrical network capacity uprating.

In selecting specific technologies for the AVM Filed Trials, it was decided to mix more established technologies such as Solar PV with more cutting edge technologies such as Vehicle 2 Grid chargers. These selections will allow us to compare and contrast the impact of technologies on the effectiveness of the control technique across a range of network configurations located in both

rural and urban environments. All AVM trial sites are located in Ireland connected to low voltage distribution networks which are operated by a single Distribution System Operator, ESB Networks. This has allowed for standardised, connection design, and monitoring and will facilitate consistent analysis of network impact.

5.2.1 Domestic Battery Field Trials

Due to the fact that electricity networks require instantaneous demand to be met by instantaneous generation the rise of intermittent renewable generation poses a complex problem. One potential solution to variable generation is the option of energy storage. Domestic scale Battery Storage systems provide a potential solution to this problem. Such systems require an inverter to couple the DC battery to the external AC network and thus are suitable for deployment of the AVM control technique.

Three separate buildings which incorporate Domestic Scale Battery systems were included as trail sites in the project. The sites comprise a mixture of domestic and institutional premises located in both urban and rural settings, some with local small scale generation in place and each with a unique local distribution network configuration. A range of 10 - 12 kVA Li-Ion batteries has been installed at each of the locations. The diverse mixture of usage profiles at each of these locations coupled with the parallel engagement of a commercial aggregator in the operation of the battery systems has produced interesting results with regard to the benefit of the AVM control technique across a range of scenarios.

Figure 5-1 Battery Storage System installed at a rural Domestic Dwelling

5.2.2 Solar PV Field Trial

Of the inverter based technologies which are part of the RESERVE AVM Field Trials, Solar PV Arrays are possibly the most mature (see Figure 5-2) . In line with this level of market maturity, techniques for communication with and the control of ‘smart’ inverters associated with PV installations are quite advanced. The RESERVE AVM Solar PV Array Trial Site is located at the ESBN’s National Training Centre in Portlaoise, Co Laois. It comprises a 7.2 kW Ground Mounted Solar PV Array connected via two independent single phase inverters. The ‘smart’ single phase inverters are capable of deploying the AVM control technique in a decentralised model using the in-built functions of the inverters themselves.

Figure 5-2 Solar PV Array in NTC, Portlaoise.

5.2.3 V2G Field Trial

A move towards increased use of electric vehicles is a key component of transportation focused decarbonisation strategies. A further evolution beyond direct vehicle charging is the development of technologies that can provide bi-directional (i.e. both charge an electric vehicle and extract charge for injection back into the grid) which are known as Vehicle to Grid (V2G) chargers. Unlike standard unidirectional AC chargers, V2G systems require inverters in order to couple the eVs DC storage to the AC network and are thus suitable for the AVM solution. The RESERVE Field Trial V2G Charger installation is located at the ESB offices in Leopardstown Dublin. It is the first known V2G installation located in Ireland. The device itself is rated at 10 kVA for both charging and discharging and connect to EVs over the CHAdeMO charging protocol.

Figure 5-3 V2G Charger Trial Site in Leopardstown, Dublin, Ireland.

5.2.4 Results – Validation of Network Code Proposals

The delivery of field trials in Ireland succeeded in implementing and validating the AVM Control technique. In addition, the field trials served to validate a number of the Network Code proposals developed in the RESERVE project under real-world conditions. The Network Code proposals which were successfully validated in the Irish Field Trials are detailed below;

NC. 14: Decentralised Voltage Control

The implemented trial sites deployed a mixture of centralised and decentralised control architectures. The flexibility afforded by this menu of options allowed for the customisation of solutions for each trial site technology. The domestic scale battery trial sites, at which the inverter based equipment was owned by a commercial aggregator, were better suited to a centralised control scheme which allowed the AVM control scheme to be implemented in the cloud and avoided the installation of additional equipment locally at each site. In the case of the V2G trial site the relative immaturity of the device's control hardware necessitated the deployment of additional hardware locally to the device in order extract measure and apply AVM mandated set-points. This local hardware implementation also facilitated the AVM control scheme to be implemented at the device itself where it operated independently of external control thus implementing a decentralised architecture. This implementation proved effective in applying the AVM control technique and successfully demonstrated the implementation of decentralised voltage control in a real-world environment.

NC. 18: Reactive Power Capability of Distributed Generators

The permitted range of power factors for all devices, other than Wind Turbines, connected at Distribution Voltages is currently restricted to lagging power factors only. In Ireland this range is currently mandated as falling between 0.95 lagging and unity. This restricted range evolved from the traditionally correct assumption that all domestic and industrial loads are fundamentally inductive in nature. The technologies deployed at the RESERVE trial sites have a considerably greater performance range than traditional devices however and are thus capable of the controlled implementation of leading power factors.

The implementation of leading power factor was successfully implemented at RESERVE trial sites when mandated by the AVM control scheme. The successful implementation of a leading power factor can be viewed in Figure 5-4 which details the Voltage and Reactive Power performance of the inverter at the Killumney Domestic Scale Battery trial site. In the period between 12:54 and 12:58 the Voltage recorded at the trial site can be seen to fall from a stable 237 V to a nadir of less than 228 V. During this same period the AVM controlled inverter adjusted Reactive Power output to a point where the device exported Reactive Power. The generation/export of Reactive Power, with export value peaking at greater than 2 kVar, equates to a power factor 0.80 leading. The net impact on system Voltage can be seen in the rapid recovery of the voltage, with system voltage returning to 237 V by 13:10, following the implementation of a leading power factor.

Figure 5-4 Voltage and Reactive Power Performance at Killumney Battery Trial Site

5.3 Virtual Output Impedance (VOIP) Control Technique Field Trial

5.3.1 Overview

To test the algorithms proposed in the scenario Dynamic Voltage Stability Monitoring a new class of inverters are required. In this impedance-based approach the accurate measurement of grid impedance is a crucial step. A wideband system identification (WSI) tool has been developed to measure and extract the grid impedance by injecting small signal perturbations in the control of the inverter. The process of procuring such new class of inverters which does not exist in the market, externally, was not cost effective. Therefore, within the scope of the RESERVE project, RWTH developed a new inverter with the proposed functionalities of WSI and virtual output impedance (VOI) control algorithms.

5.3.2 Field Trial in Ireland

The new inverter developed by RWTH has been deployed at a SSAU in Ireland. The experimental setup to be used is shown in Figure 5-5. The low power inverter prototype is encapsulated within the red box.

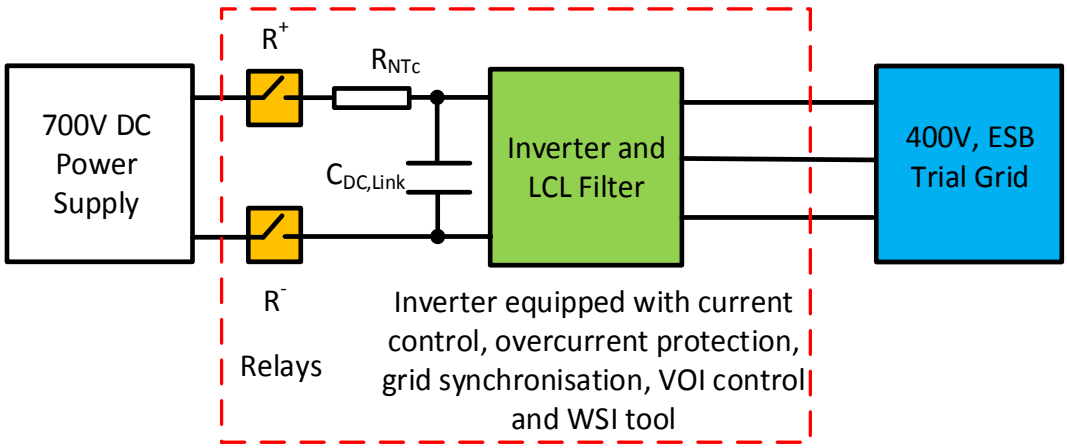

Figure 5-5 WFZ Device – Field Trial Set-up

The inverter will be operated in grid connected mode. PRBS noise will be injected for 40 ms (2 cycles) and simultaneously the voltage and current measurements are sampled. This data will be stored in a first-in-first-out (FIFO) buffer;

The stored voltage and current samples is used in the calculation of spectrum of impedance i.e., the magnitude and phase data points of the impedance are obtained for a wide range of frequencies.

The objectives of the field trial are:

(A) See the quality of extracted non-parametric impedance and evaluate the precision of the device

(B) study the impact of PRBS noise level on the extracted impedance

(D) Save data for future analysis, since we will develop stability analysis and VOI methods based on non-parametric impedance data. Such a data driven method will eradicate the requirement of system identification techniques wherein the system order needs to be predefined or assume.

The WFZ device was tested in Aachen lab with a passive load configuration and the device was evaluated for the accuracy in the measured impedance. Currently, the prototype is further tested and commissioned to operate in grid connected mode and a field trial is planned in Ireland during the first week of October 2019.

5.4 Recommendations on NC in presence of inverter-based DER

The ICT Communications recommendations are based on the requirements that were gathered and defined as part of activities in WP1 that examined the implementation of the AVM from a power systems perspective.

5.4.1 General NC features in presence of inverter-based DER

Network codes in Germany for inverter based DER mostly concentrate on power system aspects considering the interaction of the DER with the surrounding electrical distribution grid. In distribution grids, the DSO is mostly aware of holding the requirements on voltage quality in terms of voltage magnitudes, voltage unbalance and additionally on dynamic voltage stability aspects. Here, the main features that are considered can be summarized according to reactive power provision, requirements on asymmetric injection of power, adaption of active power with respect to frequency and dynamic grid support in case of a fault (e.g. short-circuit or earth fault). Thresholds and requirements on operational features considering grid interaction are therefore included in NC for low and medium voltage distribution grids. According to the German law § 9 EEG [35] larger DERs with 100kW (solar with 30kW) connected to HV and MV levels, like wind and solar power plants but also combined heat and power plants (CHPs), need to be included in a communication network, radio- or cable-based, as the DSO must have the capability to remotely control reactive power and apply curtailment.

This holds not true for small PV systems (<30kW, e.g. roof systems in LV level). In this case, a predefined reactive power characteristic is deployed and in some cases the PV injection is generally limited to 70% of the maximum power output.

5.4.2 Recommendations on ICT features in NC

In terms of ICT features, the NC in Germany do not give special recommendations with respect to integration of DER in a possible distribution grid automation. Anyway, as the number of DER is growing as well as their impact, in terms of voltage level and line current capacity, on system operation, their ability to control voltage and support in stabilizing the electricity grid requires guidelines on communication interface and structure. Consequently, aspects of ICT should be included in future NC to account for the ability of decentralized inverter-based DER. It should be stated upfront that an inclusion of hard requirements for the ICT features in NC would not be meaningful, as many different configurations and algorithms for implementation of the mentioned ancillary services like voltage control exist. In this context, an evaluation of the performance of different solutions with hard criteria is not easy to set and therefore generic recommendations on ICT features should be included as defined in the following sections.

The recommendations on general ICT aspects for each ancillary service can be regarded as guidelines for setting a common ground that is independent of the concrete implementation of the ICT structure and algorithms. Those aspects include:

- latency of the communication links (the time a data packet needs from the startpoint to its destination),
- message size (bursting protocols can cause congestions in the mobile network, especially in the older generations 2G and 3G),
- packet loss (different communication media have different probabilities of packet loss: e.g. in typical radio-based networks the chance to lose a packet is higher than in typical cable-based communication infrastructure),
- resilience (the ability to sustain high workloads and recover from disturbances and failures),
- data security (encryption and authentication) and volume (talkative protocols can congest weak communication links).

As the main focus of a DSO lies in the secure and sustainable energy supply, a special focus should be held to the high availability of the ICT system. As for example in Germany outage times per head per year are <13min, ICT system outage times should be below that value. At 99.999% this means 5.26 minutes maximum downtime per year [36].

In detail and based on our own requirements as defined in D3.7 “

Report on Requirements on scalable ICT to implement Voltage Control Concepts, V2” in Chapter 3.3, it is recommended for DSOs to setup a communication infrastructure, that allows for uni- and bi-directional communication, depending on the communication participants. The latency

recommendations are in the range of <10ms. The communication infrastructure should be able to support 1.000 devices locally and >10.000 system wide. For the power grid a high reliability in network availability and data transmission of 99.99% is to be aimed for. The support of a communication volume of at least 0.35 GB/s (up to 320kB per device for up to 1.000 devices as stated in Table 7 of D3.7 Ch. 3.3) is recommended system wide (in the data centre). For system critical infrastructure of course, a high end-to-end encryption and security is a very strong recommendation. For new communication infrastructure a DSO should aim for 20 years of operation. For the communication lightweight protocols are recommended. Good experiences have been made with MQTT (Message Queuing Telemetry Transport, an open message protocol for machine-to-machine communication) and AMQP (Advanced Message Queuing Protocol, an open standard application layer protocol for message-oriented middleware), while bad experiences have been made with the IEC 61850 GOOSE protocol (IEC 61850 is an international standard defining communication protocols for intelligent electronic devices at electrical substations; GOOSE is short for “Generic Object Oriented Substation Events”), which congests the communication network in case of message bursts.

6. Conclusion

This document describes the network code recommendations for successful implementation of the voltage control scenarios of RESERVE (SV_A and SV_B) in the future distribution networks with a high share of DERs.

Similarly, the network codes related to the dynamic voltage stability and control (scenario SV_A) are proposed and explained from both DSO perspective and the perspective of the DER inverter. The role of a 5G ICT driven decentralised control of DER inverters is proposed for the inverters. These suggestions are validated via simulations and field trials. The 5 most important network codes identified which are relevant to SV_A is provided below:

- NC.14 Decentralised Voltage Control
- NC.18 Leading Power Factor Operation
- NC.17 Dynamic Stability Margins
- NC.15 Requirements for new behaviour of RES inverters
- NC.16 New requirements for the perturbations injected from RES inverters

Similarly, some network code suggestions were proposed to support the successful implementation of the static voltage control (SV_B). According to these recommendations, the reactive power capability of different DER technologies are formulated and mathematically explained. It can be concluded that the decentralised control approach can be achieved using the VVC strategy as demonstrated by the field trials (WP5).

The 4 most important network codes identified which are relevant to SV_B is provided below:

- NC.3 Distribution system – voltage control
- NC.14 Decentralized voltage control
- NC.15 Requirements for new behaviour of RES inverters
- NC.18 Leading power factor

Both control scenarios require the successful sending and receiving signals to/from DER units. This highlights the needs for the availability of a reliable communication infrastructure in the futuristic distribution networks. Both proposed SV_A and SV_B techniques are validated to ensure that the DER Units are reacting as expected, whether it is a single/multiple RES Units on the same LV network.

7. References

[1] Zambia, “ZAMBIAN DISTRIBUTION GRID CODE,” 2016.

[2] Energinet.dk, “Technical regulation 3.2.5 for wind power plants with a power output greater than 11 kw,” 2010.

[3] T. T. GmbH, “Grid Code, - High and extra high voltage,” 2015.

[4] UK, “National Grid code,” 2017.

[5] ESB, “Distribution code,” 2016.

[6] Egyptian Distribution Network, “Solar Energy Plants Grid Connection code,” 2017.

[7] M. Braun *et al.*, “Is the distribution grid ready to accept large-scale photovoltaic deployment? State of the art, progress, and future prospects,” in *Progress in Photovoltaics: Research and Applications*, 2012.

[8] NERC, “Reliability Guideline BPS-Connected Inverter-Based Resource Performance,” 2018.

[9] H. (Cooper D. A. Markiewicz and A. (Wroclaw U. of T. Klajn, “Voltage Disturbances Standard EN 50160,” 2004.

[10] Y. Liu, J. Bebic, B. Kroposki, J. De Bedout, and W. Ren, “Distribution system voltage performance analysis for high-penetration PV,” in *2008 IEEE Energy 2030 Conference, ENERGY 2008*, 2008.

[11] CIGRE, “Capacity of Distribution Feeders for Hosting Distributed Energy Resources,” 2014.

[12] K. McKenna and A. Keane, “Open and Closed-Loop Residential Load Models for Assessment of Conservation Voltage Reduction,” *IEEE Trans. Power Syst.*, vol. PP, no. 99, 2016.

[13] Q. Wang *et al.*, “Hybrid control strategy of grid-tied inverter for harmonic and reactive power compensation,” in *Proceedings of the 13th IEEE Conference on Industrial Electronics and Applications, ICIEA 2018*, 2018.

[14] P. Garcia, M. Sumner, A. Navarro-Rodriguez, J. M. Guerrero, and J. Garcia, “Observer-Based Pulsed Signal Injection for Grid Impedance Estimation in Three-Phase Systems,” *IEEE Trans. Ind. Electron.*, 2018.

[15] X. Wang, F. Blaabjerg, and W. Wu, “Modeling and analysis of harmonic stability in an AC power-electronics- based power system,” *IEEE Trans. Power Electron.*, 2014.

[16] A. O’Connell, “Unbalanced distribution system voltage optimisation,” in *PES Innovative Smart Grid Technologies Conference Europe (ISGT-Europe), 2016 IEEE*, 2016, pp. 1–6.

[17] P. Richardson, D. Flynn, and A. Keane, “Local Versus Centralized Charging Strategies for Electric Vehicles in Low Voltage Distribution Systems,” *Smart Grid, IEEE Transactions on*, vol. 3, no. 2. pp. 1020–1028, 2012.

[18] A. O’Connell, D. Flynn, and A. Keane, “Rolling Multi-Period Optimization to Control Electric Vehicle Charging in Distribution Networks,” *IEEE Trans. Power Syst.*, vol. 29, no. 1, pp. 340–348, 2014.

[19] M. Bakhtvar and A. Keane, “A study of operation strategy of small scale heat storage devices in residential distribution feeders,” in *PES Innovative Smart Grid Technologies Conference Europe (ISGT-Europe), 2017 IEEE*, 2017, pp. 1–6.

[20] L. Abdullah, “Fuzzy Multi Criteria Decision Making and its Applications: A Brief Review of Category,” *Procedia - Soc. Behav. Sci.*, 2013.

[21] C. Kahraman, “Multi-Criteria Decision Making,” *Fuzzy Multi-Criteria Decis. Mak.*, 2008.

[22] C. Long and L. F. Ochoa, “Voltage control of PV-rich LV networks: OLTC-fitted transformer and capacitor banks,” *IEEE Trans. Power Syst.*, 2016.

[23] A. Soroudi, P. Siano, and A. Keane, “Optimal DR and ESS scheduling for distribution

losses payments minimization under electricity price uncertainty," *IEEE Trans. Smart Grid*, 2016.

[24] A. O'Connell and A. Keane, "Volt-var curves for photovoltaic inverters in distribution systems," *IET Gener. Transm. Distrib.*, vol. 11, no. 3, pp. 730–739, 2017.

[25] M. Cupelli *et al.*, "Port Controlled Hamiltonian Modelling and IDA-PBC Control of Dual Active Bridge Converters for DC Microgrids," *IEEE Trans. Ind. Electron.*, 2019.

[26] R. V Meshram, M. Bhagwat, S. Khade, S. R. Wagh, A. M. Stanković, and N. M. Singh, "Port-controlled phasor hamiltonian modeling and IDA-PBC control of solid-state transformer," *IEEE Trans. Control Syst. Technol.*, vol. 27, no. 1, pp. 161–174, 2017.

[27] M. Cupelli, S. Bhanderi, S. K. Gurumurthy, and A. Monti, "A Structure Preserving Approach for Control of Future Distribution Grids and Microgrids Guaranteeing Large Signal Stability," in *2018 IEEE Conference on Control Technology and Applications (CCTA)*, 2018, pp. 1166–1173.

[28] ESBN, "Distribution Code, Version 2.0," 2007.

[29] S. K. Gurumurthy, M. Cupelli, and A. Monti, "A Generalized Framework for Synthesizing Virtual Output Impedance Control of Grid Integrated Power Electronic Converters," in *2018 IEEE International Conference on Power Electronics, Drives and Energy Systems (PEDES)*, 2018, pp. 1–6.

[30] A. Monti, S. K. Gurumurthy, R. Uhl, and M. Pitz, "Vorrichtung zur Bestimmung der Impedanz in Abhängigkeit der Frequenz eines zu messenden Versorgungsnetzes," DE 10 2019 214 533.7, 2019.

[31] M. Bienholz and G. Griepentrog, "Wide-Band Impedance Measurement for converter impedance determination in LV-Grids," in *2018 20th European Conference on Power Electronics and Applications (EPE'18 ECCE Europe)*, 2018, p. P-1.

[32] T. T. Do, M. Jordan, H. Langkowski, and D. Schulz, "Novel grid impedance measurement setups in electrical power systems," in *Applied Measurements for Power Systems (AMPS), 2016 IEEE International Workshop on*, 2016, pp. 1–6.

[33] M. Jordan, F. Grumm, H. Langkowski, T. Do Thanh, and D. Schulz, "Online network impedance identification with wave-package and inter-harmonic signals," in *Nonsinusoidal Currents and Compensation (ISNCC), 2015 International School on*, 2015, pp. 1–6.

[34] S. K. Gurumurthy, R. Uhl, M. Pitz, F. Ponci, and A. Monti, "Non-Invasive Wideband-frequency Grid Impedance Measurement Device," in *IEEE AMPS*, 2019.

[35] EEG, "No Title." [Online]. Available: https://www.gesetze-im-internet.de/eeg_2014/__9.html.

[36] Wikipedia, "No Title." [Online]. Available: https://en.wikipedia.org/wiki/High_availability.

8. Abbreviations

AVM Active Voltage Management
B2B Business to Business
BMS Building management system
CAPEX CAPital EXpenditure
CENELEC European Committee for Electro technical Standardization
CEP Complex Event Processing
COTS Commercial off-the-shelf
CPMS Charge Point Management System
CSA Cloud Security Alliance
CSV Comma Separated Values
DEMS Decentralised energy management system
DER Distributed Energy Resources
DMS Distribution Management System
DMTF Distributed Management Taskforce
DSE Domain Specific Enabler
DSO Distribution System Operator
EAC Exploitation Activities Coordinator
ERP Enterprise Resource Planning
ESB Electricity Supply Board
ESCO Energy Service Companies
ESO European Standardisation Organisations
ESS Energy Storage Systems
ETP European Technology Platform
ETSI European Telecommunications Standards Institute
GE Generic Enabler
GNC Generalised Nyquist Criterion
HEMS Home Energy Management System
HiL Hardware in the Loop
HTTP HyperText Transfer Protocol
HTTPS HyperText Transfer Protocol Secure
HV High Voltage
I2ND Interfaces to the Network and Devices
ICT Information and Communication Technology
IEC International Electro-technical Commission
IoT Internet of Things
KPI Key Performance Indicator
LTE Long Term Evolution
LV Low Voltage
M2M Machine to Machine

MPLS Multiprotocol Label Switching
MV Medium Voltage
NB-IoT Narrowband Internet of Things
NIST National Institute of Standards and Technology
O&M Operations and maintenance
OLTC On-load tap changing
OPEX OPerational Expenditure
OPF Optimal Power Flow
PCC Point of Common Coupling
PF Power Factor
PLL Phase Lock Loop
PM Project Manager
PMT Project Management Team
POC Point Of Connection
POI Points of Interest
PPP Public Private Partnership
PWM Pulse Width Modulation
PMU Phasor Measurement Unit
PV Photo Voltaic
QEG Quality Evaluation Group
QoS Quality of Service
RES Renewable Energy Source
RPP Renewable Power Production
S3C Service Capacity; Capability; Connectivity
SCADA Supervisory Control and Data Acquisition
SDH Synchronous Digital Hierarchy
SDN Software Defined Networks
SDOs Standards Development Organisations
SET Strategic Energy Technology
SET Strategic Energy Technology
SG-CG Smart Grid Coordination Group
SGSG Smart Grid Stakeholders Group
SME Small & Medium Enterprise
SoA State of the Art
SON Self Organizing Network
SRF Synchronous Reference Frame
SS Secondary Substation
SSAU Secondary Substation Automation Unit
SSH Secure Shell
TL Task Leader

TLS	Transport Layer Security
TM	Technical Manager
TRL	Technology Readiness Level
V2G	Vehicle-to-Grid
VPP	Virtual Power Plant
VVC	Volt-var Curve
VVO	Volt-var Optimisation
WP	Work Package
WPL	Work Package Leader

9. List of Figures

10. List of Tables

Simulation results

A.1 Simulation results regarding the PF limits for PV technology

The network under study is depicted in Figure 10-1. In this network it is assumed that all RES are PV units and the VVCs are obtained individually for optimizing the objective function (voltage unbalance).

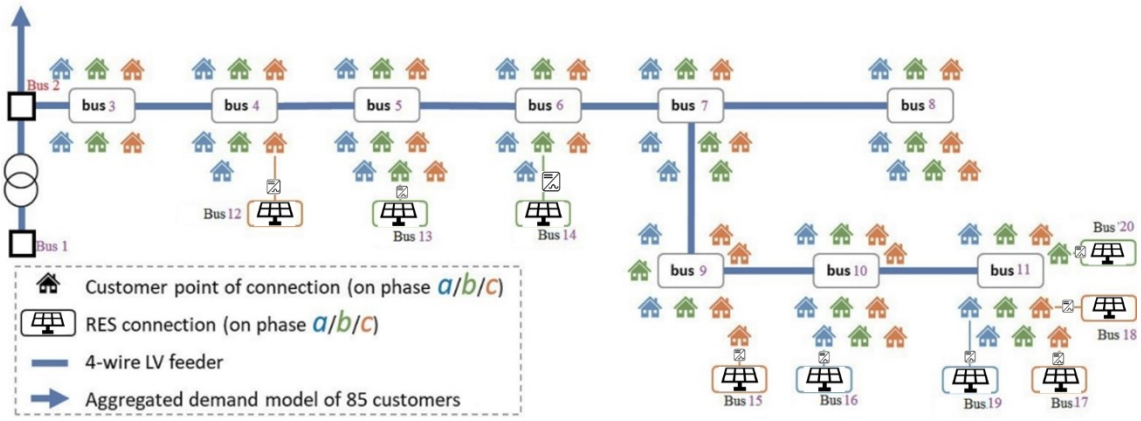

Figure 10-1 Three phase unbalance network under study

Several cases have been simulated as follows:

Case a) In this case, it is assumed that the PV units can only provide active power (unity power factor). The average voltage unbalance is calculated equal to 0.018152. The total active losses are 226.9387 kWh. The reactive power capability curve is shown in Figure 10-2.

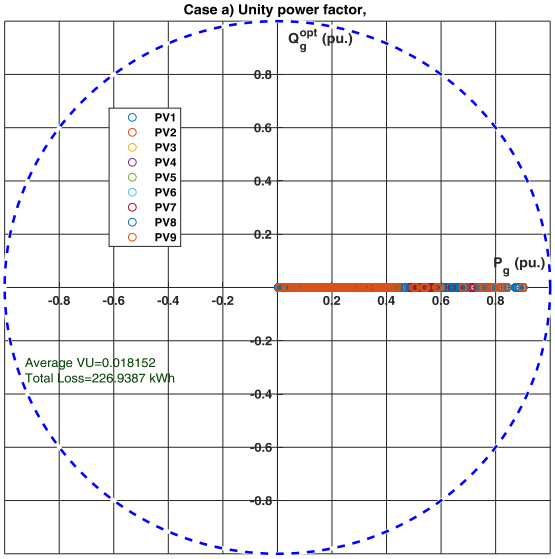

Figure 10-2 PQ capability curve of PV units with unity power factor

Case b) In this case, it is assumed that the PV units can provide lag/lead reactive power (with some limitations on the thermal capacity of the inverter). The average voltage unbalance is calculated equal to 0.010667. The total active losses are 245.764 kWh. The reactive power capability curve is shown in Figure 10-3.

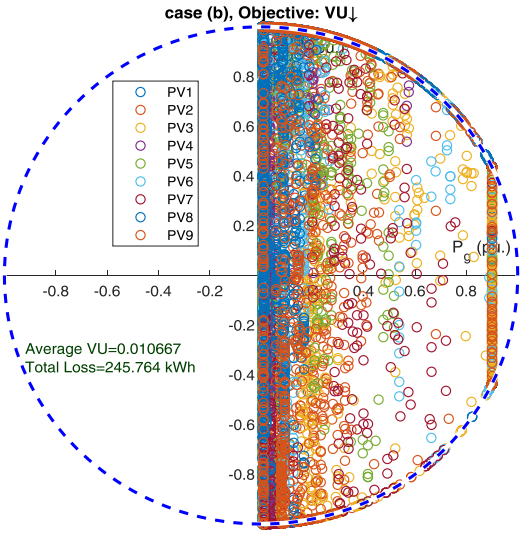

Figure 10-3 PQ capability curve of PV units with Lag/lead reactive power

Case c) In this case, it is assumed that the PV units can only provide lag reactive power (with no limitations on the reactive power). The only constraint is satisfying the thermal constraint of the inverter. The average voltage unbalance is calculated equal to 0.012174. The total active losses are 239.8162 kWh. The reactive power capability curve is shown in Figure 10-4.

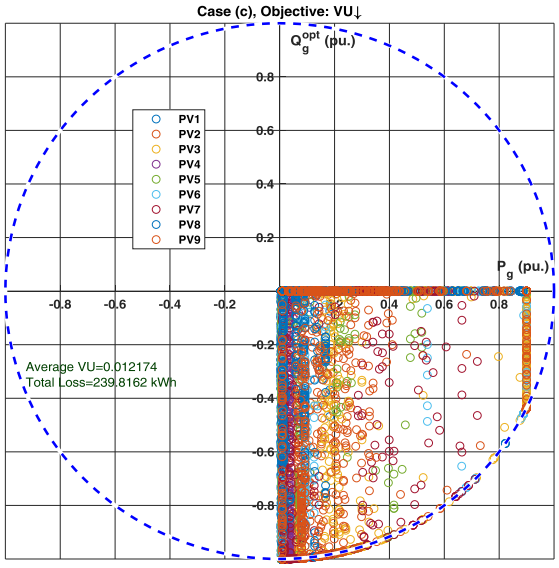

Figure 10-4 PQ capability curve of PV units with Lag reactive power

Case D) In this case, it is assumed that the PV units can only provide lag reactive power (with minimum 0.92 power factor). The average voltage unbalance is calculated equal to 0.014333. The total active losses are 229.5192 kWh. The reactive power capability curve is shown in Figure 10-5.

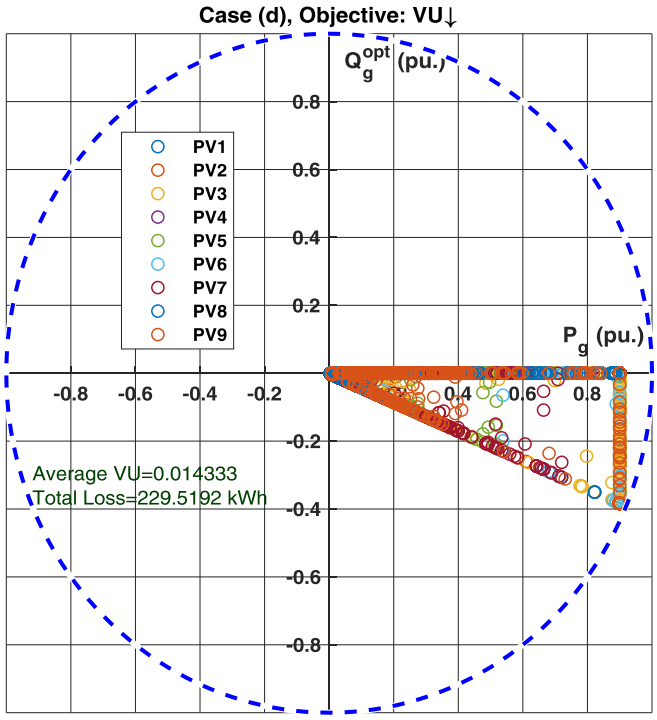

Figure 10-5 PQ capability curve of PV units with min 0.92 Lag power factor

Case e) In this case, it is assumed that the PV units can provide lag/lead reactive power (with some operational constraints of the inverter). The average voltage unbalance is calculated equal to 0.01183. The total active losses are 231.3975 kWh. The reactive power capability curve is shown in Figure 10-6.

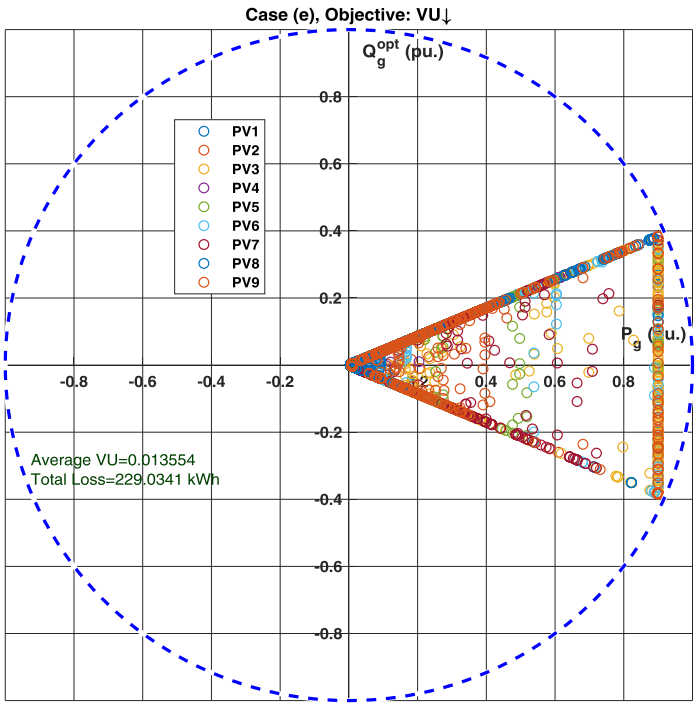

Figure 10-6 PQ capability curve of PV units with limitations on Lag/lead reactive power

The reactive power support of PV units in each case study is shown in Figure 10-7.

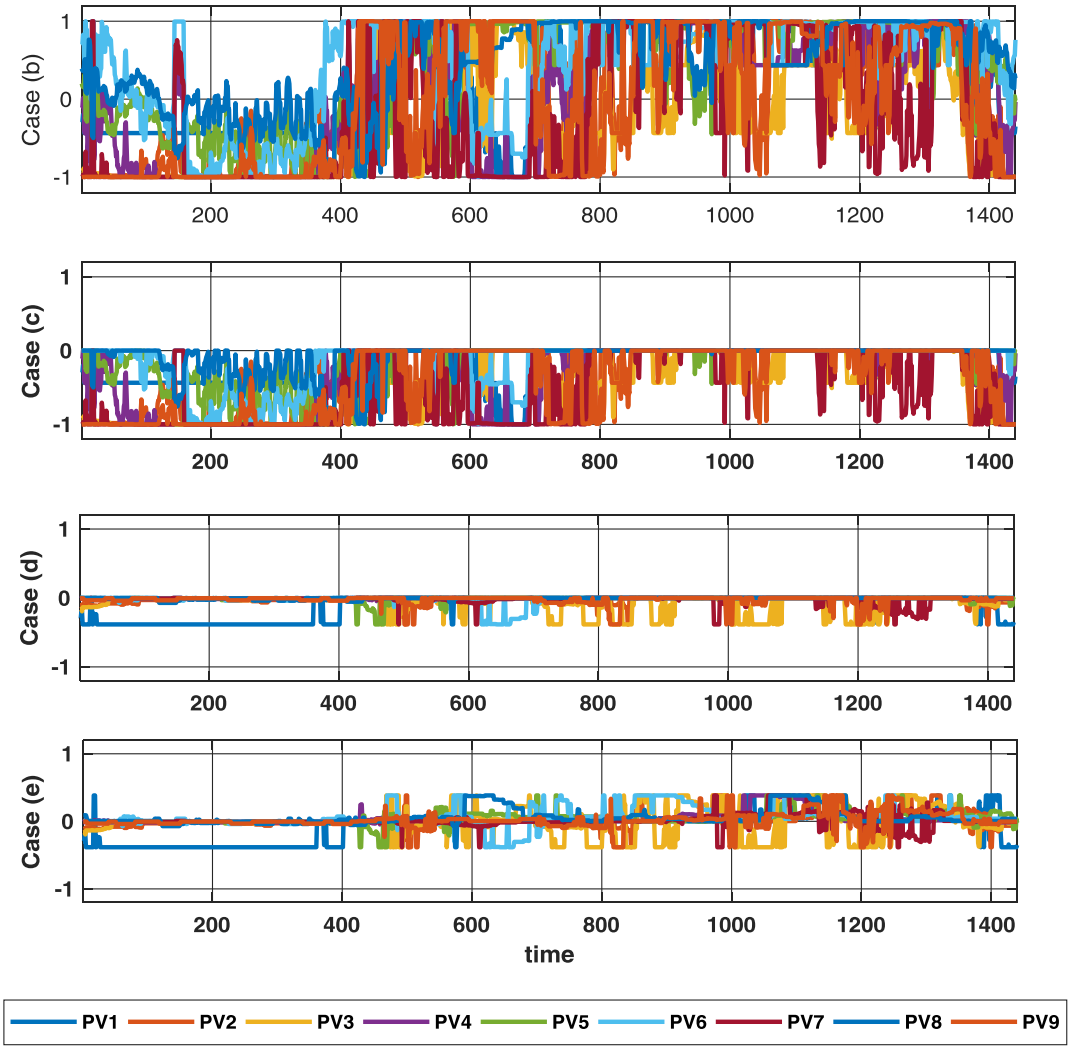

Figure 10-7 Reactive power support by PV units in each case study

The impacts of reactive power support of PV units on the network voltage magnitudes in phase **a** are shown in Figure 10-8.

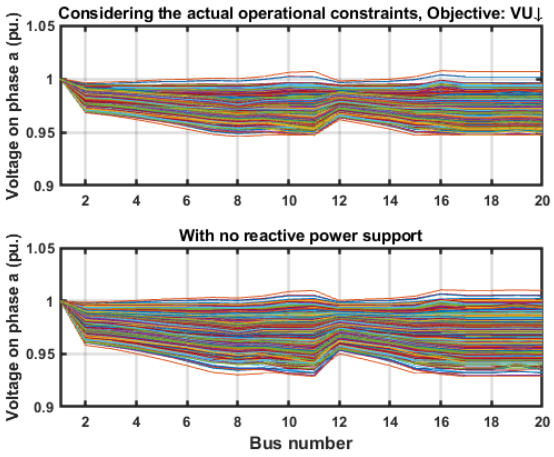

Figure 10-8 Voltage of phase (a) with/without reactive support of PV units

The impacts of reactive power support of PV units on the network voltage magnitudes in phase **b** are shown in Figure 10-9.

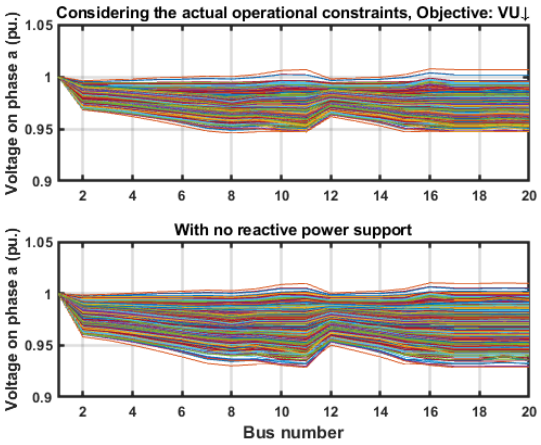

Figure 10-9 Voltage of phase (b) with/without reactive support of PV units

The impacts of reactive power support of PV units on the network voltage magnitudes in phase **c** are shown in Figure 10-10.

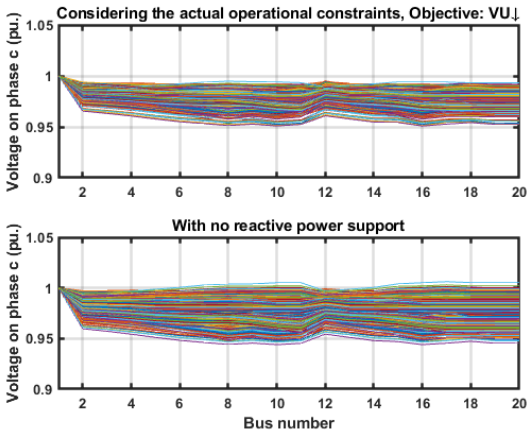

Figure 10-10 Voltage of phase (c) with/without reactive support of PV units

A.2 Simulation results on the effects of network characteristics

In this subsection, the results of applying the supervised decentralized voltage control is presented, when some of the controllable devices are not available during some periods. These will affect the optimal control strategies. The simulation is done on the sample three-phase unbalanced network as shown in Figure 10-11.

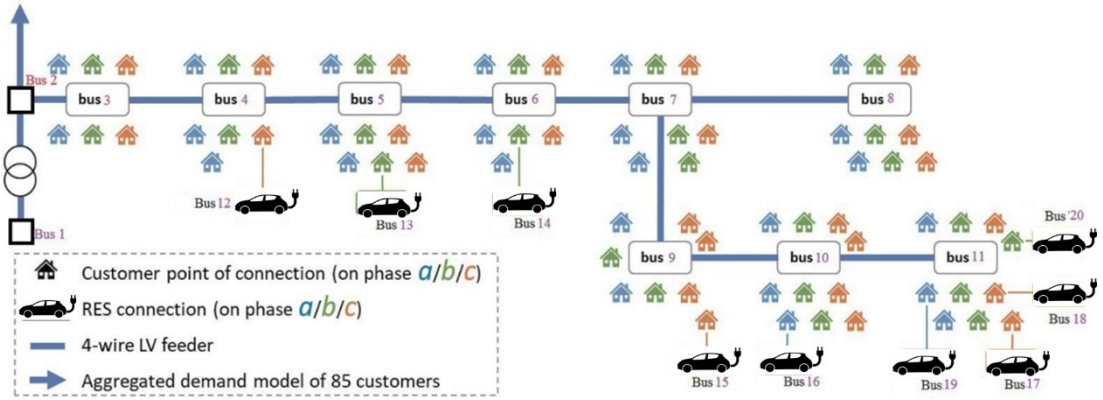

Figure 10-11 Sample three-phase unbalanced network with inverter based V2g

In order to analyse the effects that unavailability of some of the inverters have on the results of the active voltage management algorithm, first the VVCs are obtained in each connection state. A connection state is defined as a vector in which the availability of the controllable devices is specified.

In order to obtain the VVCs in case of the outage of each inverter (or probably a set of system inverters) a centralised offline simulation is conducted. The same steps as those provided in **D3.2** and **D3.3** is followed. For each possible connection state, a set of VVCs are extracted, each of which for a single controllable device.

After extracting the VVCs in each connection state, the results of applying the proposed adaptive AVM technique (which keep the VVCs' characteristics up-to-date whenever the system configuration changes) are compared with those obtained by applying the fixed VVCs which are not changed in varying system configuration.

The proposed adaptive active voltage management technique is tested on the same sample low voltage distribution system as the one which was introduced and used in **D3.3**. This system is a radial LV feeder with 85 nodes situated in Ireland [16]–[19]. The data required for conducting the simulations can be found in **D3.3** and also **D3.2**.

The inverter-based controllable devices which are considered to showcase the proposed algorithm in this subsection are nine inverter-based 2 kVA Vehicle to Grid (V2G) systems connected at different PCCs across the network of this sample system. The data on these V2G inverters can be found in **D3.3**. All the other assumptions were presented in **D3.3**. This makes it possible to compare the results of these studies to those obtained in **D3.3**. Similar to **D3.3**, in this chapter it is assumed that at the head of the feeder in the multi-scenario case, a separate feeder connection off the transformer supplies further 85 customers. The batteries of Electric Vehicles (EVs) have a considerable potential not only to provide energy for the locomotion of EVs, but also to dynamically interact with the low voltage electricity grids.

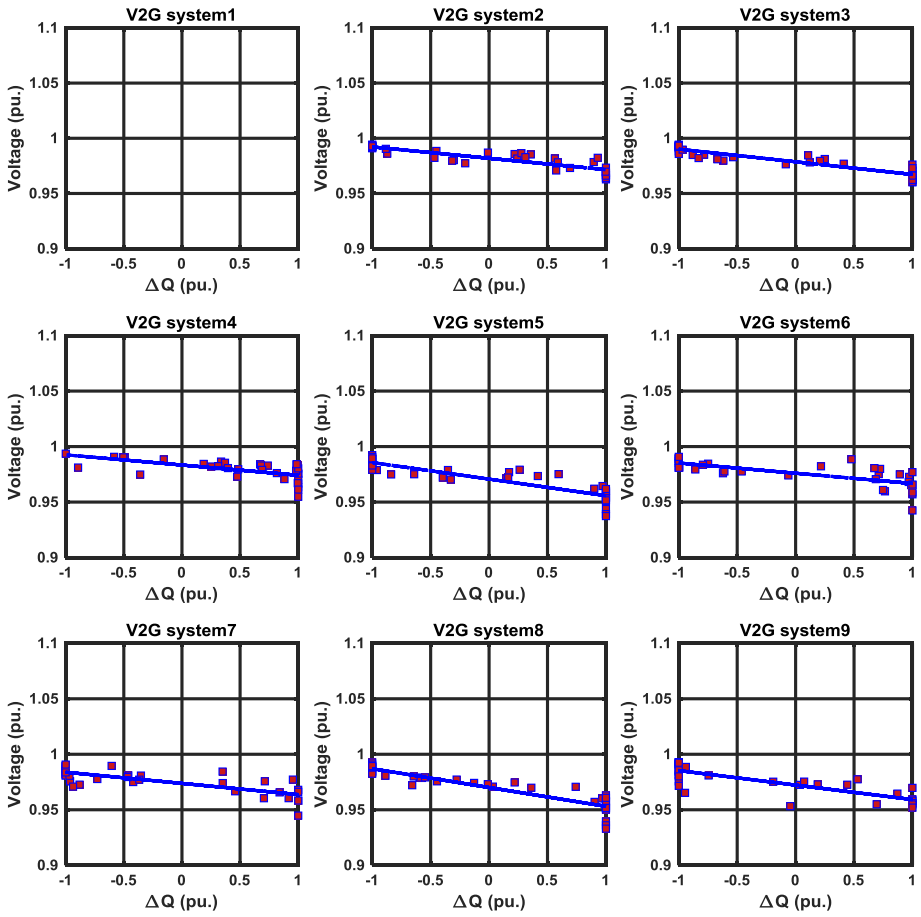

Figure 10-12 Resulting VVCs found for minimisation of voltage unbalance for V2G systems 2-9, showing intercepts and slopes assuming V2G system 1 is unavailable.

It is noticeable that a V2G system typically consumes active power, except for the systems for which both operation strategies and technical characteristics of the charging station allow battery discharge during some periods. The owners of the electric vehicles may also disagree with discharging their vehicles' batteries in the course of time that they left their vehicles to be charged at the charging station. More accurately, the interface between the distribution grid and the electrical vehicles, instead of using typical power converters that only work on unidirectional mode, need to use bidirectional power converters to charge the batteries (Grid-to-Vehicle capability) and to deliver a part of the stored energy in the batteries back to the power grid (Vehicle-to-Grid capability). A collaborative broker is needed to define and control the usage profiles. In that case, it is of utmost importance to take the requirements of the low voltage distribution systems and the convenience of the vehicle owners into account. In the simulations of this section, it has been assumed that the charging station only consumes active power. However, reactive power can be easily exchanged between the V2G system and the grid. In this fashion, the static under-voltage problem may arise as an important phenomenon that needs to be addressed. The active power consumption of the V2G systems may reduce the voltage levels at different load points of the distribution system lower than the values allowed according to the system standards. This necessitates higher levels of reactive power support that should be supplied by the V2G system inverters of the charging stations installed across the network to mitigate the unwanted voltage drop, especially at remote ends. An opposite phenomenon may be observed in distribution systems enabled with PV arrays at different connection points, since the high values of the active power injection (in case of high penetration of the solar production) may cause the voltage levels to rise.

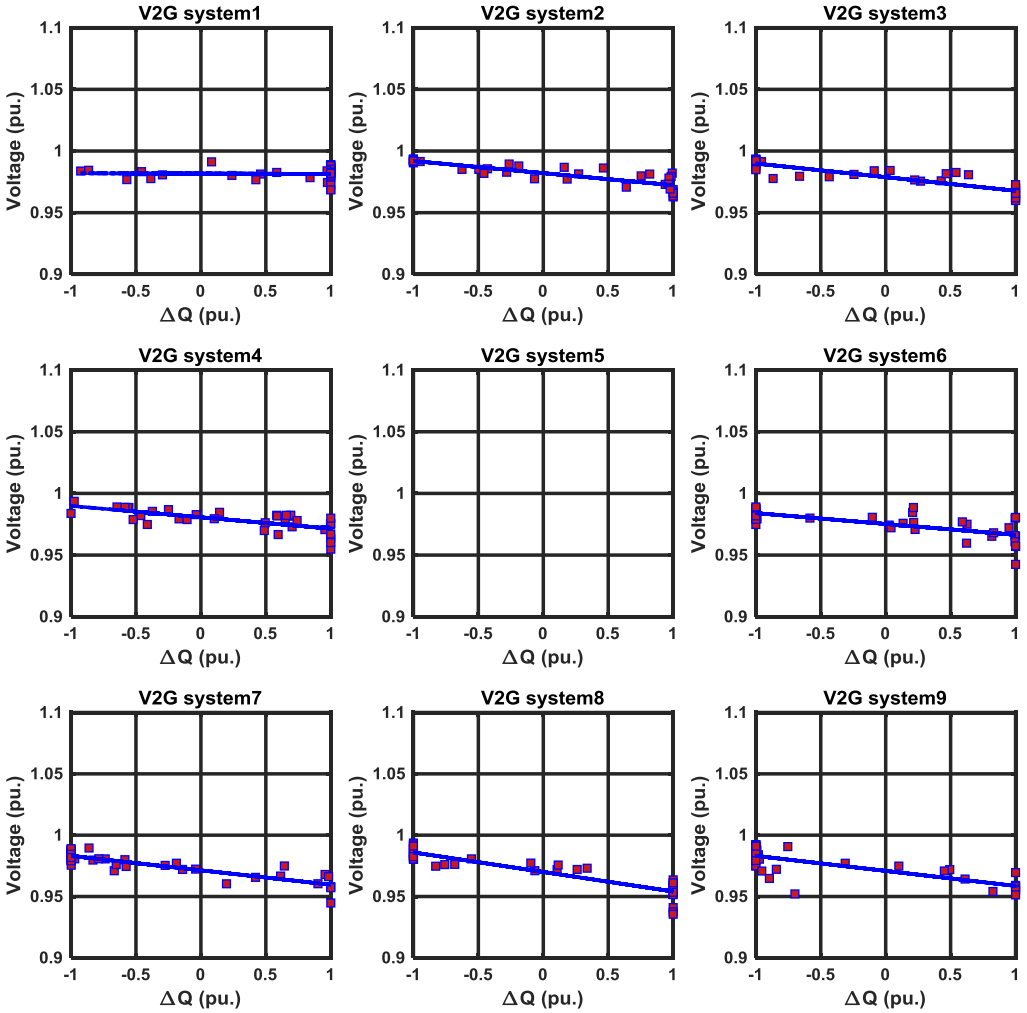

Figure 10-13 Resulting VVCs found for minimisation of voltage unbalance for V2G systems 1-4 and 6-9, showing intercepts and slopes assuming V2G system 5 is unavailable.

In **D3.3**, the VVCs were extracted for this system assuming all the inverters are available. Here, all the V2G systems are disconnected one by one and a set of VVCs are extracted for the system inverters. Figure 10-12 and Figure 10-13 show the VVCs when V2G system 1 and 5 are unavailable, respectively.

Figure 10-14 shows the optimal voltages found for the remaining system inverters in the case of the outage of each V2G systems. It should be noted that these optimal voltages should be considered as the voltage set-points in the voltage control mode of operation for the available inverters.

If the inverters follow these voltage set-points in the voltage control mode of operation, the results will be the same as those that are obtained in power control model of operation where the inverters are tasked with following the reactive power levels that are found using the extracted VVCs.

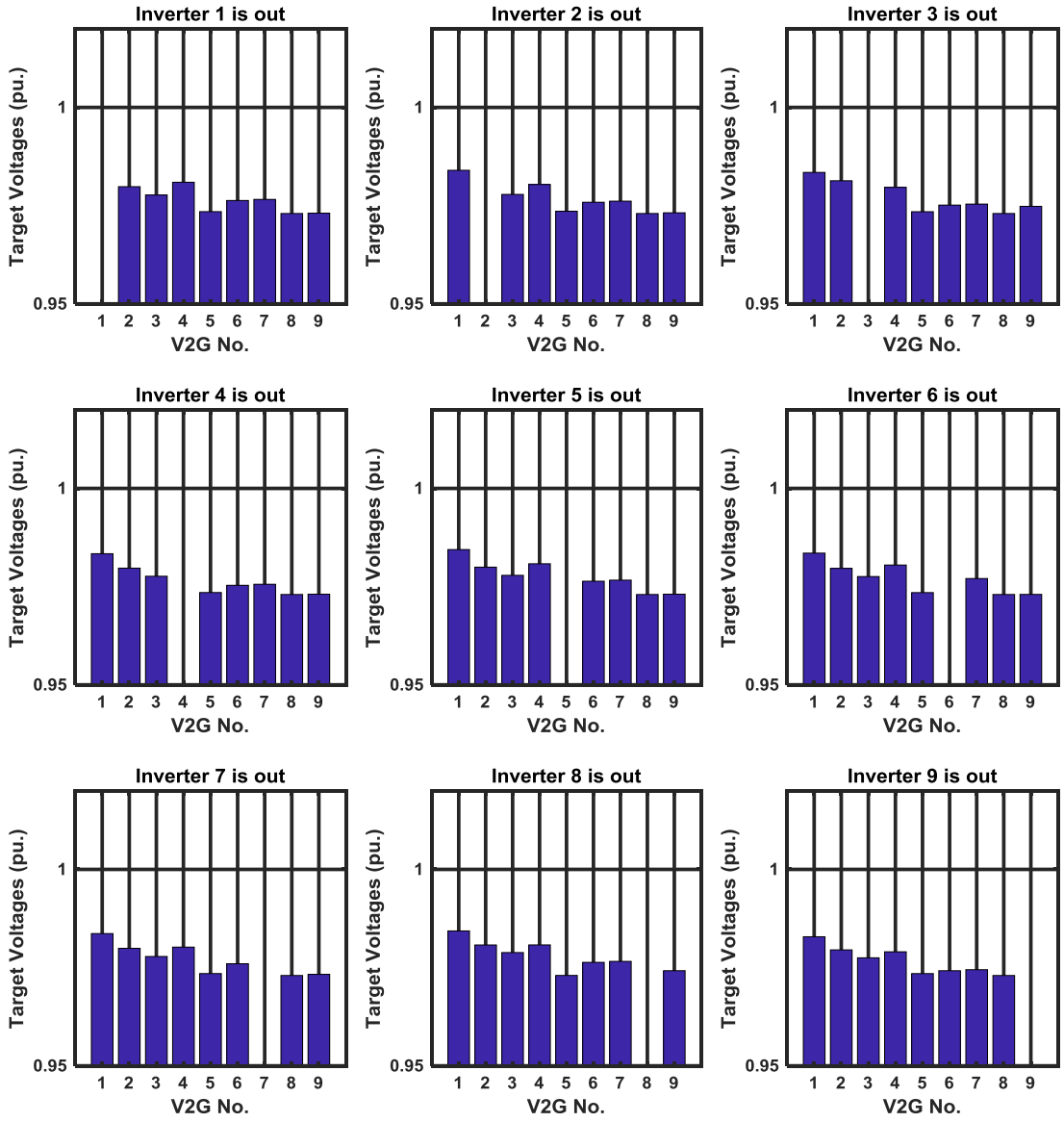

Figure 10-14 Optimal voltage levels of the remaining system inverters at their connection points after the outage of each V2G system

As can be seen in Figure 10-14 the optimal voltage levels the PCCs of the system inverters depend on the availability of the other system inverters. This indicates the necessity of developing an adaptive decentralised control scheme like the one proposed in this chapter based on the impedance identification technique. In order to increase the robustness of the algorithm proposed for the active voltage management, a supervised closed-loop decentralised control will be proposed in **D3.5**, where the system configuration is also communicated from a central control unit to the local control systems in a prodigal basis to ensure an accurate system configuration.

Table 10-1 Slopes of the VVCs in each system configuration (m constants for VVCs)

Unavailable inverter	**$V2G_1$**	**$V2G_2$**	**$V2G_3$**	**$V2G_4$**	**$V2G_5$**	**$V2G_6$**	**$V2G_7$**	**$V2G_8$**	**$V2G_9$**
Base case	-0.00120	-0.01043	-0.00939	-0.00793	-0.01368	-0.01145	-0.00935	-0.02598	-0.01178
1	-	-0.01033	-0.01148	-0.00921	-0.01493	-0.00925	-0.01006	-0.01697	-0.01306

2	-0.00079	-	-0.01141	-0.00873	-0.01545	-0.00871	-0.00969	-0.01730	-0.01394
3	-0.00161	-0.00946	-	-0.00930	-0.01565	-0.00961	-0.01102	-0.01741	-0.01244
4	-0.00426	-0.00969	-0.01091	-	-0.01604	-0.00928	-0.00858	-0.01774	-0.01366
5	-0.00020	-0.00983	-0.01106	-0.00923	-	-0.00881	-0.01174	-0.01592	-0.01225
6	-0.00417	-0.01006	-0.01101	-0.00842	-0.01602	-	-0.00828	-0.01696	-0.01349
7	-0.00408	-0.01073	-0.01074	-0.00830	-0.01499	-0.00870	-	-0.01697	-0.01290
8	0.00009	-0.00935	-0.01085	-0.00795	-0.01445	-0.01097	-0.01078	-	-0.01322
9	-0.00291	-0.01009	-0.01022	-0.00859	-0.01602	-0.00828	-0.00958	-0.01766	-

Table 10-1 presents the slopes of the VVCs in each system configuration. As can be seen, all the slopes of the VVCs are negative. This assures a positive reactive power injection when the measured voltages at PCCs are below the regarding target voltages (V_{opt}) and a negative reactive power injection (positive absorption) when the measured voltages are higher than the target voltages. This validates the successful application of the proposed active voltage management algorithm in all system configurations. This is as expected as under steady-state and stable operation (static voltage control), an injection of reactive power to the PCC will raise the voltage magnitude at this location. Similarly, a reactive power absorption at PCC reduces the voltage magnitude. Under this setup, the voltage at each PCC will always follow the regarding optimal voltage. In **D3.5**, a closed-loop control will be proposed to improve the accuracy of the voltage control scheme.

It should also be noted that the slopes of the VVCs depend on the system configuration. As discussed in D3.3, this shows that the capability of an inverter-based controllable device to adhere to a set-point is more linked to the system topology, system impedance, and the location that this inverter has been installed at.

The intercepts of the VVCs in each system configuration (outage of each inverter) are presented in Table 10-2. As can be seen, the intercepts not only depend on the system level defined objective (according to **D3.3**), but also highly depend on the system configuration (here, the availability of the system controllable devices).

As discussed in **D3.3**, the intercept *c*, should closely match the optimal voltage (V_{opt}), i.e., the voltage set-points extracted for voltage control mode of operation. This shows the efficiency of the proposed method for active voltage management based on VVCs and validates application of the optimal voltages (V_{opt}) as the voltage set-points of the system inverters in the voltage control mode of operation. Similar to **D3.3**, the relative error is defined as the relative difference between the intercept of each VVC and the regarding optimal voltage ($|c\text{-}V_{opt}|/V_{opt}$).

Table 10-2 Intercepts of the VVCs in each system configuration (c constants for VVCs)

Unavailable inverter	**V2G$_1$**	**V2G$_2$**	**V2G$_3$**	**V2G$_4$**	**V2G$_5$**	**V2G$_6$**	**V2G$_7$**	**V2G$_8$**	**V2G$_9$**
Base case	0.98545	0.98953	0.98191	0.98282	0.98103	0.98757	0.97680	0.98615	0.98353
1	-	0.98051	0.97803	0.98175	0.97254	0.97920	0.97564	0.97201	0.97280
2	0.98326	-	0.97943	0.98018	0.97278	0.97834	0.97536	0.97799	0.97300
3	0.98087	0.98369	-	0.97738	0.97046	0.97466	0.97453	0.97233	0.97978
4	0.98534	0.98059	0.97771	-	0.97357	0.97533	0.97521	0.97816	0.97247
5	0.98352	0.98167	0.98119	0.98277	-	0.97599	0.97488	0.97200	0.97234

6	0.98868	0.98009	0.97910	0.98003	0.97279	-	0.97685	0.97185	0.97243
7	0.98154	0.98032	0.97837	0.97785	0.97281	0.97563	-	0.97285	0.97261
8	0.98141	0.98354	0.97884	0.98064	0.97028	0.97455	0.97626	-	0.97815
9	0.98074	0.97958	0.97585	0.97677	0.97598	0.97378	0.97465	0.97300	-

Table 10-3 shows the relative errors between the intercepts of VVCs and the regarding optimal voltages in voltage mode of operation for different system configurations. It is noticeable that in no configuration these relative errors exceed 0.25%. Another indication of the successful implementation of the proposed active voltage management technique on this sample system in different configurations.

Table 10-3 Relative errors between the intercepts of VVCs and the regarding optimal voltages in voltage mode of operation (100*|c-V_{opt}|/V_{opt}) in percent

Unavailable inverter	**V2G$_1$**	**V2G$_2$**	**V2G$_3$**	**V2G$_4$**	**V2G$_5$**	**V2G$_6$**	**V2G$_7$**	**V2G$_8$**	**V2G$_9$**
Base case	0.16000	0.04500	0.02300	0.13200	0.25100	0.24500	0.07400	0.14300	0.21800
1	-	0.06937	0.03364	0.08141	0.09551	0.01136	0.09667	0.10167	0.02943
2	0.07477	-	0.05874	0.02050	0.08107	0.05305	0.08024	0.10338	0.01824
3	0.05943	0.03569	-	0.02750	0.10184	0.04852	0.08839	0.06895	0.00378
4	0.00397	0.09041	0.00631	-	0.09557	0.00037	0.03973	0.08617	0.06157
5	0.09248	0.07236	0.03196	0.00585	-	0.03936	0.18095	0.10272	0.07563
6	0.01520	0.04585	0.05452	0.04783	0.07136	-	0.02162	0.11778	0.06106
7	0.01289	0.04236	0.05447	0.03807	0.06969	0.03595	-	0.11834	0.06956
8	0.09468	0.07844	0.00062	0.01431	0.07564	0.18327	0.03304	-	0.10976
9	0.01199	0.00701	0.03645	0.02606	0.05221	0.04484	0.01821	0.10279	-

In D3.3, the voltage profiles are compared with and without applying the proposed control algorithm. The necessity of keeping the VVC parameters updated for each inverter needs to be shown and the effectiveness of the adaptive voltage control framework should be validated. For this purpose, two new studies are conducted.

For both studies, the minute by minute active and reactive power demands at all load points and also the other required data are collected for one week and for each minute a three-phase unbalanced power flow has been conducted to find the three-phase voltages. The input data were presented in **D3.3** and are not repeated here for the sake of brevity.

For both studies the proposed AVM algorithm is implemented in a one week period to keep the reactive power dispatch up-to-date. During each day of the study week a certain inverter is assumed to be unavailable. In the first day the first V2G system is unavailable, in the second day the second V2G system is unavailable and so on. V2G 8 and 9 are always available.

First study: In the week-long time-series power flow, the V2G systems on this sample LV feeder are tasked with following their assigned VVCs found in **D3.3**. In other words, the VVCs are not updated according to the availability of the V2G systems.

Second study: In a week-long time-series power flow, the V2G systems on this sample LV feeder are tasked with following their assigned VVCs found in this subsection. It means during each day, the set of VVCs are updated according to the outage of the regarding V2G system.

Table 10-4 shows the system energy loss and voltage unbalance index for the first and second studies, respectively. Each study has been repeated for the objectives of minimisation of the voltage unbalance and loss minimisation with different assumptions for the limitations that should be considered for the reactive power support capability of the system inverters. The details of such assumptions and also the definitions of the voltage unbalance index and total energy loss are provided in **D3.3** and is not repeated here for the sake of brevity.

Table 10-4 Energy loss and voltage unbalance for the First Study

Objective function and constraints		Total Energy Loss (kWh)	Average Voltage Unbalance
Min. Voltage Unbalance		301.0221	0.014872
Min. V. Unbalance with accurate operational constraints		302.2134	**0.013912**
Min. Voltage Unbalance Available NC Recommendation, Lagging PF>0.92		296.7859	0.015067
Min. Power Loss [kW]		288.9155	0.016153
Min. Power Loss with accurate operational constraints		**287.8015**	0.015543
Min. Power Loss [kW] NC recommendation Lagging PF>0.92		290.8570	0.016221
Fixed Power Factor	0.95 Lag Power factor	297.1450	0.017371
	Unity Power factor	298.9494	0.017235
	0.95 Lead Power factor	301.1108	0.017186

Table 10-5 Energy loss and voltage unbalance for the Second Study

Objective function and constraints		Total Energy Loss (kWh)	Average Voltage Unbalance
Min. Voltage Unbalance		308.4233	0.012621
Min. V. Unbalance with accurate operational constraints		305.2320	**0.012180**
Min. Voltage Unbalance Available NC Recommendation, Lagging PF>0.92		298.7541	0.015032
Min. Power Loss [kW]		284.8322	0.016503
Min. Power Loss with accurate operational constraints		**283.0875**	0.015854
Min. Power Loss [kW] NC recommendation Lagging PF>0.92		289.4841	0.016723
Fixed Power Factor	0.95 Lag Power factor	297.1450	0.017371
	Unity Power factor	298.9494	0.017235

	0.95 Lead Power factor	301.1108	0.017186

As can be seen in Table 10-5 with the objective of minimisation of the voltage unbalance the value of the optimal voltage unbalance index is reduced at least by 14% in the second study compared to the first study.

The value of the total energy loss is reduced at least by 1.66% in the second study comparing to the first study where the loss minimisation is chosen as the system level objective function.

A.1 Simulation results on multi-agent based AVM

Table 10-6 gives the results of the offline studies producing the following characteristics for the V2G connections under examination. Parameters of the VVCs (*m* and *c*) and also the target voltages are given in this table.

As discussed in **D3.3**, active voltage management include different control modes for the inverter-based resources to optimise performance depending on whether the generator is connected to the grid, or in island mode. Therefore, they can be set to maintain the voltage (voltage control mode), the PF (power factor control mode) or the reactive power (power control mode). Here, we assume that the inverters can be operated in both power control mode and voltage control modes of operation.

In the online simulations of this subsection, the extracted VVCs (see **Table** 10-6) are applied to find the optimal reactive support of the inverters of this sample system in power control mode of operation. It should be noted that the target voltages reported in **Table** 10-6 can be considered as the voltage set-points in the voltage control mode of operation for these controllable devices.

If the inverters follow these target voltage set-points in the voltage control mode of operation, the results will be the same as those that are obtained in power control model of operation where the inverters are tasked with following the reactive power levels that are found using the VVCs. In other words, in both control modes, the controllable devices should try to follow the optimal voltages as accurate as possible considering the operational limitations which depend on the type of the controllable devices connected to the system. These limitations were introduced in **D3.3** for different types of RESs.

Table 10-6 Optimal inverter voltages (for voltage control mode), slope and intercept of V2G systems for power control mode. Objective: Multi-objective (Simultaneous minimisation of loss and voltage unbalance)

V2G system	Power control mode of operation			Voltage control mode of operation	Relative Error %
	m **(pu/kVAR)**	***c*** **(pu)**	**Reactive power control equation** $\Delta Q=\alpha.V_{pcc}+\beta$	V_{opt} **(pu)**	
1	-0.00057	0.98373	$\Delta Q= -1752.1544 V_{pcc} + 1723.6444$	0.9847	0.0971
2	-0.00884	0.98499	$\Delta Q= -113.1492 V_{pcc} + 111.4510$	0.9853	0.0360
3	-0.01007	0.98033	$\Delta Q= -99.2938 V_{pcc} + 97.3407$	0.9802	0.0103

4	-0.00810	0.98042	$\Delta Q = -123.4866 V_{pcc} + 121.0683$	0.9816	0.1228
5	-0.01549	0.97520	$\Delta Q = -64.5687 V_{pcc} + 62.9674$	0.9762	0.0974
6	-0.00897	0.98110	$\Delta Q = -111.4642 V_{pcc} + 109.3574$	0.9825	0.1426
7	-0.00817	0.97606	$\Delta Q = -122.3467 V_{pcc} + 119.4177$	0.9764	0.0374
8	-0.01750	0.97501	$\Delta Q = -57.1446 V_{pcc} + 55.7168$	0.9761	0.1157
9	-0.01158	0.97876	$\Delta Q = -86.3402 V_{pcc} + 84.5063$	0.9802	0.1493

All the slopes of the VVCs are negative. This leads to a positive reactive power injection when the measured voltages at PCCs are below the regarding target voltages (V_{opt}) and a negative reactive power injection (positive absorption) when the measured voltages are higher than the target voltages presented in **Table** 10-6.

This validates the successful application of the proposed AVM algorithm. This is as expected as, under stable operation (static voltage control), an injection of reactive power at the connecting bus of a controllable inverter increases the voltage magnitude at this location and a reactive power absorption at this node reduces this voltage.

The intercept ***c***, closely matches the optimal voltage (V_{opt}). This indicates the effectiveness of the proposed method for active voltage management based on VVCs and validates application of the optimal voltages (V_{opt}) as the voltage set-points of the system inverters in the voltage control mode of operation as explained in **D3.3**. The relative error is presented in **Table** 10-6 for each V2G system. The VVCs of all 9 V2G systems are presented in **Figure** 10-15.

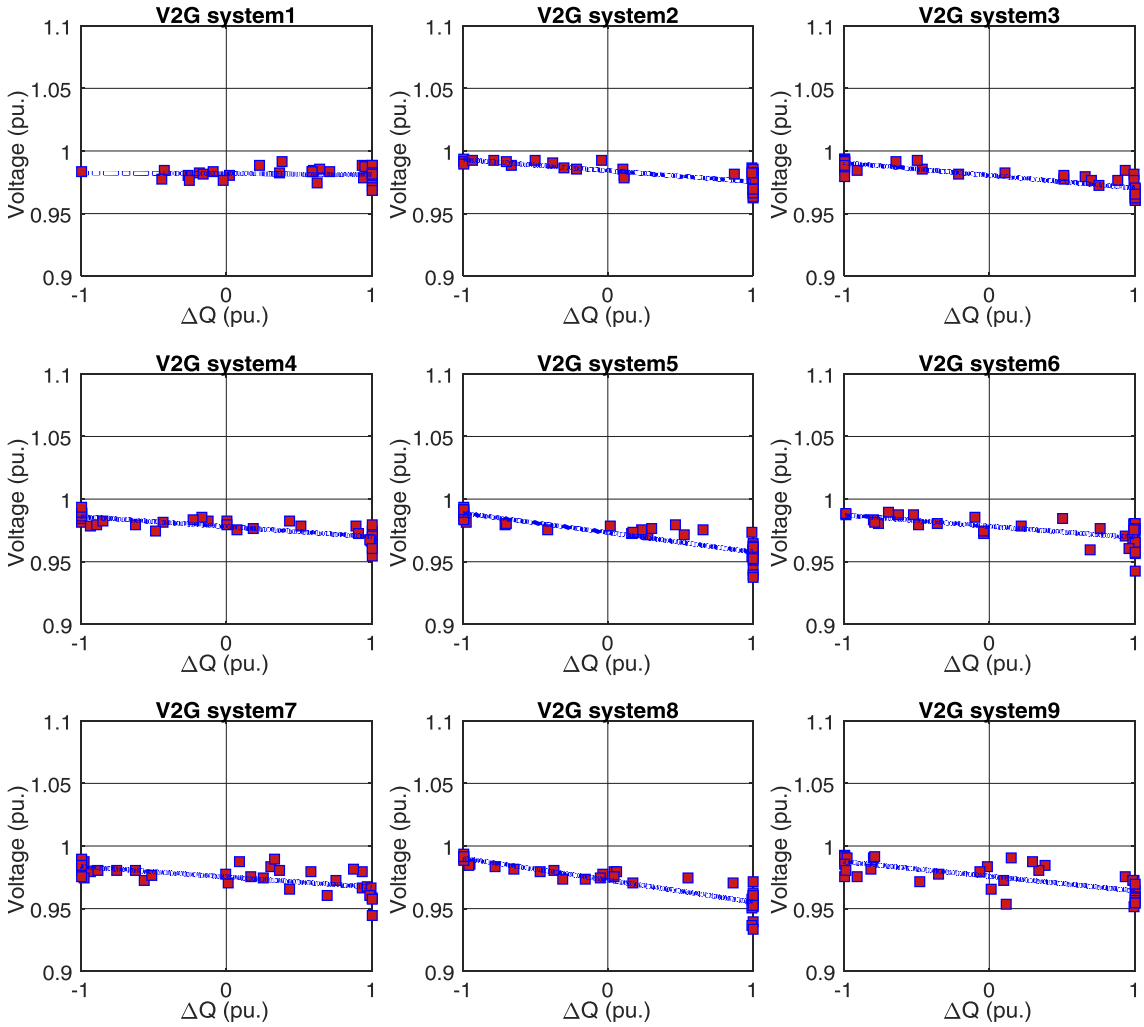

Figure 10-15 Resulting VVCs found for the simultaneous minimisation of the power loss and voltage unbalance for V2G systems 1-9, showing intercepts and slopes

Similar to D3.3, in order to validate the ability of the adopted 3-phase power flow algorithm to converge to a stable solution while there are many controllable devices connected to the low voltage distribution system under study, and also to assess the voltage controllability of the inverters, the three-phase voltages are presented in **Figure** 10-16. The voltage of each inverter is fixed on the values presented for target voltages in the multi-objective study.

Figure 10-17 presents the value of the reactive power that each inverter should supply at PCC. Some of these reactive power injection values are negative, signifying reactive power consumption by these inverters. No active power injection/consumption is allowed by these V2G systems in the calculation of the reactive power injections presented in **Figure** 10-17. This means all the capacity of each inverter can be dedicated to reactive power support. The active and reactive power demands at all load points and other load characteristics have been set to the values regarding the most probable scenario. See **D3.3** for more information and observations.

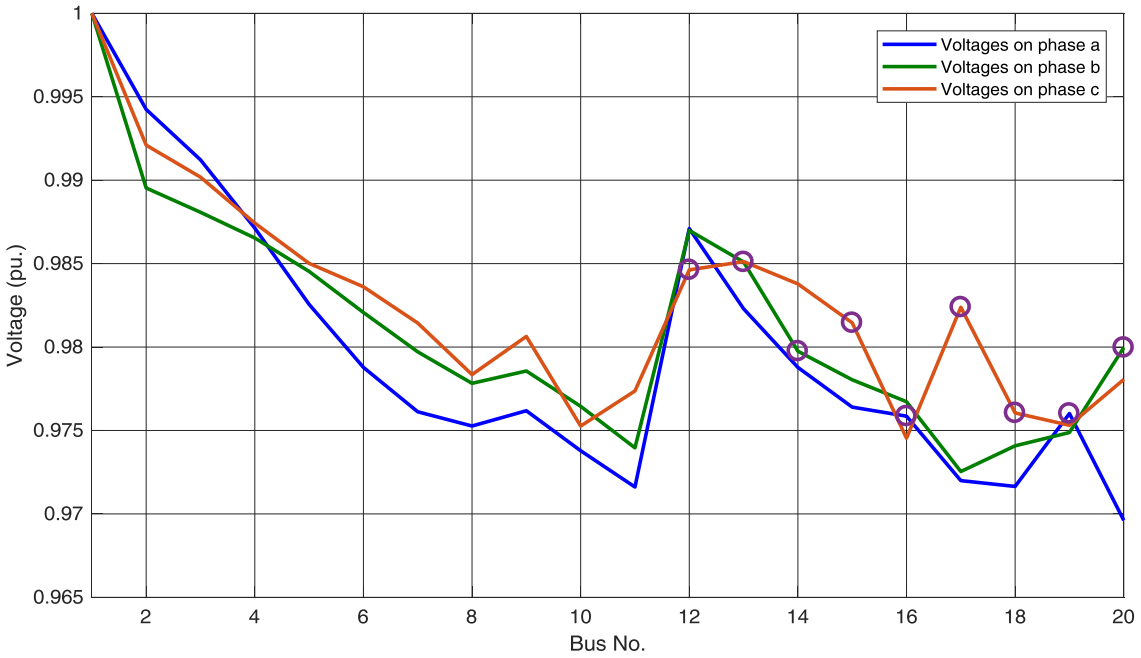

Figure 10-16 Voltage levels at different system buses, buses 12-20 are the PCCs of the V2G systems (Multi-objective)

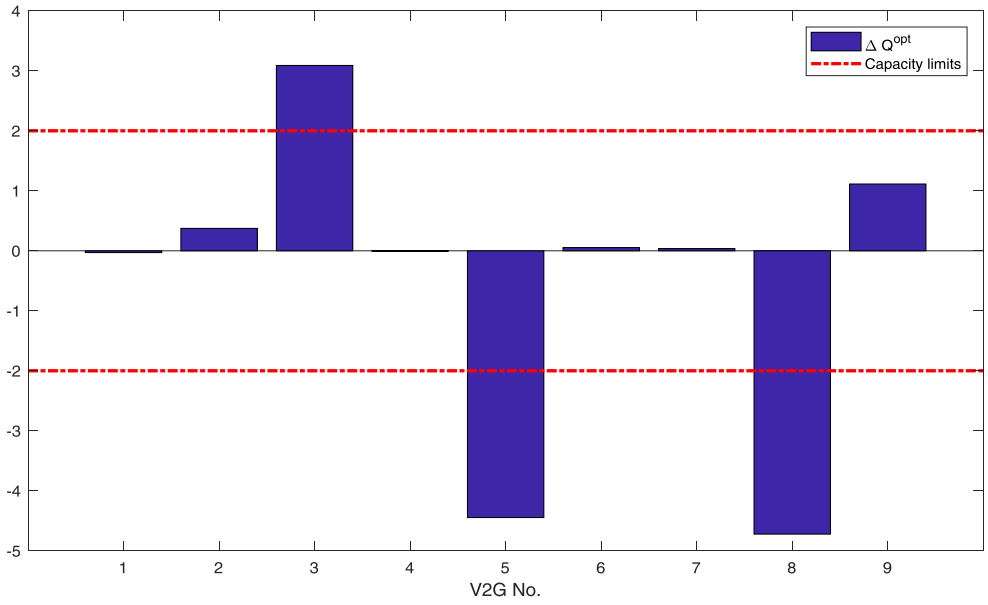

Figure 10-17 Reactive power injection of each V2G inverter in order to achieve the target voltage levels for each inverter (Multi-objective)

In order to show how the proposed multi-objective framework makes a compromise between the first and second objectives in this study, Figure 10-18 presents the average values of the voltage unbalance at different load points (buses 2-11) of this sample system. As can be seen, with the multi-objective framework, the value of the average voltage unbalance at most of the load points is between the values of this parameter for the first and the second objectives, i.e., minimisation of the voltage unbalance and loss minimisation.

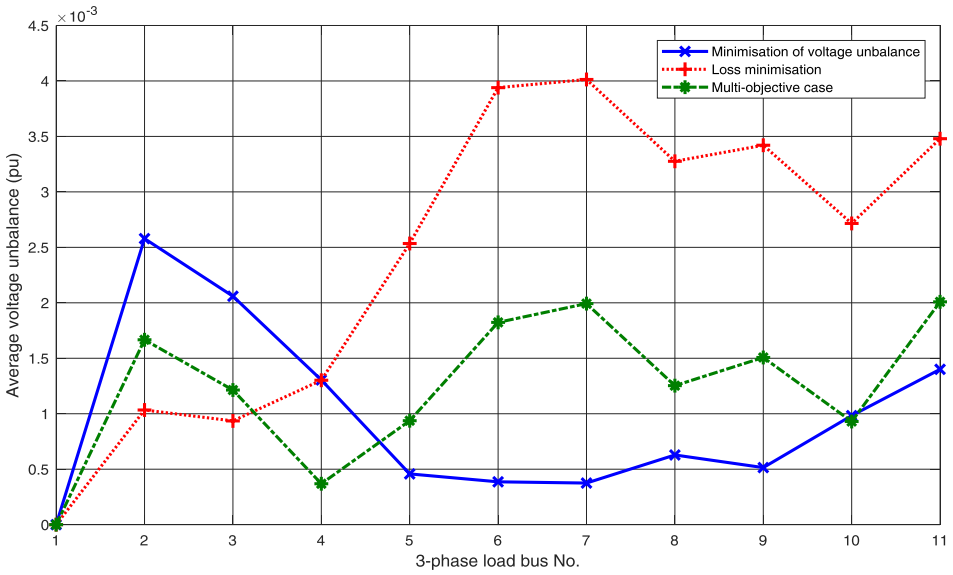

Figure 10-18 Average voltage unbalance at 3-phase load buses with different objectives (Minimisation of Voltage Unbalance, Loss Minimisation, Multi-objective)

To validate the effectiveness of the proposed multi-objective active voltage management framework, the minute by minute active and reactive power demands at all load points and also the other required data are considered to be similar to those assumed for validation of the proposed single objective AVM algorithm in **D3.3**. This enables us to compare the results of the single and multi-objective AVM algorithm. In a week-long period, the V2G systems on this LV feeder are tasked with following their assigned VVCs found using the multi-objective AVM algorithm, i.e., the VVCs presented in Figure 10-17.

In three separate studies, the three different fixed power factor operation strategies are assumed for the V2G systems connected to this low voltage distribution system, i.e., 0.95 inductive, 1 and 0.95 capacitive. These settings constrain the reactive power support of each V2G inverter to absorb roughly one-third of the value of active power consumed by the V2G charger, zero and inject about one-third of the value of active power consumed by the V2G charger. A fixed power factor is typical for an inverter based controllable device connected to a low voltage distribution system to reduce the voltage-rise effect caused by the excessive active power injections. The operation of the set-points extracted using the VVCs are compared to the operation at the aforementioned fixed power factor strategies.

The effects of different constraints on the effectiveness of the multi-objective framework are also investigated. Similar to **D3.3**, the results are also compared to those obtained with the case that the capacity constraints are considered as the only constraints and also the results of the fixed power factor criteria. The observed voltage measurement at the terminals of the V2G systems are mapped to their set-point operation of reactive power using 9 different studies.

More information regarding the week-long validation of the local voltage control algorithm can be found in **D3.3**. Here, the main focus is on analyzing the results of multi-objective AVM algorithm. As mentioned in **D3.3**, the values gained for the average voltage unbalance and weekly energy loss considering the minimisation of the average voltage unbalance and loss minimisation in Table 10-7 suggests that there may be some strategies that can reduce the voltage unbalance and energy loss simultaneously. Here, this strategy is found using the proposed multi-objective framework.

According to the results provided in Table 10-7 for multi-objective framework, we can analyse how the sets of constraints considered for the operation of the inverter-based controllable devices can affect the performance of the proposed AVM algorithm. With the accurate constraint modelling (see the simulation results provided in **D3.3**), the results of applying the proposed AVM algorithm for optimising the reactive power dispatch to simultaneously minimise the voltage unbalance and power loss are even better than those obtained for the case with capacity

constraint as the only constraint on the operation of the system inverters. For the single objective studies, the same phenomenon is observed. The reasons were discussed in **D3.3**.

For the case study with a maximum lagging power factor of 0.92, the proposed multi-objective AVM algorithm leads to a total loss and voltages unbalance lower than the best energy loss and voltage unbalance attained with the fixed power factor assumption. This shows the efficiency of the proposed active voltage management algorithm even with such restricted feasible area is considered for the reactive power injection of the system inverters.

The more important point that should be noted is that in all studies presented in Table 10-7, for multi-objective case, the value of the voltage unbalance is better than the voltage unbalance found for the regarding single objective loss minimisation study. However, this voltage unbalance is not lower than the one obtained for the regarding single objective minimisation of the voltage unbalance. For the weekly energy loss, the results of the multi objective algorithm is better than those obtained for the single objective minimisation of the voltage unbalance but not as optimal as those obtained for the single objective loss minimisation case. Multi-objective framework leads to an energy loss 6.61% lower than the energy loss found for the single objective minimisation of the voltage unbalance, but only 0.61% higher than the loss found for the single objective minimisation of the power loss. The value of the voltage unbalance is 23.5% lower for multi objective framework comparing to the voltage unbalance obtained with single objective loss minimisation while with the multi-objective framework the value of this value is only 5.94% higher than the one obtained for single objective minimisation of the voltage unbalance. This indicates the acceptable efficiency of the proposed multi-objective decentralized active voltage management. The effects of different constraints on the PQ capability curve and also the active and reactive power injections of all the inverters in multi-objective case are presented in **Figure** 10-19.

Table 10-7 Comparison of active power loss and voltage metrics

Objective		Total Energy Loss (kWh)	Average Voltage Unbalance
Min. Voltage Unbalance		313.4432	0.012584
Min. V. Unbalance with accurate operational constraints		303.5436	**0.012124**
Min. Voltage Unbalance Available NC Recommendation, Lagging PF>0.92		297.6478	0.015234
Min. Power Loss [kW]		283.9466	0.015801
Min. Power Loss with accurate operational constraints		**282.9815**	0.015244
Min. Power Loss [kW] NC recommendation Lagging PF>0.92		290.4841	0.015918
Multi-objective		297.4471	0.013176
Multi-objective with accurate operational constraints		**284.7254**	**0.012890**
Multi-objective [kW] NC recommendation Lagging PF>0.92		293.2985	0.015334
	0.95 Lag Power factor	297.1450	0.017371

Fixed Power Factor	Unity Power factor	298.9494	0.017235
	0.95 Lead Power factor	301.1108	0.017186

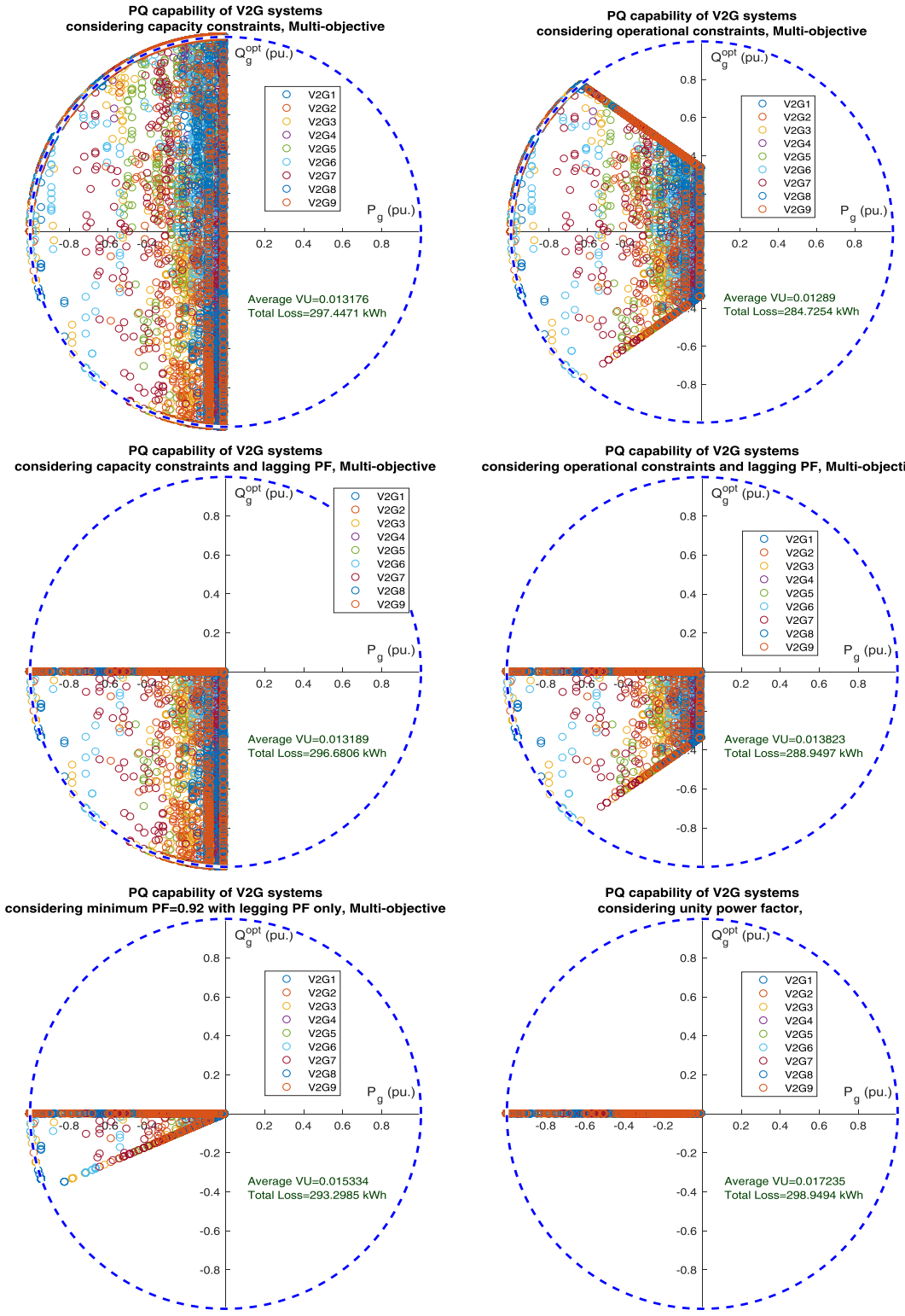

Figure 10-19 Active and reactive power capability curves, Multi-objective optimisation for simultaneous minimisation of the total energy loss and average voltage unbalance.

A.2 Simulation Results Regarding Perturbations Injected from RES Inverters

The converter parameters of the WFZ device defined in Table 3-1 are used to for the simulation test cases. The device is simulated in both grid forming and grid feeding mode. PRBS perturbations are introduced in into the control loops, first in the D-axis and then in the Q-axis with a time delay of 0.02 s between the D and Q axis perturbations in order to enable any transients to settle. A 11-bit shift register is used to generate the PRBS signal. The perturbed output currents and voltages are measured following which the parametric impedance is measured. As mentioned in Section 3.6, the impedance is obtained until half the switching frequency i.e. 25 kHz and accurate measurements are obtained until 10 kHz.

A.2.1 Grid Feeding Case

A.2.1.1 Case 1: Known passive grid impedance

A passive impedance branch of known impedance is chosen as the grid impedance such that the analytical impedance can be calculated as a reference. Figure 10-20 shows the perturbations injected in the grid injected current in both D and Q axis. Notice how only one axis is perturbed at a time.

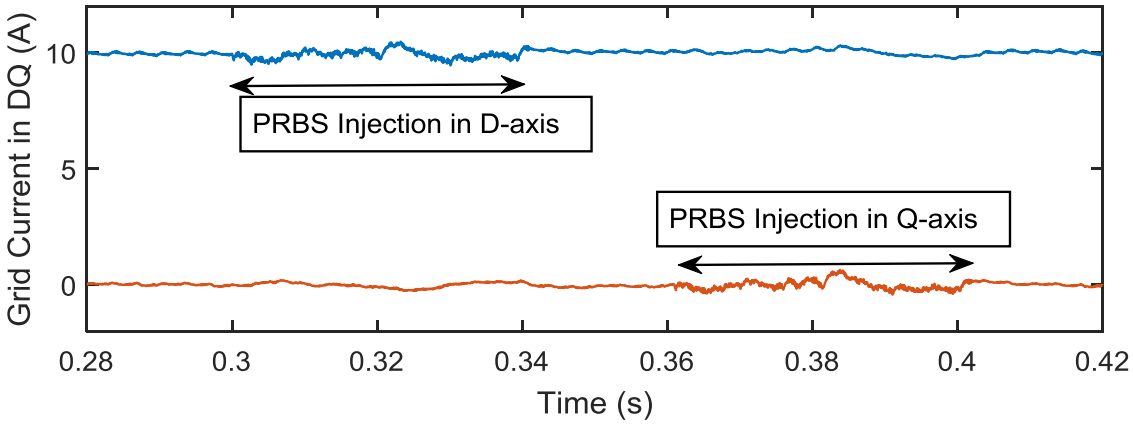

Figure 10-20 DQ Current during PRBS injection

Following the WSI technique described in D3.4, the non-parametric wideband grid impedance is obtained, and the analytical impedance is also evaluated at all those frequencies. Figure 10-21 and Figure 10-22 shows the magnitude and phase plot of the measured impedance. An excellent fit is observed until 10 kHz. These simulations were validated for a wide range of impedances and high accuracy was not until 10 kHz.

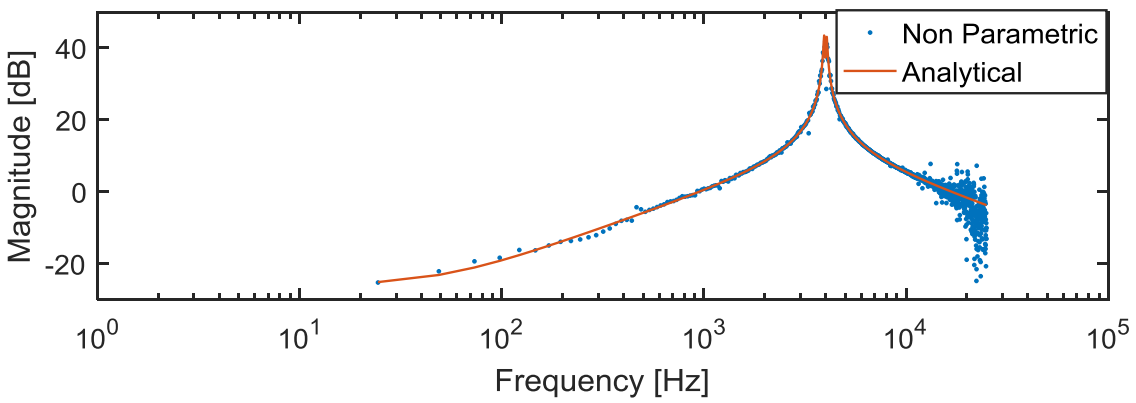

Figure 10-21 Grid-Feeding Mode - Non-parametric grid impedance

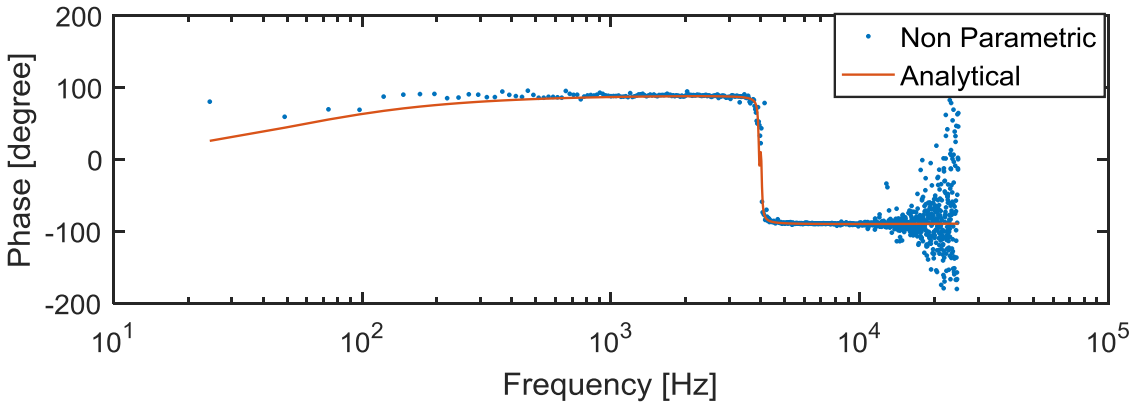

Figure 10-22 Grid-Feeding Mode - Non-parametric grid phase

A.2.1.2 Case 2: Unknown grid impedance – Active grid scenario with parallel connected inverter

Consider a case where an active source such as a PV inverter is connected in parallel to the device. The WFZ device would measure an impedance which is the Thevenin equivalent of the parallel connected inverter and the grid impedance which was used for Case 1. Figure 10-23 shows the non-parametric magnitude and Figure 10-24 shows the non-parametric phase respectively. Clearly, two resonant peaks are observed in Figure 10-23 when compared to Figure 10-21, where only one resonance peak is existed. This is known as parallel resonance and the proposed device can measure such parallel resonance phenomenon. Notice that in Figure 10-24, the phase below the accuracy range of the device of 10 kHz goes above +90 or -90 degrees, clearly indicating the presence of an active grid impedance.

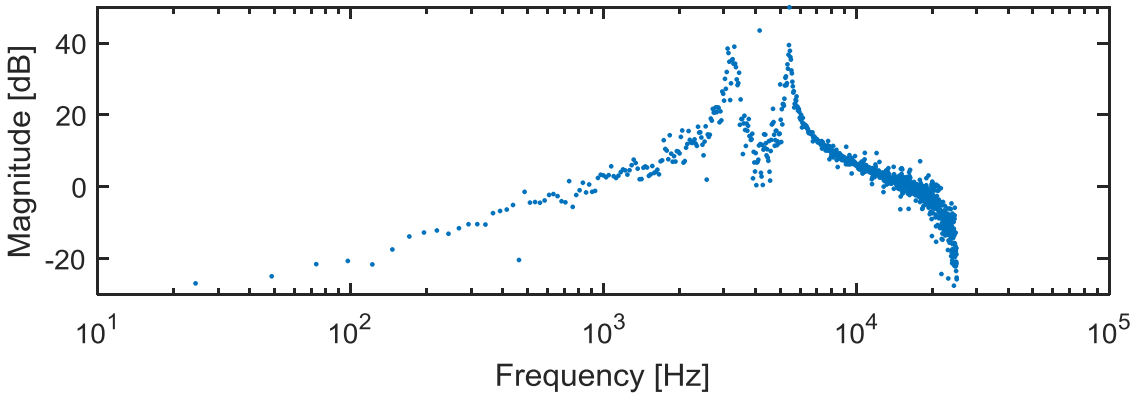

Figure 10-23 Grid-Feeding Mode - Non-parametric grid impedance magnitude – With Parallel Inverter

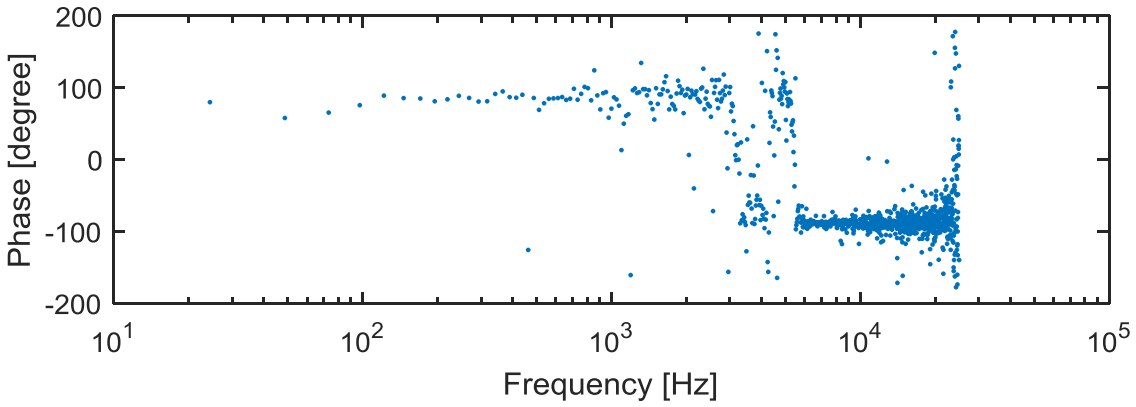

Figure 10-24 Grid-Feeding Mode - Non-parametric grid impedance phase – With Parallel Inverter

A.2.2 Grid Forming Case

The simulation cases presented here are identical to the cases used in the testing of WFZ device in Section 3.6. These simulation tests cases represent a preliminary step before obtaining experimental results; a two-fold validation process. Figure 10-25 shows the perturbed load currents during PRBS injection. Figure 10-26 shows the non-parametric impedance magnitude and Figure 10-27 shows the corresponding phase obtained after post-processing using WSI technique. Excellent accuracy in the impedance measurements are obtained until 10 kHz concurring with the accuracy observed in the experimental validation.

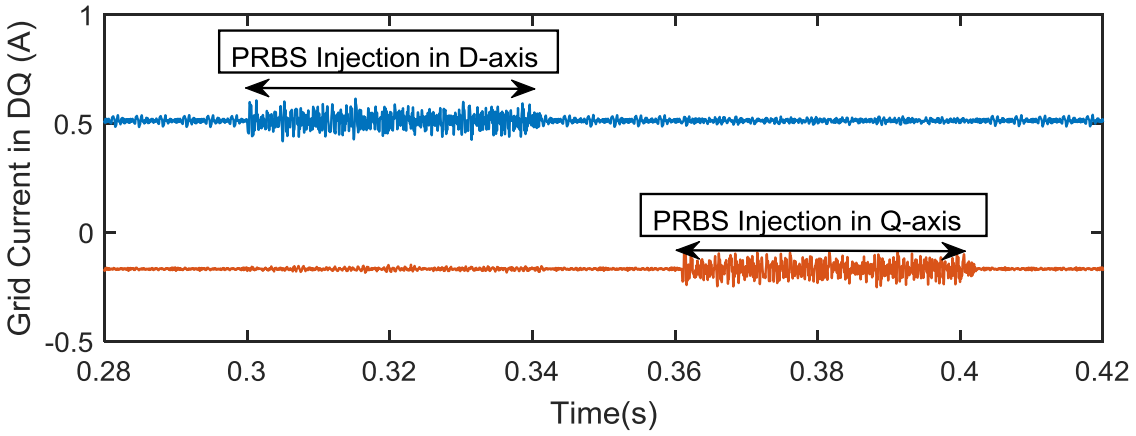

Figure 10-25 DQ Current during PRBS injection

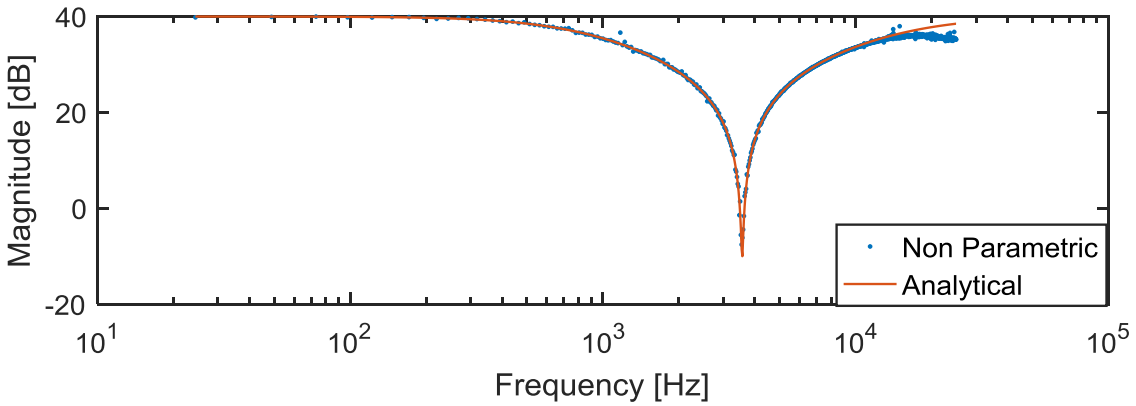

Figure 10-26 Grid-Forming Mode - Non-parametric grid impedance

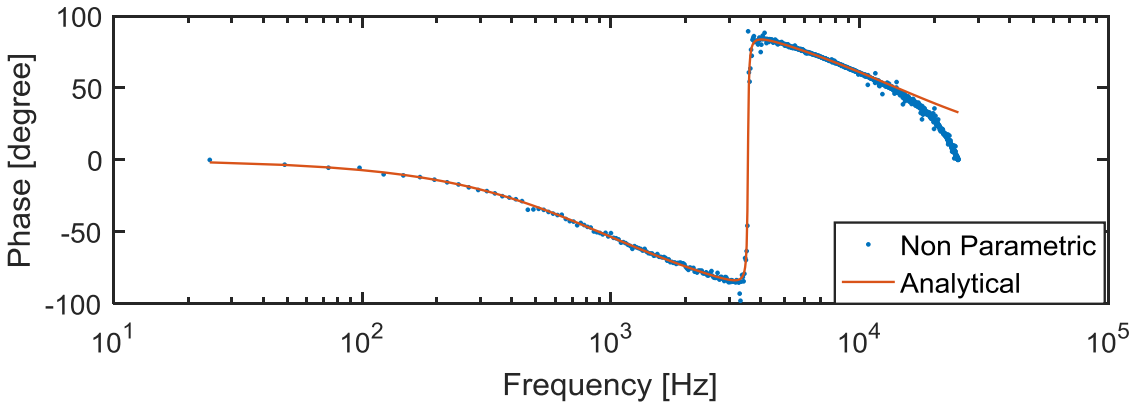

Figure 10-27 Grid-Forming Mode - Non-parametric grid phase

A.3 Frequency Domain Results of VOI Control

A stability analysis is conducted for the VOI control procedure explained in deliverable **D3.5**. Both low and high frequency dynamics of the inverter can be shaped by the VOI controller. VOI controller synthesis is parameterized by the choice of weighting function. The cut-off frequency of the weighting function is varied which results in different loop shape for closed loop output impedance at both low and high frequency ranges. Figure 10-28 shows the variation of closed-loop output admittance for both low and high frequency ranges as the bandwidth parameter of weighting function is varied. This analysis was done considering a fixed grid impedance model, since the VOI controller synthesis process considers grid impedance model. Changes to the grid impedance model will naturally result in a different VOI controller. Therefore, to effectively study the impact of weighting parameters, the grid impedance model is fixed.

Considering a given grid impedance, a class of stabilizing VOI control can be synthesized with the proposed generalized framework in **D3.5**. To show how stability at the PCC can be improved, the weighting function parameters M_u and ω_u are varied and the resulting VOI controller is used to calculate the inverter output admittance. Using the Generalized Nyquist Criterion (GNC), as defined in **D3.2** and **D3.3**, the characteristic loci of eigen values are calculated and are shown in Figure 10-29 to Figure 10-32. Increasing M_u and ω_u moves the GNC plot away from the critical point, thereby increase the gain and phase margins. The system becomes highly stable for the case M_u=0.4, ω_u=50.

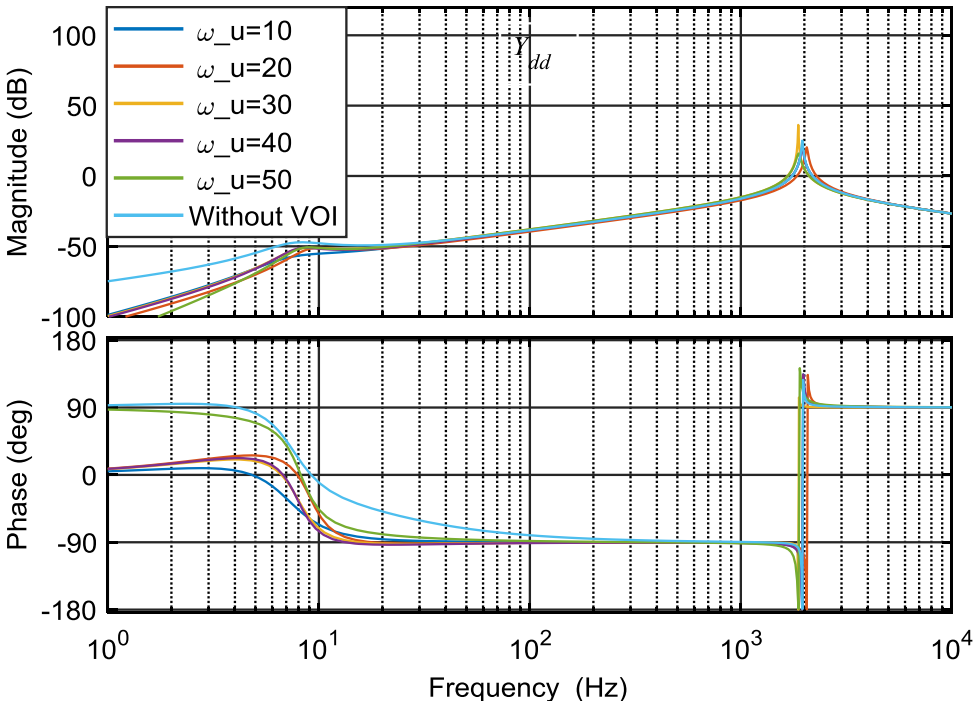

Low Frequency Variation

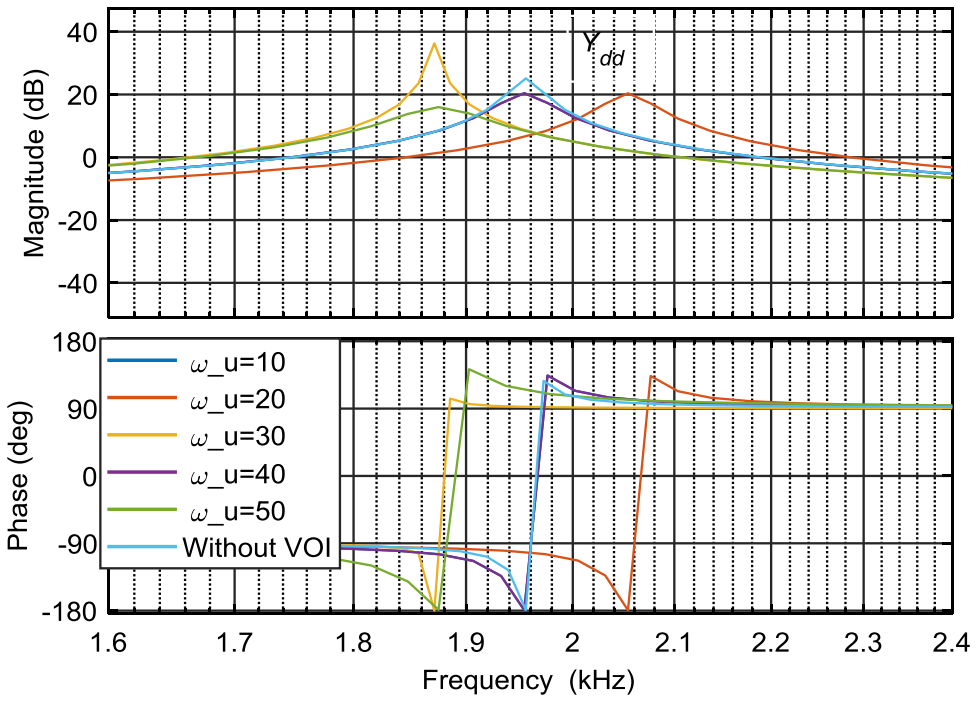

Zoomed Plot – High frequency variation

Figure 10-28 Variation of closed loop output admittance Y_{dd} of inverter with VOI control weighting function parameter

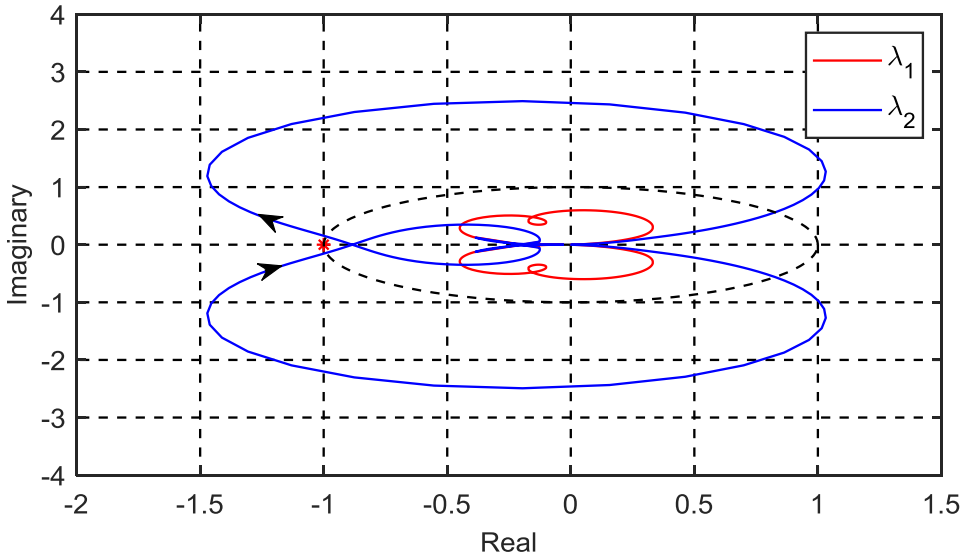

Figure 10-29 GNC for weighting function parameters M_u=0.1, ω_u=10

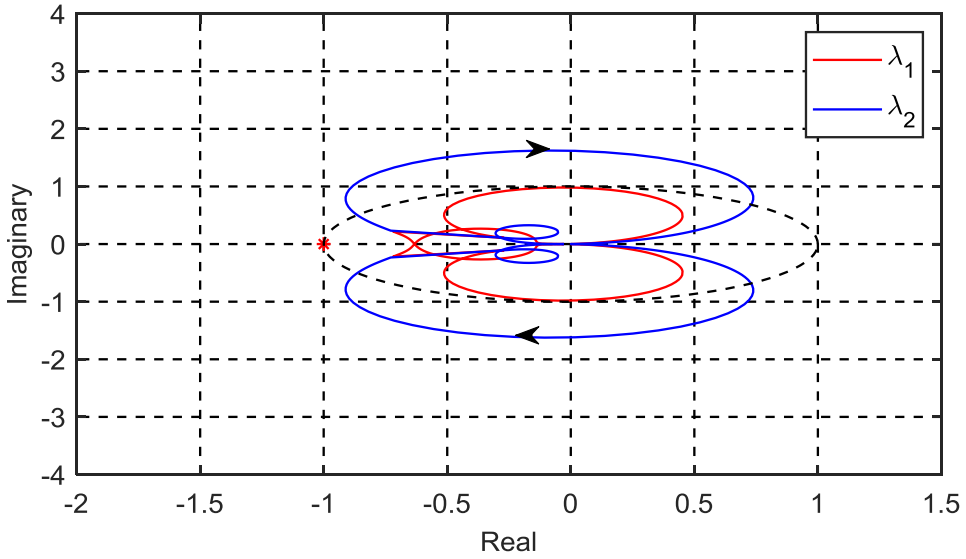

Figure 10-30 GNC for weighting function parameters M_u=0.1, ω_u=50

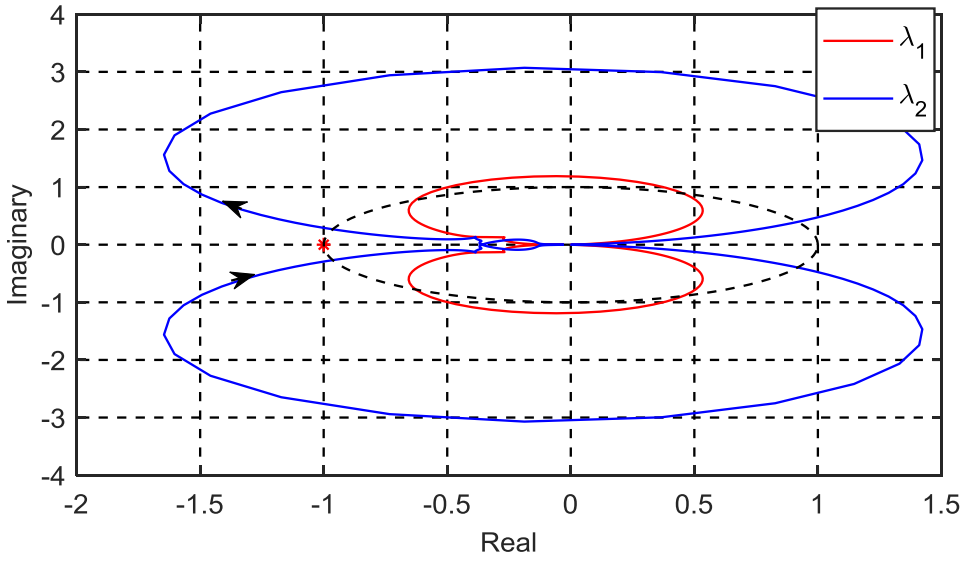

Figure 10-31 GNC for weighting function parameters M_u=0.4, ω_u=10

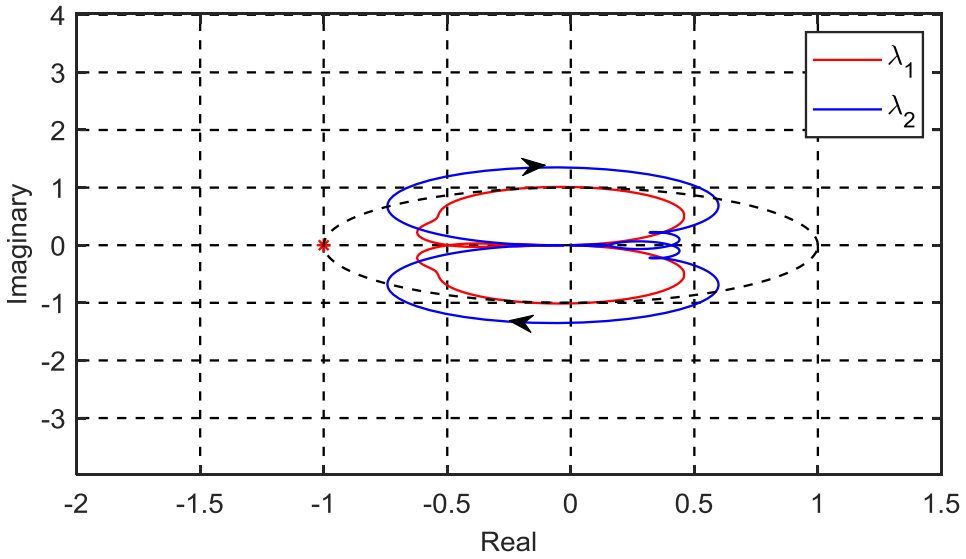

Figure 10-32 GNC for weighting function parameters M_u=0.4, ω_u=50

A.4 VOI Control Real-Time Simulation

A.4.1 RT-Simulation Description

Table 10-8 presents the parameters of the three-phase grid connected inverter. The table includes operational parameters, filter parameters and control parameters. The grid connected inverter has an LCL output filter with no physical damping or passive damping filter as shown in Figure 10-33.

Table 10-8 Inverter Parameters

Converter Parameters	Values
DC Link Voltage	1000 V

Grid Voltage and Frequency	400 V, 50 Hz
Switching Frequency	5 kHz
Converter Side Choke	3.8 mH, 0.1Ω
Grid Side Choke	3.8 mH, 0.1Ω
Filter Capacitance Co	19.8 µF
Control Parameters (Kp, Ki)	1.832E-4, 1.832

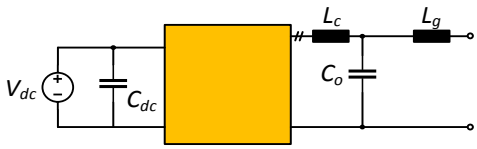

Figure 10-33 Grid connected inverter with LCL Filter

The grid impedance connected the output of the inverter is shown in Figure 10-34. This impedance is fixed in such a way that it introduces a resonance within the control bandwidth of the inverter.

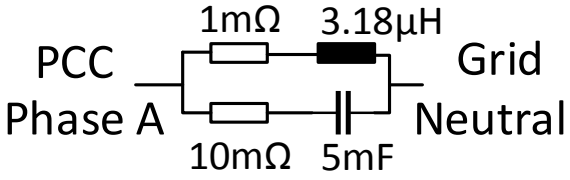

Figure 10-34 Grid Impedance

The VOI controller is designed to emulate the behavior of a passive shunt RC damper. The filter structure of a shunt RC damper is shown in Figure 10-35

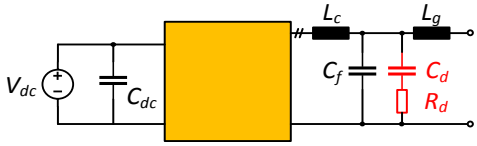

Figure 10-35 Passive damping filter structure to be emulated by VOI controller

Comparing Figure 10-33 and Figure 10-35, the overall capacitance C_o is split into capacitances C_f and C_d. For simplicity, the split ratio can be half, which means $C_d = C_f = C_o/2$. By calculating the characteristic impedance of the LCL filter and choosing an optimal quality factor, the damping resistor R_d can be calculated. For a split ratio of half, the optimal quality factor is 9. The VOI control structure that actively emulates the passive damping structure in Figure is given by the following equation.

$$K_{voi} = K_d . \frac{s}{s + \frac{1}{R_d C_d}}$$

Here R_d and C_d refers to the damping resistance and capacitance respectively. By considering an optimal quality factor of 9, the damping resistance R_d is calculated as 88.14 Ω. The control gain K_d is fixed as 0.2. The frequency domain response of the result VOI controller is shown in Figure 10-36.

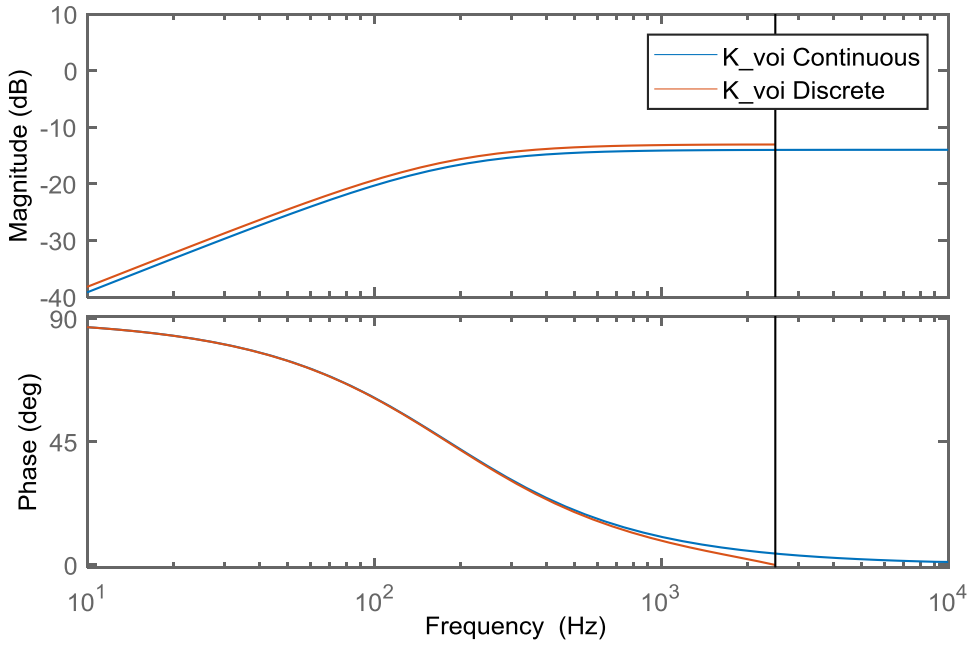

Figure 10-36 VOI Controller in Frequency Domain

Thus, as explained in D3.5, we have two controllers, one PI controller with grid voltage feedforward taking care of output current reference tracking while the other is the VOI controller, which reshapes the output impedance for improving dynamic stability and reducing harmonic distortions.

A.4.2 RT-Simulation Results

The real-time simulation is run at a time step of 10 µs, without any overruns which means the solver can solve the power system within the specified time step of 10 µs. As mentioned earlier, the chosen grid impedance for this converter introduces harmonic instability. Hence, the simulation is started under the presence of VOI. The control parameters are designed by discretizing the system transfer functions at 5 kHz of sampling frequency and a discrete domain PLL is designed by considering settling time of 30 ms and damping ratio of 0.7 which leads to a highly stable PLL design.

At time t=0.3 seconds, the VOI controller is disengaged and only the output reference tracking controller is active. Thus, the virtual damping provided by the VOI controller is not available. It can be noted from t=0.3 s onwards, the harmonic distortion grows, and system becomes unstable. Figure 10-37 and Figure 10-38 shows the grid injected currents in ABC domain and Figure 10-39 shows the grid injected current in DQ domain.

At time t=3.05 seconds, the VOI controller is engaged which introduces virtual damping through the shaped impedance. Through, the presence of damping, the harmonic distortions in grid current are damped and the system goes back to its stable state.

The overall control signal before scaling, i.e PI control with grid voltage feedforward and VOI controller is shown in Figure 10-40. Without the VOI controller, the traditional PI with feedforward cannot stabilize the system.

The time domain response of the VOI controller is shown in Figure 10-41. For time less than 3 seconds, it can be seen the VOI controller is applying higher order harmonics to damp the harmonic interaction between the inverter and grid impedance and when the VOI controller is disengaged at t=3 s, the system becomes unstable. At time t=3.05 seconds, the VOI controller is engaged and it can be noted from Figure 10-41 that the VOI controller tries to apply higher order harmonics to damp the resonance.

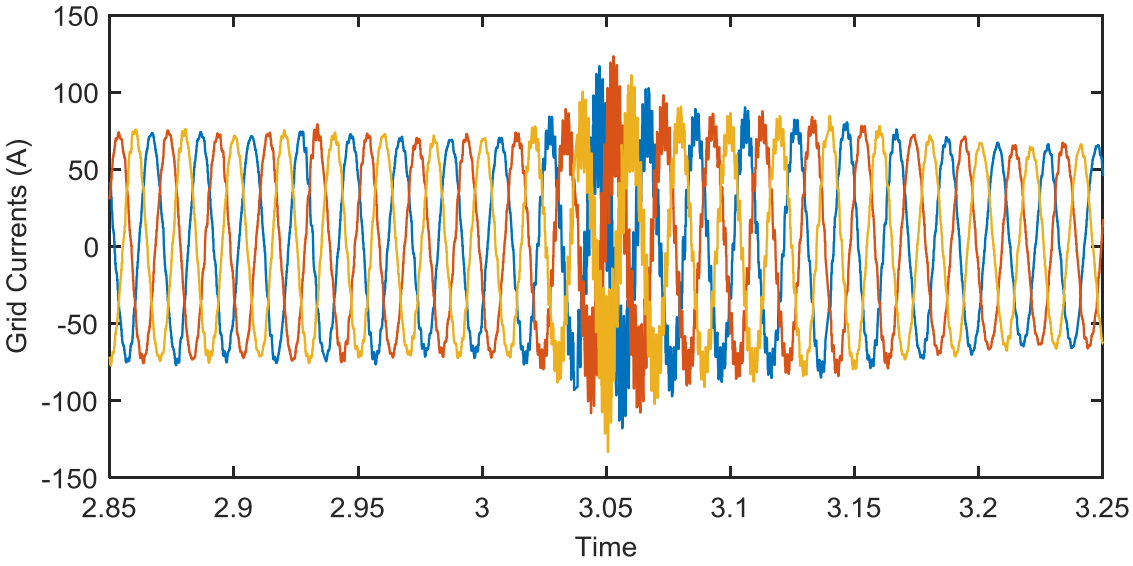

Figure 10-37 Grid Current in ABC frame

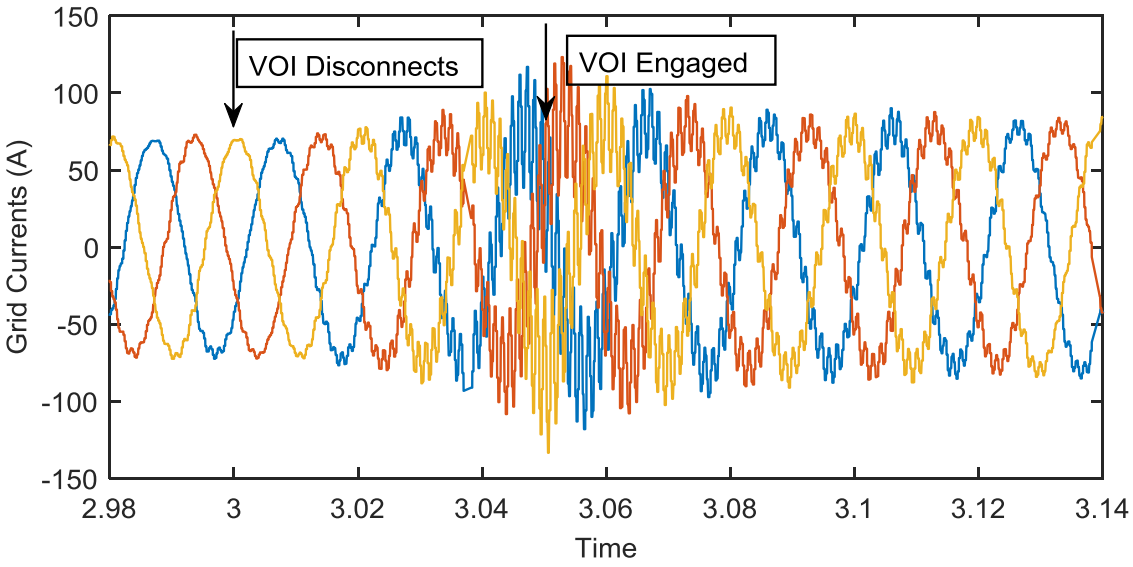

Figure 10-38 Grid Current in ABC Frame (zoomed) - Showing Harmonic Instability due to absence of VOI Controller

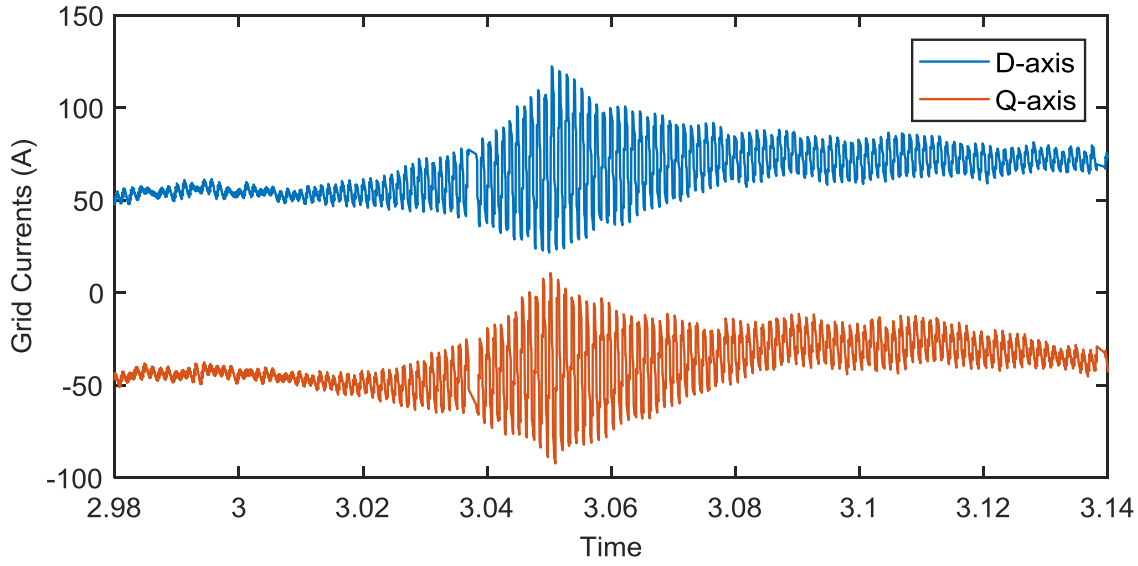

Figure 10-39 Grid Current in DQ Frame (zoomed) - Showing Harmonic Instability due to absence of VOI Controller

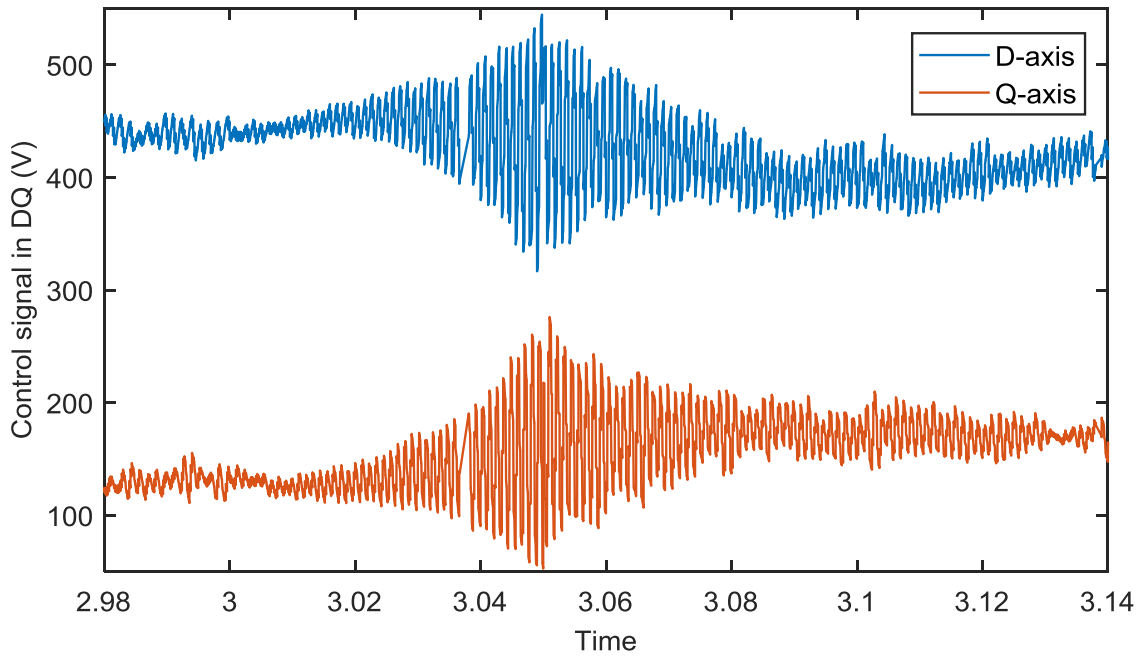

Figure 10-40 Overall controller response (PI+VOI)

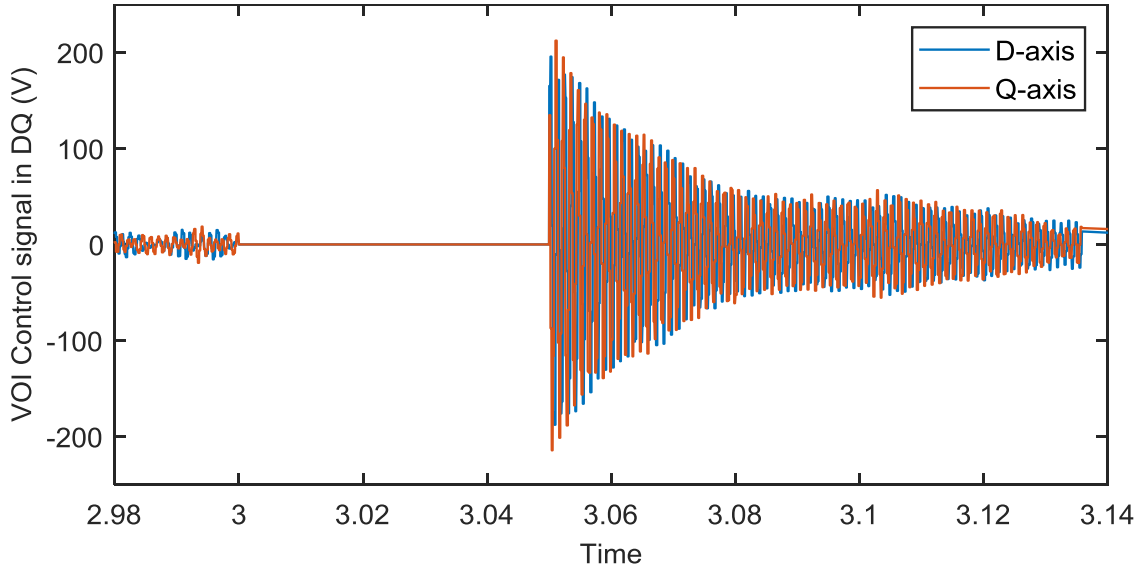

Figure 10-41 VOI Controller Response